STUDY OF HIGH β RELAXED STATE OF PLASMA

MUHAMMAD IQBAL

DEPARTMENT OF PHYSICS
QUAID-I-AZAM UNIVERSITY
ISLAMABAD PAKISTAN

2001

STUDY OF HIGH β RELAXED STATE OF PLASMA

MUHAMMAD IQBAL

DEPARTMENT OF PHYSICS
QUAID-I-AZAM UNIVERSITY
ISLAMABAD PAKISTAN

2001

This work is submitted as a thesis in
partial fulfillment of
the requirement for the award of the degree of

DOCTOR OF PHILOSOPHY
in
PHYSICS

Department of Physics
Quaid-i-Azam University
Islamabad, Pakistan

CERTIFICATE

Certified that the work contained in this thesis was carried out by **Mr. Muhammad Iqbal** under my supervision.

(Prof. Dr. G. Murtaza)
Supervisor
Salam Prof. of Physics
Government College,
Lahore, Pakistan.

Submitted through

(Prof. Dr. M. Aslam Baig)
Chairman
Department of Physics
Quaid-i-Azam University,
Islamabad, Pakistan.

Acknowledgments

All praises to Almighty Allah, the most benevolent and merciful, the creator of the universe, who enabled me to complete this thesis. I also pay my all respects to the Holy Prophet MUHAMMAD (peace be upon him) whose life is forever a source of guidance and knowledge for humanity as a whole.

I acknowledge my deepest gratitude to Professor G. Murtaza for providing me invaluable guidance and support. He has guided me not only in Physics but in other aspects of life also.

My immense gratitude goes to Professor Z. Yoshida, University of Tokyo, Japan, for introducing me to the field of Plasma Relaxation and providing me an opportunity to do research work at the University of Tokyo. He has stimulated my imagination and his encouraging discussions enabled me in broadening and improving my research capabilities.

I am also grateful to Dr. A. M. Mirza who extended me every possible help whenever needed. Special thanks are due to Dr. Zakaullah, Dr. H. Saleem, Dr. M. S. Qaiser, Dr. T. J. Baig, Dr. M. H. Nasim, Dr. N. A. D. Khattak and Zahoor Ahmad for their encouragement, guidance and moral support throughout the task of this research work.

I am grateful to Professor M. Aslam Baig, Chairman, Department of Physics, for providing me all the research facilities. I also wish to thank all my teachers and friends (especially A. H. Gilani, Ashfaq Khosa and Dr. A. Q. Hashmi) for their liberal cooperation during the completion of this work.

My heartiest thanks to all members of Plasma Physics Group both at the Quaid-i-Azam University (Anisa Qamar, Mukhtar Talha, Ajmal Khan and Ansar Mahmood) and at Salam Chair in Physics, Government College, Lahore (Rubilah, Shahid Ali, Faisal Yaqoob and Usman) who helped me in one way or the other. I also wish to thank Dr. I. M. Ghouri, Director, Center for Advanced Studies in Physics (CASP) and Dr. Riaz Ahmad for their kind hospitality and cooperation during my stay at CASP.

I would like to acknowledge the financial assistance provided by Japanese Ministry of Education, Science, Sports and Culture (Monbusho) and by the office of External Activities of the Abdus Salam International Center for Theoretical Physics, Trieste, Italy.

I also express my deep indebtedness to my parents, brothers and sisters who infused in me a spirit of steadfastness, patience and perservence to continue this task of research work.

Last but not the least, I wish to record my deepest obligations to my children and my wife for their sustained love and cooperation.

(Muhammad Iqbal)

Abstract

Beltrami fields, eigenfunctions of the curl operator, represent the static force-free relaxed state of a single-fluid MHD plasma and correspond to the alignment of magnetic field and current density. The double Beltrami fields which are the superposition of two different Beltrami fields, express a more general relaxed state of a two-fluid MHD plasma. The new relaxed states, despite its simple mathematical structure, encompass a wide class of steady states in mathematical Physics and explain interesting phenomena. Plasma configurations are investigated employing the double Beltrami fields. Our numerical results reveal that relaxed states of plasma exhibiting ultrahigh β associated with minimum values of field-aligned current and flow can be created which are suitable for the advanced fusion concept.

Furthermore, a set of algebraic equations is derived which relates the parameters of double Beltrami field (amplitudes and eigenvalues) and the ideal invariants (energy and helicities) of the system. These equations can be used to study the existence of solutions and catastrophic change of structures in relaxed equilibria in different plasma configurations. For a given set of energy and helicities, the catastrophic loss of equilibrium is observed when flux loops are compressed by varying the control parameter. This study could be very helpful to understand the eruptive events in solar corona.

List of Publications

(The reference number 3, 4 and 8 have been included in the thesis)

1. A theoretical model for a finite thickness gas puff Z-theta pinch

   Modern Phys. Lett. **B 7**, 1665 (1993).

   A. M. Mirza, **M. Iqbal**, N. A. D. Khattak and G. Murtaza

2. Fusion conditions in a finite thickness gas puff staged Z pinch

   J. Plasma Physics **52**, 365 (1994).

   A. M. Mirza, N. A. D. Khattak, **M. Iqbal**, and G. Murtaza.

3. High beta relaxed states of plasma with internal conductor plasma configuration

   Phys. Plasmas **8**, 1559 (2001).

   M. Iqbal, A. M. Mirza, G. Murtaza and Z. Yoshida

4. Beltrami fields in Plasmas: High-confinement mode boundary layers and high beta equilibria

   Phys. Plasmas **8**, 2125 (2001).

   Z. Yoshida, S. M. Mahajan, S. Ohsaki, M. Iqbal, and N. Shatashvili

Conference Proceedings

5. High-beta equilibrium of non-neutral plasma

   Meeting abstracts of the Physical Society of Japan, Vol. 53, Issue 2, part 4, page 939, Sep. 25-28, 1998.

   M. Iqbal, S. M. Mahajan, Z. Yoshida

6. Toroidal confinement of non-neutral plasma -a new approach to high-beta equilibrium-

   Proceedings of 17th IAEA Conference on Fusion Energy, Yokohama, 1998, IAEA-CN-69/ICP/10(R).

   Z. Yoshida, Y. Ogawa, J. Morikawa, H. Himura, S. Kondo, M. Hashimoto, T. Hirotsu, K. Takemura, H. Kakuno, C. Nakashima, N. Shibayama, S. Tahara, **M. Iqbal**, S. M. Mahajan

7. Toroidal magnetic confinement of non-neutral plasmas

   Proceedings of AIP Conference on Non-Neutral Plasma Physics, New Jersey, 1999, edited by J. J. Bollinger, R. L. Spencer and R. C. Davidson (American Institute of Physics, 1999) CP**498**, p. 397.

   Z. Yoshida, Y. Ogawa, J. Morikawa, H. Himura, S. Kondo, C. Nakashima, S. Kakuno, **M. Iqbal**, F. Volponi, N. Shibayama, S. Tahara

8. Optimization of double Beltrami equilibrium with ultra high beta

   Meeting abstracts of the Physical Society of Japan, Vol. **56**, March 22-25, 2000.

   M. Iqbal, S. Ohsaki, Z. Yoshida

Contents

Chapter 1

Introduction

1.1 Motivation

There is abundant evidence that certain constrained turbulent fluid systems naturally evolve toward states that exhibit some form of order on long length scales. These include two-dimensional (or geostrophic) fluids such as hurricanes on Earth and the Great Red Spot on Jupiter, the formation of isolated vortices in two-dimensional Navier-Stokes flow, the evolution of solitons in fluid and optical systems, guiding-center plasmas, pure electron plasmas, as well as two and three dimensional magnetofluids such as reversed-field pinches and spheromaks. In all cases, one physical quantity acquires long range order while another physical quantity suffers from short range disorder and takes care of the increase of entropy. The ordered structure thus appears in a particular physical quantity. In many cases, the detailed structure of these ordered states is found to be remarkably robust in the sense that they remain relatively invariant and their properties are independent of the way the system is prepared. This phenomenon has been called "self-organization" [1].

The process in which a plasma attains a state of minimum energy that is a stable state from an unstable one is termed as "Plasma Relaxation" and is a remarkable example of self-organization. Due to its importance in fusion power reactor, different devices e.g., Tokamak, Reversed-Field Pinch and Spheromak have been used to study this phenomenon. It has been observed that creation of this state is independent of the initial conditions of the system and depends only on a few global parameters such as total current or magnetic flux, and the inherent

geometry of the particular device [1]-[3].

The self-organization occurring in a variety of continuous media exhibit several common features [1]-[3]. First, they self-organize or relax to large scale structures i.e., to structures as large as allowed by boundary conditions. Second, the systems are described by nonlinear differential equations with dissipation. Third, there are ideal invariants for each system, i.e., quantities that are conserved in the absence of dissipation. Fourth, in presence of resistivity, it is often the case that at least one of the ideal invariants is more strongly affected by the dissipation than the others.

Theoretically, the relaxed state is often described by a variational principle based on selective decay hypothesis. The selective decay hypothesis is characterized by the following. If "ideal invariants" of a system are considered in the presence of a small amount of dissipation, it is often found that one of the invariants is better conserved or more rugged than others. The minimization of the expression for the poorly conserved invariant subject to the constraint that the rugged invariant is conserved using the technique of Lagrange multipliers, yields the Euler equation for the field variable.

Relaxation occurs throughout the universe. The magnetized plasmas under the topological constraints of magnetic fields relax to the natural state of lowest energy. The topology of magnetic field lines play a vital role in the relaxation process in various plasma systems. Much work has been done, therefore, to understand the so called "dynamo process" i.e., the origin and mechanism of sustainment of magnetic fields in earth and other astrophysical systems. Specifically, the magnetic field configurations of celestial objects have been an interest of astrophysicists ever since the 1934 "antidynamo" theorem of Cowling [4]. This theorem essentially states that, within the context of resistive magnetohydrodynamics (MHD), a magnetic field configuration containing a closed field line can not be sustained against resistive dissipation. Then in 1954, Lüst and Schlüter elicited astrophysical interest in force-free magnetic field configurations [5]. A few years later, this interest culminated with the well-known variational principle of Woltjer and Chandrasekhar [6]-[8].

Woltjer pointed out the importance of magnetic helicity which is a measure of "knottedness" of magnetic field [9] and acts as an invariant within a flux tube in a perfectly conducting plasma.

Mathematically, it is expressed as

$$H = \frac{1}{2}\int_v \mathbf{A}\cdot\mathrm{B}dv,$$

where $\nabla \times \mathbf{A} = \mathrm{B}$, v is the entire volume and dv is the volume element. The magnetic helicity remains unchanged while the magnetic energy $W = \frac{1}{2}\int_v B^2 dv$ decays toward a "ground state" in the presence of viscous dissipation. This energy relaxation self-organizes the magnetic field and is characterized by a selective decay of magnetic energy to a given helicity. The variational principle reads as $\delta(W-\lambda H) = 0$, where λ is the Lagrange multiplier. For appropriate boundary conditions, the resulting Euler equation is

$$\nabla \times \mathrm{B} = \lambda \mathrm{B}, \tag{1.1}$$

and expresses the force-free state of the system.

Taylor [10] formulated an equivalent variational principle but he conjectured that the energy dissipation proceeds faster than the change of the magnetic helicity in a slightly resistive plasma.

Originally, force-free fields attracted attention because of their importance in astrophysics. They play a conspicuous role in stellar atmospheres, in particular in the solar corona. Much attention has been paid to so called linear force-free fields, or fields with constant λ. Many astrophysical and space plasmas suggest the creation of linear force-free fields such as magnetic flux ropes created through interactions between the magnetosphere and the interplanetary magnetic fields [11] and the galactic jets [12].

One aspect of force-free fields with constant λ was introduced by Arnold and Moffatt [13]. They found only this kind of equilibrium field has the potential to stochastic field lines. As pointed out by Moffatt, an analogy exists between magnetic equilibrium and Euler flow of arbitrarily complex topology; the constant λ flow is equivalent to Beltrami flow. Thus studying the force-free fields gives an insight into fluid dynamics. Many authors studied the statistical mechanical properties of the force-free relaxed state using the Beltrami functions to expand fields [14]-[16]. A detailed description of the Beltrami functions and their application is given by Yoshida [17]. Eigenfunctions of the curl derivative are used in representing the circularly polarized waves [18], inverse source problems for acoustic and electromagnetic equations [19, 20],

and more practically, the superconducting magnet design problem [21]. Some laboratory experiments have also shown that the relaxed state generated through turbulence is well described as solution of the force-free equation [22, 23].

Much work has been devoted to the construction of force-free configurations. On one hand, one can construct the field lines of a configuration given an analytic expression for the field. It is in this way that stochastic lines of force have been found. On the other hand, one of the outstanding problems of the solar corona is to construct the field configuration from observation of the photospheric field. More importantly, the constant λ field is regarded as a final state after reconnection of the lines of force and subsequent reconnections of the field, as suggested by Taylor [22]. This well-known hypothesis has been used to explain the magnetic structures in laboratory plasmas such as multipinch, reverse-field Pinch (RFP), and spheromak.

Multipinch is an axisymmetric toroidal discharge and the poloidal cross section exhibits an equatorial, or up-down symmetry. The predictions of the Taylor's theory for the multipinch configuration were borne out by experiment conducted by LaHaye et al., [24]. Taylor's theory gives an accurate description of plasma relaxation in the case of the multipinch [2].

Reverse field configuration representing equilibrium state of plasma were discovered accidently in a toroidal pinch experiment called Zeta [25]. In this configuration, toroidal magnetic field reverses direction in the poloidal cross section of the plasma and such type of configuration might be used for the containment of plasma in a thermonuclear fusion. Various experimental results show that the reverse field can be created either by inducing axial current beyond the limit of kink instability or by artificially reversing the toroidal magnetic field near the conducting wall. In all the reverse field pinch devices, the magnetic field configuration at the field reversal are found to have structures that seem to justify Taylor's conjecture of minimum energy. This fit is quite good but departures from the Taylor force-free state have been noted in spheromaks [26]. Moreover, it has had less success predicting tokamak behavior and does not apply at all to field-reversed configurations (FRC). The Taylor's model based on the conservation of magnetic helicity represents a "stationary (no flow)" force-free macroscopic state of plasma. This model also suffers from critical short falls concerning the plasma edge conditions and the effect of finite pressure gradient. However, the practical magnetofluids in space and in fusion experiments are not generally force-free, i.e., they exhibit significant fluid pressure. Thus force-free fields

are obviously useless for confining plasmas. From an experimental perspective, there is strong evidence that confined magnetofluids in tokamaks [27] and in spheromaks [28, 29] have large organized flows. As pointed out by Frisch et al., [30], if large scale magnetic structures develop then large scale velocity fields will necessarily be generated by the $\mathbf{j} \times \mathbf{B}$ term in the equation of motion (Lorentz force). The inverse cascade then proceeds through the interaction of the velocity fields with the large scale magnetic fields.

Many studies have been done to obtain a relaxed state with a flow by introducing a number of constraints on the system. It is due to Sudan's pioneering work [31] that the two fluid (Hall) effect is considered to play an important role in the relaxation phenomena with plasma flows. He has derived the force-free ($\nabla p = 0$) equilibrium using a generalized variational principle. Turner [32] constructed a model of magnetofluid relaxation and showed that presence of nonvanishing fluid vorticity is necessary for the existence of relaxed magnetic field configurations that confine a finite plasma pressure. He showed that inclusion of Hall's term in Ohm's law in single fluid magnetohydrodynamic (MHD) equations under certain boundary conditions admits an invariant of the type $H = \int_v \mathbf{P} \cdot \nabla \times \mathbf{P} dv$, where $\mathbf{P} = (m\mathbf{V}/c + \mathbf{A}/c)$; $\mathbf{A}$ is the vector potential, $\mathbf{V}$ is velocity of the fluid, m and q represent the mass and charge respectively. Later it was shown by Avinash and Taylor [33, 34] that within multifluid approximation such an invariant is admitted by each fluid separately. Steinhauer and Ishida [35, 36] constructed the transport equations for the said invariants called self-helicities which are basically the canonical composites of the fluid and magnetic momenta. They developed a relaxation theory using these transport equations for two-species magnetofluid considering self-helicities, one for each species, as an invariant. It is shown that relaxed state characterizes finite pressure and sheared flow.

More recently a possible approach of creating relaxed state of a high β plasma with strong flow has been proposed by Mahajan and Yoshida [37]. This simplest theoretical approach takes into account the Hall effect and the equilibrium state of two-species ideal magnetofluid can be described as a linear combination of two different Beltrami fields with two spatial scale lengths in contrast to conventional Beltrami fields that are characterized by only a single scale length to yield force-free equilibrium. It is fortuitous that the equilibrium state can also be derived from a general principle of constrained minimization by assuming that the magnetofluid energy seeks the minimum value compatible with the constrained helicities. The new formalism explicitly

describes the strong coupling between the fluid and the electromagnetic natures of the plasma and through the Bernoulli mechanism make it possible to confine a finite plasma pressure. This treatment gives a much wider class of special equilibrium solutions. The general solvability of the double curl Beltrami system has been proved by Yoshida et al., [38]. The new set of solutions being more general consists of field configurations satisfied by constant λ Beltrami fields and also contains field configurations which are qualitatively different from constant λ force-free Beltrami magnetic fields. The larger new set may help us understand a variety of structures in Plasmas. It also makes possible to do experiments with altogether different configurations some of which may lead to a novel regime of high-pressure plasma confinement.

Yoshida et al., [39, 40] have applied the plasma confining characteristic of this formalism and successfully demonstrated the steady-state confinement of a pure electron plasma using an internal conductor toroidal confinement device, Proto-RT. They have examined the basic mechanisms to produce and confine non-neutral plasma having high β and strong flows. Such type of plasmas are considered to be suitable for advanced fusion.

A collisionless self-organizing model for the high-confinement (H-mode) boundary layer developed in the tokamak plasma [41]-[47] based on double curl Beltrami treatment is presented [48, 49] and the analysis shows the predicted values of the layer width and the poloidal flow velocity are in good agreement with experimental observations. Furthermore, numerical analysis of toroidal equilibria clearly shows that high-β equilibrium states can be achieved by double Beltrami fields [49].

The double curl Beltrami formalism yields structures which are much more complex, interesting and richer than the ones contained in the conventional conducting-fluid model. This model bears a higher potential to study the dynamics and morphology of a variety of space, astrophysical and laboratory plasmas.

In this thesis, using Mahajan-Yoshida model as a paradigm, we have studied the plasma dynamics in cylindrical and annular plasma configurations for different Beltrami parameters and boundary conditions. Analytical solutions for the annular plasma system are presented and high β relaxed states with minimum values of field aligned current and flows are investigated [50]. Optimization of β and components of flow and current is performed, and a comparison of the two configurations is also presented.

A set of algebraic relations is derived that relates the eigenvalues and amplitudes of the double Beltrami field with the macroscopic constants of motion (helicities and energy). Employing these relations, the existence of solutions and catastrophic change of structures is studied [49].

1.2 Layout of thesis

This thesis is arranged as follows. In chapter one, we have given a justification for studying high-β relaxed state of a plasma and layout of the dissertation. In chapter two, basic concepts related with single Beltrami fields are reviewed. Introducing the concept of helicity, self-organization in magnetohydrodynamics (MHD) is discussed and the expression of relaxed magnetic field is derived using Woltjer's hypothesis. Taylor's conjecture about the relaxation has also been described. Explicit solutions of constant λ force free fields are presented and the solution in the plane geometry is used to model magnetic arcade configurations in the solar atmosphere for two and three dimensional cases. Chapter 3 deals with different models of relaxation based on double Beltrami fields. Steinhauer-Ishida model based on concept of self-helicity constraint satisfied by each species is described in detail. In the same chapter, Mahajan-Yoshida model characterized by a superposition of two different Beltrami fields is presented and proved using the variational technique. The two models are compared at the end of this chapter. In chapter 4, we have presented the analytical solution for the axisymmetric cylindrical geometries using Mahajan-Yoshida model. First, simple cylindrical plasma configuration is discussed. Radial profiles for magnetic field, flows and pressure are given and the results obtained are discussed briefly. We have extended this work using new configuration namely internal conductor plasma configuration. Presenting analytical solution for this new configuration, radial profiles of different physical quantities are given subject to different boundary values and eigenvalues. The results are discussed and comparison between two geometries is made at the end of this chapter. In chapter 5, parameters associated with the double Beltrami fields are evaluated by invoking the constant of motion of the evolution equation. The characteristics of the relaxed states are studied by slowly changing the control parameter. In the last chapter, we summarize and discuss the results obtained after employing Mahajan-Yoshida model to different plasma configurations.

Chapter 2

Beltrami Fields

The Beltrami fields, eigenfunctions of the curl operator, may be used to represent the essential characteristics of sheared, spiral, chiral, or helical structures in various vector fields. Since the magnetic field is the key player in labelling and determining the state of a typical plasma, it stands to reason that one could describe and understand the possible self-organized states of a plasma in terms of Beltrami fields. Self-organization basically refers to a generic process of spontaneous formation of an ordered structure. In plasmas, self-organization process has long been considered to be a process that an unstable equilibrium relaxes into a minimum energy state. In the next section, we will discuss the self-organization and the related physical concept.

2.1 Self-organization in MHD System

MHD, the science of motion of electrically conducting fluids under magnetic fields, deals with the situation of mutual interaction between the fluid velocity field and the electromagnetic field. As a result of nonlinear induction effect and its reciprocal Lorentz force, MHD systems are more complicated than those of ordinary fluid mechanics. Surprisingly, however, three-dimensional MHD systems exhibit a greater degree of regularity than does an ordinary incompressible three-dimensional fluid. Observations of space and laboratory plasmas alike reveal that the magnetic field of the plasma tends to self-organize through a turbulent phase of relaxation into a simple spiral configuration. This phenomenon resembles the self-organization in two dimensional fluids. Dynamics of two-dimensional fluid is rather ordered in comparison with that of a three

dimensional fluid. The conservation of the enstrophy is considered to make this difference.

For the case of MHD relaxation, there is one topological invariant namely the magnetic helicity invariant, that plays a central role and is defined as follows. Let s be any closed surface moving with the fluid on which the condition $\mathbf{n} \cdot \mathbf{B} = 0$ is satisfied where $\mathbf{n}$ is the unit normal vector on the surface. Assuming a fixed gauge, let $\mathbf{A}$ be a vector potential for $\mathbf{B}$ i.e., $\mathbf{B} = \nabla \times \mathbf{A}$, the magnetic helicity H in the volume v inside s is defined by the integral

$$H = \int_v \mathbf{A} \cdot \mathbf{B} dv. \tag{2.1}$$

In the study of geometric structure of streamlines, the helicity plays an essential role to characterize the linkage and twist. In the following section we describe helicity.

2.1.1 Helicity

The helicity density of any vector field $\mathbf{A}$ is defined by the quantity $\mathbf{A} \cdot (\nabla \times \mathbf{A})$. The volume integral of helicity density yields the helicity of the field. Helicity density is the scalar product of a polar vector and an axial vector. It is therefore, a pseudo-scalar quantity and changes sign under the change from a right-handed to a left-handed frame of reference.

The magnetic helicity is a measure of the structural complexity of the magnetic field. It is related to the interconnection of the field and is well defined if it is gauge invariant. For a given magnetic field configuration, the vector potential is defined within a gauge transformation. We consider the gauge transformation

$$\mathbf{A} \rightarrow \acute{\mathbf{A}} = \mathbf{A} + \nabla \chi, \tag{2.2}$$

where χ is an arbitrary scalar function of position. The corresponding change in helicity given by (2.1) is

$$\mathbf{H} \rightarrow \acute{\mathbf{H}} = \mathbf{H} + \int_v \mathbf{B} \cdot \nabla \chi dv. \tag{2.3}$$

Using the fact that $\nabla \cdot \mathbf{B} = 0$, we find that

$$\acute{\mathbf{H}} - \mathbf{H} = \int_v \nabla \cdot (\chi \mathbf{B})\, dv = \int_s \mathbf{n} \cdot \mathbf{B} \chi ds, \tag{2.4}$$

where s is the surface bounding the volume over which helicity is calculated. It shows that helicity is well defined if and only if $\mathbf{n} \cdot \mathbf{B} = 0$ on the bounding surface.

In order to show the significance of magnetic helicity, we consider two infinitesimal flux tubes that occupy volumes V_1 and V_2. The tubes follow the curves C_1 and C_2 and let ϕ_1 and ϕ_2 be the respective magnetic fluxes. The flux tubes link each other once and we assume that $\mathbf{B} = 0$ outside the tubes. The flux of each tube is given by

$$\phi_j = \int_{s_j} \mathbf{n} \cdot \mathbf{B} ds. \qquad (j = 1, 2) \tag{2.5}$$

Here $\mathbf{n}$ is the unit normal vector on s_j and ds is the surface element. We assume slender tubes where $\mathbf{n} \cdot \mathbf{B}$ is constant on s_j. Thus, for the flux tube V_1, we can replace $\mathbf{B}dv = \mathbf{n} \cdot \mathbf{B} ds dl = \phi_1 dl$, therefore the expression for H_1 may be written approximately as

$$\begin{aligned} H_1 &= \int_{s_1} \mathbf{n} \cdot \mathbf{B} ds \oint_{C_1} \mathbf{A} \cdot d\mathbf{l}, \\ &= \phi_1 \int_{\Sigma_1} \mathbf{n} \cdot \mathbf{B} ds \\ &= \phi_1 \phi_2 \end{aligned} \tag{2.6}$$

where Σ_1 is an open surface spanning C_1. In writing down the above expression of H_1, we have used the fact that $\mathbf{B}$ is approximately normal to s_1, that is a cross section of the flux tube V_1. Thus the integral over s_1 is ϕ_1, the flux of the tube V_1, and the closed integral yields ϕ_2, the flux of the tube V_2.

Similarly, H_2 has the same value given as

$$H_2 = \phi_1 \phi_2. \tag{2.7}$$

The total magnetic helicity H is given by the sum of the helicities of all the tubes, that is

$$\begin{aligned} H &= H_1 + H_2 \\ &= 2\phi_1 \phi_2. \end{aligned} \tag{2.8}$$

Thus the integrals H_1 and H_2 measure the linkage of two flux tubes. If the tubes were not

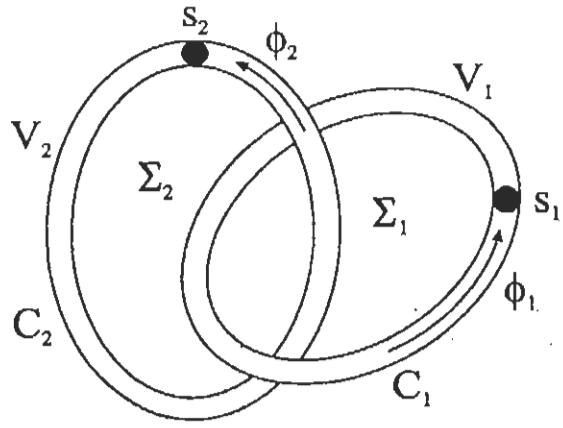

Figure 2-1: A schematic representation of two linked flux tubes.

interlinked, the line integrals would vanish.

More generally, if two flux tubes wind around each other N times (i.e., N is the "winding number" of C_1 relative to C_2), then

$$H_1 = H_2 = \pm N\phi_1\phi_2, \tag{2.9}$$

and

$$H = \pm 2N\phi_1\phi_2, \tag{2.10}$$

where the sign depends on the relative orientation of the magnetic field in the two flux tubes. The field direction in the two interlinked tubes as shown in figure (2-1) has a right-handed orientation relative to each other. If field direction is reversed in one of the tubes, then the relative orientation becomes left-handed and if both are reversed, it remains right-handed.

In ideal MHD, the integrals H_1 and H_2, representing the topological property of the field are preserved throughout the motion. According to frozen field property, if a condition is satisfied at time zero, then it is satisfied for all times. Therefore, the flux tubes can not be broken or reconnected in a perfectly conducting plasma.

In the next sub-section, we will address the problem of the invariance of magnetic helicity in a perfectly conducting plasma.

2.2 Woltjer's Theorem

Suppose that the magnetic field $\mathbf{B}$ *satisfies the induction equation* $\partial\mathbf{B}/\partial t = \nabla \times (\mathbf{V} \times \mathbf{B})$. *Then for a plasma confined by a perfectly conducting boundary* $(\mathrm{n} \times \mathbf{E})$, *the helicity is conserved.*

According to Woltjer [6], for a perfectly conducting plasma there are infinite number of constraints defined by

$$H_l = \int_{v_l} \mathbf{A} \cdot \mathbf{B} dv, \qquad l = 1, 2, ..., \infty$$

where v_l is the volume of the lth flux tube, whose close bounding surface is s_l. The rate of change of H_l can be written as follows

$$\frac{dH_l}{dt} = \int_{v_l} (\frac{\partial \mathbf{A}}{\partial t} \cdot \mathbf{B} + \mathbf{A} \cdot \frac{\partial \mathbf{B}}{\partial t}) dv + \int_{s_l} (\mathbf{A} \cdot \mathbf{B})(\mathrm{n} \cdot \mathbf{V}) ds. \tag{2.11}$$

The last term on the right-hand side of above equation arises because surface of flux tube is considered to move with a velocity $\mathbf{V}$. By noting $\partial\mathbf{B}/\partial t = \nabla \times (\mathbf{V} \times \mathbf{B})$,

$$\int_{v_l} \mathbf{A} \cdot \frac{\partial \mathbf{B}}{\partial t} dv = -\int_{v_l} \nabla \cdot [\mathbf{A} \times (\mathbf{V} \times \mathbf{B})] dv + \int_{v_l} (\mathbf{V} \times \mathbf{B}) \cdot (\nabla \times \mathbf{A}) dv \tag{2.12}$$

is obtained. Here the second term of the right hand side vanishes identically. By using the Gauss theorem,

$$\int_{v_l} \nabla \cdot [\mathbf{A} \times (\mathbf{V} \times \mathbf{B})] dv = \int_{s_l} [(\mathbf{A} \cdot \mathbf{B})(\mathbf{V} \cdot \mathrm{n}) - (\mathbf{A} \cdot \mathbf{V})(\mathbf{B} \cdot \mathrm{n})] ds, \tag{2.13}$$

and from the definition of the infinitesimal flux tube $\mathbf{n} \cdot \mathbf{B} = 0$. Then the above equations give

$$\frac{dH_l}{dt} = \int_{v_l} (\frac{\partial \mathbf{A}}{\partial t} \cdot \mathbf{B}) dv. \tag{2.14}$$

Substituting $\mathbf{E} = -\nabla\phi - \partial\mathbf{A}/\partial t$ into equation (2.14), we get

$$\frac{dH_l}{dt} = -\int_{v_l} (\mathbf{E} \cdot \mathbf{B} + \nabla\phi \cdot \mathbf{B}) dv, \tag{2.15}$$

Using $\mathbf{E} = -\mathbf{V} \times \mathbf{B} + \eta \mathbf{j}$ in the above equation, we get

$$\frac{dH_l}{dt} = -\int_{v_l} (-\mathbf{V} \times \mathbf{B} \cdot \mathbf{B} + \eta \mathbf{j} \cdot \mathbf{B} + \nabla \phi \cdot \mathbf{B}) dv, \tag{2.16}$$

The first term vanishes identically and we get from the above equation

$$\begin{aligned} \frac{dH_l}{dt} &= -\int_{v_l} \eta \mathbf{j} \cdot \mathbf{B} dv - \int_{v_l} \nabla \cdot (\phi \mathbf{B})\, dv, \\ &= -\int_{v_l} \eta \mathbf{j} \cdot \mathbf{B} dv - \int_{s_l} \phi \mathbf{n} \cdot \mathbf{B} ds. \end{aligned} \tag{2.17}$$

For a perfect plasma $\eta = 0$ and by noting $\mathbf{n} \cdot \mathbf{B} = 0$ for the flux tube surrounding a closed line of force, we confirm

$$\frac{dH_l}{dt} = 0. \tag{2.18}$$

Thus each of the integral H_l is invariant in a perfectly conducting plasma. This invariant being essentially topological involves the identification of lines of force and represents the linkage of lines of force with one another. If one closed field line initially links another n-times then in a perfectly conducting plasma, the two loops must remain linked n-times during any plasma motion.

If we minimize the magnetic energy,

$$W = \frac{1}{2} \int_v B^2 dv \tag{2.19}$$

subject to the constraint of magnetic helicity conservation as described above, then for a plasma confined by a perfectly conducting shell, the Euler equation describing the equilibrium can be deduced as follows:

$$\delta (W - \lambda H) = 0, \tag{2.20}$$

where

$$\delta W = \int_v \mathbf{B} \cdot \delta \mathbf{B} dv, \tag{2.21}$$

and

$$\delta H = \frac{1}{2}\int_v (\delta \mathbf{A}\cdot\mathbf{B} + \mathbf{A}\cdot\delta\mathbf{B})\, dv, \tag{2.22}$$

so that

$$\int_v \mathbf{B}\cdot\delta\mathbf{B} dv = \frac{\lambda}{2}\int_v (\delta\mathbf{A}\cdot\mathbf{B} + \mathbf{A}\cdot\delta\mathbf{B})\, dv,$$

or

$$\int_v \mathbf{B}\cdot\nabla\times\delta\mathbf{A} dv = \frac{\lambda}{2}\int_v (\delta\mathbf{A}\cdot\mathbf{B} + \mathbf{A}\cdot\nabla\times\delta\mathbf{A})\, dv.$$

Using identity $\nabla\cdot(\mathbf{a}\times\mathbf{b}) = \mathbf{b}\cdot\nabla\times\mathbf{a} - \mathbf{a}\cdot\nabla\times\mathbf{b}$, and noting that the surface integrals vanish due to boundary conditions, we obtain

$$\int_v \delta\mathbf{A}\cdot(\nabla\times\mathbf{B})\, dv - \lambda\int_v \delta\mathbf{A}\cdot\mathbf{B} dv = 0,$$

or

$$\int_v \delta\mathbf{A}\cdot(\nabla\times\mathbf{B} - \lambda\mathbf{B})\, dv = 0.$$

This expression holds good for any arbitrary value of $\delta\mathbf{A}$, therefore

$$\nabla\times\mathbf{B} = \lambda\mathbf{B}. \tag{2.23}$$

This represents the force free relaxed state configuration of magnetic fields. However, the above discussion can not be the appropriate description of the quiescent state. In order to determine λ, one would have to calculate the invariant H for each closed field line and relate it to its initial value. Hence, far from being universal and independent of initial conditions, the state defined by equation (2.23) depends on every detail of the initial state. A way out of this dilemma was proposed by Taylor [10, 22]. He argued that in presence of resistivity, helicity acts as a global constraint. In the following subsection, we will describe Taylor's conjecture.

2.2.1 Taylor's Conjecture

The real plasmas, especially turbulent ones, are never perfectly conducting. In the presence of resistivity, however small, the topological properties of lines of force are no longer preserved. Lines of force may break and reconnect even though the resistive diffusion time may be very

long and there is insignificant flux dissipation. Mathematically the situation is one of non-uniform convergence; when $\eta = 0$ the equations do not permit changes in the topology of field lines, whereas such changes may occur when $\eta \neq 0$, even in the limit of small η. Physically, as $\eta \to 0$ the region over which resistivity acts get smaller but the field gradients get larger and the rate of reconnection does not diminish as fast as η or may not diminish at all. This situation is similar to driven reconnection. It concludes that in a turbulent resistive plasma, flux tubes have no continuous independent existence.

Taylor hypothesized that in a resistive plasma, all the topological invariants H cease to be relevant, not because the magnetic flux changes significantly because it is no longer possible to identify the field by which the flux changes. However, the sum of all the invariants, that is, the integral of $\mathbf{A} \cdot \mathbf{B}$ over the total plasma volume V_0, is independent of any topological considerations and of the need to identify particular field lines. Therefore, it remains a good invariant so long as the resistivity is small.

To obtain the relaxed state of a slightly resistive plasma, therefore, we should minimize the energy subject to the single constraint that the total magnetic helicity

$$H_0 = \frac{1}{2} \int_{v_0} \mathbf{A} \cdot \mathbf{B} dv \tag{2.24}$$

remains invariant. Following the similar procedure as given in the previous section, the minimization of energy subject to the constraint of total magnetic helicity using the variational principle $\delta(W - \lambda H_0) = 0$, and taking into account the requirement for the gauge invariance that the normal component of magnetic field vanishes at the boundary, we can easily get the following condition

$$\nabla \times \mathbf{B} = \lambda \mathbf{B} \tag{2.25}$$

for the equilibrium of a plasma enclosed by a perfectly conducting shell where λ is a constant. This relaxed state depends only on a single parameter λ and is independent of the initial conditions. Hence, this relaxed state differs significantly from the relaxed state defined by equation (2.23) which depends on the initial conditions.

When $\eta \neq 0$ in the plasma and $\mathbf{n} \cdot \mathbf{B} = 0$ at the conducting boundary, we see directly from

equation (2.17) that H_0 is not invariant, it decays at a rate

$$\frac{dH_0}{dt} = -\int_{v_0} \eta \mathbf{j} \cdot \mathbf{B} dv, \tag{2.26}$$

where v_0 is the total volume and the magnetic energy decay can be calculated as follows

$$\begin{aligned} \frac{dW}{dt} &= \int_{v_0} \mathbf{B} \cdot \frac{\partial \mathbf{B}}{\partial t} dv, \\ &= -\int_{v_0} \mathbf{B} \cdot \boldsymbol{\nabla} \times \mathbf{E} dv, \qquad (2.27) \\ &= -\int_{v_0} \boldsymbol{\nabla} \cdot (\mathbf{B} \times \mathbf{E})\, dv - \int_{v_0} \mathbf{E} \cdot (\boldsymbol{\nabla} \times \mathbf{B})\, dv, \qquad (2.28) \end{aligned}$$

The first integral vanishes due to boundary condition and putting the value of $\mathbf{E} = -\mathbf{V} \times \mathbf{B} + \eta \mathbf{j}$, we get

$$\frac{dW}{dt} = \int_{v_0} \mathbf{V} \times \mathbf{B} \cdot (\boldsymbol{\nabla} \times \mathbf{B})\, dv - \int_{v_0} \eta \mathbf{j} \cdot (\boldsymbol{\nabla} \times \mathbf{B})\, dv, \tag{2.29}$$

The first integral vanishes identically and we get

$$\frac{dW}{dt} = -\int_{v_0} \eta \mathbf{j}^2 dv. \tag{2.30}$$

From (2.26) and (2.30), we obtain

$$\frac{|dH_0/dt|}{|dW/dt|} = \frac{|\eta \mathbf{j} \mathbf{B}|}{|\eta \mathbf{j}^2|} = \frac{B}{j} = \mu_0 L. \tag{2.31}$$

where we have used the relation $\mu_0 \mathbf{j} = \boldsymbol{\nabla} \times \mathbf{B}$. Since L is small compared to the system size, H_0 changes more slowly than W. Dissipation of helicity in a resistive plasma does not effect the applicability of Taylor's conjecture. The relaxed states defined by (2.25) are the end results of some characteristic plasma dynamics. The time scales associated with the dynamics controlling relaxation process are important. The relaxation theory does not require that the magnetic helicity H_0 must be absolutely invariant. It only requires that the dynamical process responsible for the relaxation dissipate energy faster than helicity. Thus, it is the relative invariance of helicity with respect to energy that is important.

2.3 Beltrami Fields

Any vector field having its curl proportional to itself is termed as Beltrami field. The Beltrami magnetic field where $\mathbf{j} \times \mathbf{B}$ vanishes because $\mathbf{j}$ is parallel to $\mathbf{B}$ is known as "force-free" field.

A variety of complex phenomena, which are introduced by the nonlinear magnetohydrodynamics (MHD), make it impossible to construct a nontrivial theory by direct analysis of the basic equations. Therefore, we must apply a reduction of the model with appealing to scale separations, singular perturbations, coarse graining (averaging), etc., in order to elucidate a specific phenomenon. Let us consider a slow motion (or a steady state) low-pressure magnetized plasma. In the standard normalized unit, the general MHD equations read as

$$\partial_t \mathbf{v} = -(\mathbf{V}\cdot\nabla)\mathbf{v} + \epsilon_A^{-2}(\nabla\times\mathbf{B})\times\mathbf{B} - \beta\nabla p + \epsilon_R\triangle\mathbf{V}, \qquad \nabla\cdot\mathbf{V} = 0. \tag{2.32}$$

$$\partial_t \mathbf{B} = \nabla\times(\mathbf{V}\times\nabla) - \epsilon_L\nabla\times(\nabla\times\mathbf{B}). \tag{2.33}$$

Unknown variables are the magnetic field $\mathbf{B}$, the flow velocity $\mathbf{V}$ and the pressure p. Alfvén number ϵ_A, Lundquist number ϵ_L^{-1}, and the beta ratio β are the dimensionless coefficients. To determine the evolution of the pressure p, we may use some barotropic relation or, simply, the incompressibility condition $\nabla\cdot\mathbf{V} = 0$.

In the limit of $\epsilon_A \to 0$, with assuming slow time scale, we obtain

$$(\nabla\times\mathbf{B})\times\mathbf{B} = 0, \tag{2.34}$$

which is equivalent to

$$\nabla\times\mathbf{B} = \lambda\mathbf{B}, \tag{2.35}$$

where λ is a certain scalar function. By taking the divergence of both sides of equation (2.35), and using $\nabla\cdot\mathbf{B} = 0$, we obtain

$$\mathbf{B}\cdot\nabla\lambda = 0. \tag{2.36}$$

Equation (2.36) implies that the scalar function λ must be constant along the magnetic field line (streamline of $\mathbf{B}$). When the magnetic field lines cover a volume V, equation (2.36) demands that λ is constant in V. Therefore, the Beltrami field with a constant λ is amenable to the

singular limit of $\epsilon_A \to 0$ with chaotic magnetic field.

Let us now represent two cases as an explicit solutions of the Beltrami condition (2.35), the first solution has helical symmetry, and the second one is fully three dimensional.

2.3.1 Chandrasekhar-Kendall Functions

Chandrasekhar and Kendall [51] gave explicit solutions of (2.35) in the (r, θ, z) cylindrical coordinates. For a cylindrical domain with radius a and a periodicity in z with length L, the following one scalar-field representation, known as the Chandrasekhar-Kendall function

$$\mathbf{B} = \lambda(\nabla\psi \times \nabla z) + \nabla \times (\nabla\psi \times \nabla z), \tag{2.37}$$

solves (2.35) provided

$$\lambda = \pm(\mu^2 + k^2)^{1/2}, \tag{2.38}$$

and ψ obeys

$$\Delta\psi + \lambda^2\psi = 0, \tag{2.39}$$

where μ and k are constants. In cylindrical geometry, ψ may be represented as

$$\psi = \phi(r)e^{i(m\theta - kz)},$$

with $\phi(r)$ satisfying the Bessel equation. Therefore, completely explicit solution of (2.39) is

$$\psi = J_m(\mu r)e^{i(m\theta - kz)}, \tag{2.40}$$

where J_m is the Bessel function of order m $(= 0, 1, 2, ...)$, $k = \pm 2\pi n/L$ $(n = 0, 1, 2, ...)$. The solution is periodic in θ with a period 2π. The eigenvalue λ is determined by the boundary condition demanding that the normal component of $\mathbf{B}$ vanish on the surface of the cylindrical domain. This condition is trivial for $k = m = 0$, and μ can take any real (and also complex) value. Hence, continuous eigenvalues λ are obtained that span the entire complex plane.

When a solenoidal vector field has an ignorable coordinate (i.e., a symmetry), the corresponding streamline equation becomes integrable. The Chandrasekhar-Kendall function has a

"helical" symmetry, i.e., the function ψ depends only on a particular combination of θ and z and is independent of the orthogonal combination. In that sense there is an ignorable coordinate and hence, the associated streamline equation becomes integrable. For a Fourier mode with k and m, we may write equation (2.37) to obtain

$$\mathbf{B} = \nabla\Psi \times \nabla z + B_z(km^{-1}r^2\nabla\theta + \nabla z), \tag{2.41}$$

where

$$\begin{aligned} \Psi &= \lambda\psi - km^{-1}r\partial_r\psi, \\ B_z &= -(\triangle + k^2)\psi. \end{aligned}$$

We call this new Ψ as the "helical flux function". We easily find

$$\mathbf{B} \cdot \nabla\Psi = 0,$$

which implies that a level set of Ψ is an integral surface of the streamline equation.

2.3.2 ABC flow

In the (x, y, z) cartesian coordinates, we consider a magnetic field given by the ABC flow [52];

$$\mathbf{B} = \begin{pmatrix} A\sin\lambda z + C\cos\lambda y \\ B\sin\lambda x + A\cos\lambda z \\ C\sin\lambda y + B\cos\lambda x \end{pmatrix} \tag{2.42}$$

where A, B, C and λ are real constants. We easily verify that this ABC flow named after Arnold, Beltrami and Childress, satisfies the Beltrami condition (2.35). Since $\mathbf{B}$ is periodic in x, y and z of period $2\pi/\lambda$, we can identify every $x + 2n\pi$, $y + 2n'\pi$ and $z + 2n''\pi$ $(n, n', n'' \in Z)$ with the fundamental domain $0 \leq x, y, z < 2\pi$.

First we assume that $A = 0$. Then, $\mathbf{B}(x, y)$ is two-dimensional. By defining

$$\psi(x, y) = \lambda^{-1}(B\cos\lambda x + C\sin\lambda y),$$

we can write (2.42) in the form of

$$\mathbf{B} = \nabla\psi \times \nabla z + \lambda\psi\nabla z, \tag{2.43}$$

Therefore, this $\psi(x, y)$ is the Hamiltonian of the corresponding field-line equation.
If none of A, B, and C are zero, $\mathbf{B}(x, y, z)$ is three dimensional. For this case we can not find the equivalent of ψ of the preceding example of helical symmetry. In fact we may write (2.42) in the form

$$\begin{aligned}
\mathbf{B} &= \nabla\psi \times \nabla z - \nabla\chi \times \nabla y, \\
\chi &= -\lambda^{-1}(B\sin\lambda x + A\cos\lambda z) - Cx\sin\lambda y, \\
\psi &= \lambda^{-1}(C\sin\lambda y + B\cos\lambda x) - Ax\cos\lambda z,
\end{aligned}$$

but this ψ is a function of all three coordinates and the streamline becomes chaotic.

2.4 Solar Coronal Loops

The close proximity of the solar corona to our earth provides an opportunity to understand the dynamics of naturally occurring magnetized plasmas. The eclipse and spacecraft images of the corona reveal that the corona is highly structured, and that the hot plasma making up the corona is confined to intricate the magnetic field pattern. The eruptive events such as solar flares, erupting prominences, and coronal mass ejections are generally considered to be the source of the sudden release of magnetic energy. The solar eruptive events have been conventionally studied through magnetohydrodynamic tools [53, 54]. Most of the models that attempt to explain the eruptive processes are based on the assumption of force-free ($\mathbf{j} \times \mathbf{B} = 0$) coronal field [55]. The kinetic pressure in the solar corona is strongly dominated by the magnetic pressure. Specifically, for a small β (ratio of the kinetic pressure and the magnetic pressure) in the solar corona, the magnetic field demands the Beltrami condition.

The solar corona is highly inhomogeneous, and structures of different shapes and sizes are seen to pervade it. There are radial structures called coronal holes along which the plasma flows into the solar wind and are often found near poles. Over the rest of the solar surface, the

coronal structures generally form loops or large arches that link magnetically active regions of different polarity [56]. The solar corona, or the outer atmosphere of the sun, consists of a hot, tenuous plasma permeated with a magnetic field. The coronal magnetic field is anchored in the photosphere which is the dense visible surface of the sun. The coronal plasma displays a rich variety of dynamical activity. The coronal magnetic field is induced by convective motions in the photosphere. The motions in photosphere cause the feet of the coronal magnetic field lines to move about constantly and produces continual stirring of coronal plasma. Sunspots and their associated strong magnetic fields interact with each other and make the magnetic field lines to twist into loops and arcades resembling croquet hoops. The loop or arch-like configurations have been observed in the solar corona in the emissions at ultraviolet (UV), extreme ultraviolet (EUV) and X-ray wavelengths [57]. Plasma flows are also observed in the loops. The entire loop may have body oscillations [58]. The loops vary greatly over their lifetimes from tens of minutes to several hours.

Numerical solution given in figure (2-2) show the structure of streamlines in the two dimension whereas figure (2-3) depicts the magnetic field structure for three dimensional solutions. In figure (2-2), we have taken $C = 0$ and the magnetic field lines are representing arcade type structures which look very similar to the loops and arcades observed in solar corona [49].
On the other hand, for three dimensional solutions, we get chaos of streamlines as is obvious in figure (2-3).
Beltrami functions represent a special class of steady states in fluids and plasmas. Uniform Beltrami functions, which are the eigenfunctions of the curl operator, are well understood on a rigorous mathematical basis. They are applied in a wide area of physics. A complete set of eigenfunctions can be used to expand a solenoidal field such as a magnetic field or an incompressible fluid velocity. Streamlines defined by a uniform Beltrami function may yield a well-defined chaos, and this fact opens up a new paradigm of modern physics.

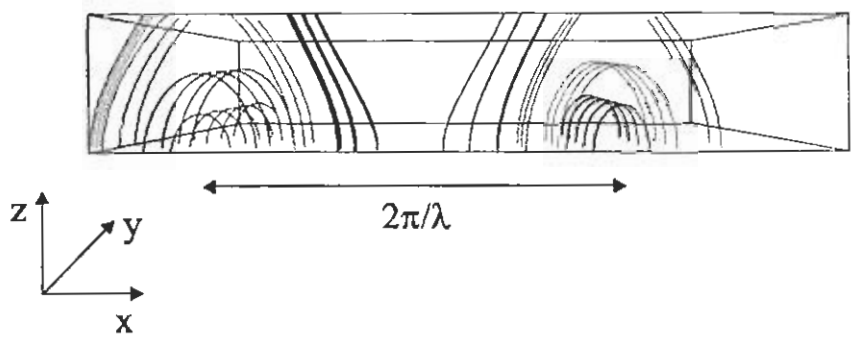

Figure 2-2: Magnetic field line structure for $A = 0.5$, $B = 1.0$, $C = 0$ and $\lambda = 2.0$ resembling a coronal arcade.

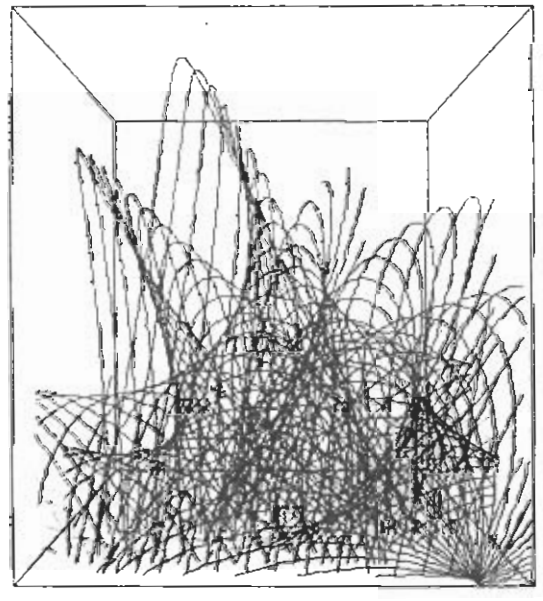

Figure 2-3: Chaotic structure of magnetic field lines for $A = 0.5$, $B = 1.0$, $C = 0.8$ and $\lambda = 1.0$.

Chapter 3

Double Beltrami Fields

The theory of relaxation of turbulent plasma has been very successful in predicting and interpreting the results of plasma experiments such as Reverse Field Pinch, Spheromak and Multipinch [10, 22]. According to this theory the plasma relaxes to a configuration of minimum energy subject to the constraint of constant total magnetic helicity. In the resulting equilibria, the fluid velocity is zero and the magnetic field satisfies the "Beltrami condition,"

$$\nabla \times \mathbf{B} = \lambda \mathbf{B} \tag{3.1}$$

Here λ is a scalar field that must satisfy $\mathbf{B} \cdot \nabla \lambda = 0$ to insure $\nabla \cdot \mathbf{B} = 0$. The Beltrami magnetic field represents a "stationary (no flow)" force-free ($\mathbf{j} \times \mathbf{B} = 1/\mu_0 (\nabla \times \mathbf{B}) \times \mathbf{B} = 0$) macroscopic plasma state.

Knowledge of a system's invariants often leads to an elegant qualitative picture of its behavior, particularly that such constraints cause it to self-organize into relaxed state [3]. Helicity constraints constitute an important and interesting set of constraints admitted by magneto-hydrodynamics (MHD) equations. Examples of such constraints are magnetic helicity, cross helicity and fluid helicity in hydrodynamics [6, 7, 9, 59]. These constraints represent linking properties of lines of some vector field, e.g., magnetic helicity represents self-linkage of magnetic field lines, cross helicity represents mutual linkage of magnetic and vortex field lines, while fluid helicity represents self-linkage of vortex field lines. These helicities are usually defined within the framework of a single fluid MHD and the invariance of these helicities have fostered suc-

cessful predictions of self-organization by certain classes of magnetofluid into force-free states, i.e., equilibria with no coupling force between the system's fluid and the field elements [10, 22]. However, practical magnetofluids in space and in fusion experiments are not generally force free, i.e., they exhibit significant fluid pressure. Further, significant flows (not predicted by the MHD theory) are a nearly ubiquitous feature of practical plasmas. Several authors have attempted, by introducing a number of constraints, to obtain relaxed states with plasma flow. In a multifluid system, self-helicities which are canonical composite of the fluid and magnetic momenta have been proposed as invariants by many authors [32, 33, 34, 60]. Steinhauer and Ishida [35, 36] have described the two-fluid relaxation theory considering self-helicities as system's invariants. In the next section, we will describe the model of Steinhauer and Ishida.

3.1 Steinhauer-Ishida Model

The relaxation theory of a two-species magnetofluid presented by Steinhauer and Ishida generalizes the familiar magnetohydrodynamics (one-fluid) theory. The invariants of the two-fluid are the self-helicities,

$$H_\alpha = (c^2/8\pi q_\alpha^2) \int \mathrm{P}_\alpha \cdot \Omega_\alpha dv, \tag{3.2}$$

where dv is a volume increment; and the integral is over entire system volume. These are the composite helicities, combining fluid and field behavior through the canonical momentum and the generalized vorticity:

$$\mathrm{P}_\alpha = m_\alpha \mathrm{u}_\alpha + q_\alpha \mathrm{A}/c, \qquad \Omega_\alpha = \nabla \times \mathrm{P}_\alpha. \tag{3.3}$$

Here $\mathbf{A}$ is the vector potential of the fields, and each species (denoted by index α) has the charge, mass, density, pressure, and flow velocity, $q_\alpha, m_\alpha, n_\alpha, p_\alpha, \mathrm{u}_\alpha$, respectively. The dimensional constant, $c^2/8\pi q_\alpha^2$ is chosen to give k_α energy-length units. In this theory

- The transport equations for the self-helicities are derived.
- Local and global invariance of self-helicities is presented.
- Relaxed states are found by minimizing the magnetofluid energy subject to constrained self-helicities.

In the next subsection helicity transport equations are given.

3.1.1 Helicity Transport Equations

The equation governing the evolution of a local helicity has been called the helicity transport equation. To obtain helicity transport equations, first basic equations (Maxwell's equations, equation of motion) will be arranged in forms that (a) reference the evolution to a particular species by using the total derivative, $D_\alpha/Dt = \partial/\partial t + \mathbf{u}_\alpha \cdot \nabla$ (following [61]); and (b) replace the electric field in favor of the Lorentz force on a particle of species α:

$$\mathbf{F}_\alpha = n_\alpha q_\alpha (\mathbf{E} + \mathbf{u}_\alpha \times \mathbf{B}/c), \tag{3.4}$$

where $\mathbf{E}$ and $\mathbf{B}$ are the electric and magnetic fields, and c is the speed of light in vacuum. The evolution of fluid and field quantities are expressed as companion pairs of equations: the first in each pair expresses the evolution of a vector quantity; and its companion expresses the evolution of the curl of that vector.

Consider first the evolution of $\mathbf{A}$. For this use the expression of electric field in terms of potentials $\mathbf{A}$ and ϕ as

$$\mathbf{E} = -\nabla\phi - (1/c)\partial\mathbf{A}/\partial t. \tag{3.5}$$

Putting the above expression in equation (3.4), get

$$\partial\mathbf{A}/\partial t = -\frac{c\mathbf{F}}{q_\alpha n_\alpha} + \mathbf{u}_\alpha \times \mathbf{B} - c\nabla\phi. \tag{3.6}$$

Adding $\mathbf{u}_\alpha \cdot \mathbf{A}$ on both side of the above equation, we get the total derivative of $\mathbf{A}$ as

$$\frac{D_\alpha \mathbf{A}}{Dt} = -\frac{c\mathbf{F}}{q_\alpha n_\alpha} + \mathbf{u}_\alpha \times \mathbf{B} - c\nabla\phi + \mathbf{u}_\alpha \cdot \nabla\mathbf{A}. \tag{3.7}$$

The companion field equation arises from Faraday's Law

$$\frac{\partial \mathbf{B}}{\partial t} = -c(\nabla \times \mathbf{E}). \tag{3.8}$$

Replace $\mathbf{E}$ in favor of the Lorentz force using equation (3.4), get

$$\frac{\partial \mathbf{B}}{\partial t} = -\frac{c}{q_\alpha}\nabla \times (\frac{\mathbf{F}_\alpha}{n_\alpha}) + \mathbf{u}_\alpha(\nabla \cdot \mathbf{B}) - \mathbf{B}(\nabla \cdot \mathbf{u}_\alpha) + (\mathbf{B} \cdot \nabla)\mathbf{u}_\alpha - (\mathbf{u}_\alpha \cdot \nabla)\mathbf{B}. \tag{3.9}$$

Adding $\mathbf{u}_\alpha \cdot \nabla \mathbf{B}$ and $\mathbf{B}$ times a form of continuity equation $\left(n_\alpha \frac{D_\alpha}{Dt}(1/n_\alpha) = \nabla \cdot \mathbf{u}_\alpha\right)$ and simplify with the identity $\nabla \times (\mathbf{u}_\alpha \times \mathbf{B}) = \mathbf{u}_\alpha \nabla \cdot \mathbf{B} - \mathbf{B}\nabla \cdot \mathbf{u}_\alpha + \mathbf{B} \cdot \nabla \mathbf{u}_\alpha - \mathbf{u}_\alpha \cdot \nabla \mathbf{B}$ and $\nabla \cdot \mathbf{B} = 0$. Then

$$n_\alpha \frac{D_\alpha}{Dt}(\frac{\mathbf{B}}{n_\alpha}) = -\frac{c}{q_\alpha}\nabla \times (\frac{\mathbf{F}_\alpha}{n_\alpha}) + (\mathbf{B} \cdot \nabla)\mathbf{u}_\alpha. \tag{3.10}$$

Consider next the pair of equations for the fluid motion. Using the barotropic function, $h_\alpha \equiv \int dp_\alpha / m_\alpha n_\alpha$, the equation of motion for species α is

$$m_\alpha \frac{D_\alpha \mathbf{u}_\alpha}{Dt} = -\nabla h_\alpha + \frac{\mathbf{F}_\alpha}{n_\alpha} + \frac{\mathbf{R}_\alpha}{n_\alpha}, \tag{3.11}$$

where $\mathbf{R}_\alpha$ is frictional force density. An equation for the fluid vorticity, $\boldsymbol{\omega}_\alpha = \nabla \times \mathbf{u}_\alpha$, follows by taking curl of (3.11), adding $\boldsymbol{\omega}_\alpha$ times the continuity equation, and using vector identities $\mathbf{u}_\alpha \cdot \nabla \mathbf{u}_\alpha = \nabla - \mathbf{u}_\alpha \times (\nabla \times \mathbf{u}_\alpha)$ and $\nabla \times (\mathbf{u}_\alpha \times \boldsymbol{\omega}_\alpha) = \mathbf{u}_\alpha \nabla \cdot \boldsymbol{\omega}_\alpha - \boldsymbol{\omega}_\alpha \nabla \cdot \mathbf{u}_\alpha + \boldsymbol{\omega}_\alpha \cdot \nabla \mathbf{u}_\alpha - \mathbf{u}_\alpha \cdot \nabla \boldsymbol{\omega}_\alpha$ and taking $\nabla \cdot \boldsymbol{\omega}_\alpha = 0$. Then

$$m_\alpha n_\alpha \frac{D_\alpha}{Dt}(\frac{\boldsymbol{\omega}_\alpha}{n_\alpha}) = \nabla \times \frac{\mathbf{F}_\alpha}{n_\alpha} + \nabla \times \frac{\mathbf{R}_\alpha}{n_\alpha} + m_\alpha \boldsymbol{\omega}_\alpha \cdot \nabla \mathbf{u}_\alpha. \tag{3.12}$$

Finally, consider a pair of equations that combine a fluid species and the fields to form the canonical momentum $\mathbf{P}_\alpha$, and its companion the generalized vorticity, $\boldsymbol{\Omega}_\alpha$. The evolution of $\mathbf{P}_\alpha$ follows from combining $q_\alpha/c \cdot$ [Eq. (3.7)]+[Eq. (3.11)]:

$$\frac{D_\alpha \mathbf{P}_\alpha}{Dt} = \frac{q_\alpha}{c}(\mathbf{u}_\alpha \times \mathbf{B} + \mathbf{u}_\alpha . \nabla \mathbf{A}) - \nabla + \frac{\mathbf{R}_\alpha}{n_\alpha}. \tag{3.13}$$

Its companion follows from combining $q_\alpha/c \cdot$ [Eq. (3.10)]+[Eq. (3.12)]:

$$n_\alpha \frac{D_\alpha}{Dt}(\frac{\boldsymbol{\Omega}_\alpha}{n_\alpha}) = \boldsymbol{\Omega}_\alpha \cdot \nabla \mathbf{u}_\alpha + \nabla \times (\frac{\mathbf{R}_\alpha}{n_\alpha}). \tag{3.14}$$

We have now three pairs of equations governing evolution of the quantities $\mathbf{A}$, u_α, and $\mathbf{P}_\alpha$ and their "specific" curl forms $\mathrm{B}/n_\alpha, \omega_\alpha/n_\alpha$, and $\mathbf{\Omega}_\alpha/n_\alpha$ (specific means per particle). In each case the evolution is referenced to a species using the total derivative. In two pairs the electromechanical coupling (Lorentz force, $\mathbf{F}_\alpha$) appear explicitly. Significantly, in the third pair $\mathbf{F}_\alpha$ is absent, suggesting that $\mathbf{P}_\alpha$ and $\mathbf{\Omega}_\alpha/n_\alpha$ express the natural-field coupling.

The next step is to find the helicity transport equations for the quadratic elements by combining the above derived equations. The specific form of these helicities are $\mathrm{u}_\alpha \cdot \mathbf{\Omega}_\alpha/n_\alpha$ (kinetic helicity); $\mathbf{A} \cdot \mathrm{B}/n_\alpha$ (magnetic helicity); $\mathrm{u}_\alpha \cdot \mathrm{B}_\alpha/n_\alpha$ (cross helicity); and $\mathbf{P}_\alpha \cdot \mathbf{\Omega}_\alpha/n_\alpha$ (self-helicity). The transport equations have already been derived for the kinetic [9], magnetic [9, 62, 63, 64] and cross helicities [9].

The kinetic helicity transport equation arises as follows: construct $\omega_\alpha \cdot$ [Eq.(3.11)] + $\mathrm{u}_\alpha \cdot$ [Eq.(3.12)]; simplify with the identity $\mathrm{u}_\alpha \cdot (\omega_\alpha \cdot \nabla \mathrm{u}_\alpha) = \omega_\alpha \cdot \nabla u^2/2$; and integrate $\nabla \times \mathbf{F}_\alpha$, $\nabla \times (\mathrm{R}_\alpha/n_\alpha)$ and $\omega_\alpha \cdot \nabla$ terms by parts. We get

$$\begin{aligned} m_\alpha n_\alpha \frac{D_\alpha}{Dt}\left(\frac{\mathrm{u}_\alpha \cdot \omega_\alpha}{n_\alpha}\right) &= \nabla \cdot \left[\left(m_\alpha \frac{u_\alpha^2}{2} - h_\alpha\right)\omega_\alpha + \mathrm{u}_\alpha \times \mathbf{F}_\alpha + \mathrm{u}_\alpha \times \frac{\mathrm{R}_\alpha}{n_\alpha}\right] \\ &\quad + 2\mathrm{u}_\alpha \cdot \nabla \times \mathbf{F}_\alpha + 2\mathrm{u}_\alpha \cdot \nabla \times \frac{\mathrm{R}_\alpha}{n_\alpha}. \end{aligned} \tag{3.15}$$

The magnetic helicity transport equation is found as follows: construct $\mathrm{B} \cdot$ [Eq.(3.7)] + $\mathbf{A} \cdot$ [Eq.(3.10)]; simplify with the identity $\mathbf{A} \cdot (\mathrm{B} \cdot \nabla \mathrm{u}_\alpha) = \mathrm{B} \cdot \nabla(\mathrm{u}_\alpha \cdot \mathbf{A}) - \mathrm{B} \cdot (\mathrm{u}_\alpha \cdot \nabla \mathbf{A})$; integrate by parts the $\nabla \times \mathbf{F}_\alpha$ and $\mathrm{B} \cdot \nabla$ terms, recognizing that $\nabla \cdot \mathrm{B} = 0$. Then

$$n_\alpha \frac{D_\alpha}{Dt}\left(\frac{\mathbf{A} \cdot \mathrm{B}}{n_\alpha}\right) = \nabla \cdot \left[(\mathrm{u}_\alpha \cdot \mathbf{A} - c\phi)\,\mathrm{B} + \frac{c}{q_\alpha}\mathbf{A} \times \mathbf{F}_\alpha\right] - 2\frac{c}{q_\alpha}\mathrm{B} \cdot \frac{\mathbf{F}_\alpha}{n_\alpha}. \tag{3.16}$$

The cross helicity transport equation is found as follows: construct $m_\alpha \mathrm{u}_\alpha \cdot$ [Eq.(3.10)] + $\mathrm{B} \cdot$ [Eq.(3.11)]; and integrate by parts the $\nabla \times \mathbf{F}_\alpha$ and $\mathrm{B} \cdot \nabla$ terms. Then

$$\begin{aligned} m_\alpha n_\alpha \frac{D_\alpha}{Dt}\left(\frac{\mathrm{u}_\alpha \cdot \mathrm{B}}{n_\alpha}\right) &= \nabla \cdot \left[(m_\alpha \frac{u_\alpha^2}{2} - h_\alpha)\mathrm{B} + m_\alpha \frac{c}{q_\alpha}\mathrm{u}_\alpha \times \frac{\mathbf{F}_\alpha}{n_\alpha}\right] \\ &\quad + \frac{c}{q_\alpha}\frac{\mathbf{F}_\alpha}{n_\alpha} \cdot \left[\nabla \times \left(\frac{q_\alpha}{c}\mathbf{A} - m_\alpha \mathrm{u}_\alpha\right)\right] + \mathrm{B} \cdot \frac{\mathrm{R}_\alpha}{n_\alpha}. \end{aligned} \tag{3.17}$$

The transport equations for the self-helicities are found as follows: construct $\Omega_\alpha \cdot$[Eq.(3.13)]+ $\mathrm{P}_\alpha \cdot$[Eq.(3.14)]; simplify with the identity $\mathrm{P}_\alpha \cdot (\Omega_\alpha \cdot \nabla \mathrm{u}_\alpha) = \Omega_\alpha \cdot \nabla(\mathrm{P}_\alpha \cdot \mathrm{u}_\alpha) - \Omega_\alpha \cdot (\mathrm{u}_\alpha \cdot \nabla \mathrm{P}_\alpha)$; substitute $\mathrm{P}_\alpha = m_\alpha \mathrm{u}_\alpha + q_\alpha \mathrm{A}_\alpha / c$; expand $\mathrm{u}_\alpha \cdot \nabla \mathrm{u}_\alpha = \nabla u_\alpha^2/2 - \mathrm{u}_\alpha \times \nabla \mathrm{u}_\alpha$; and integrate by parts $\Omega_\alpha \cdot \nabla$ and $(\nabla \times \mathrm{P}_\alpha) \cdot \mathrm{R}_\alpha$ terms. Then

$$n_\alpha \frac{D_\alpha}{Dt}\left(\frac{\mathrm{P}_\alpha \cdot \Omega_\alpha}{n_\alpha}\right) = \nabla \cdot \left[\left(\mathrm{u}_\alpha \cdot \mathrm{P}_\alpha - \frac{1}{2} m_\alpha u_\alpha^2 - m_\alpha h_\alpha - q_\alpha \phi\right) \Omega_\alpha - \mathrm{P}_\alpha \times \frac{\mathrm{R}_\alpha}{n_\alpha}\right] + 2\Omega_\alpha \cdot \frac{\mathrm{R}_\alpha}{n_\alpha}. \tag{3.18}$$

Physically, the self-helicities represent a measure of the self-linkage, or knottedness, of the generalized vorticity [32]. The helicity transport equations derived in above equations (3.15 - 3.18) reference the evolution of a particular species using the total derivative. Each right hand side of transport equations is the sum of a divergence term, and force terms for the friction $\mathrm{R}_\alpha / n_\alpha$ and the electromechanical coupling F_α. In the event that the divergence operates on a scalar times a vector, then the vector define integral curves or "lines of force" associated with the helicity.

3.2 Local and Global Invariance of Helicities

3.2.1 Local invariance

Local invariance follows from transport equations. It is related to the families of integral curves defined by divergence terms in the helicity transport equations. For the ideal case, i.e., setting the frictional term to zero; if the coupling term vanishes, then the helicity is invariant on the characteristic lines that are tangential to the vector in the divergence term. This shows that the helicity is locally invariant. It remains constant on each characteristic line that doesn't intercept the system boundary. These characteristic lines convect with a particular species. Consider MHD, which is the reduced case of single fluid ($\alpha = i$). Here the simplified form of Ohm's law is $\mathrm{F} = 0$. Then in each of the transport equations for the three simple helicities given in equations (3.15) - (3.17), the right side become divergences of a scalar times the vector which defines the lines of force. But on the other hand, self-helicities described in equation

(3.18) are invariant without reducing assumptions. This is because electromagnetic coupling is absent from their transport equations. Their characteristic lines convect with the particular specie.

3.2.2 Global invariance

Global invariance concerns the global forms of a helicity. The global invariance relies on the vanishing normal component of generalized vorticity at the boundary i.e., $(\Omega_\alpha)_n = \Omega_\alpha \cdot \hat{\mathbf{n}} = 0$. If initially $(\Omega_\alpha)_n = 0$ everywhere on the boundary, and there is no flow through the boundary, $\mathbf{u}_\alpha \cdot \hat{\mathbf{n}} = 0$, then $(\Omega_\alpha)_n = 0$ will always remain zero in the ideal (frictionless) case. To prove the global invariance of self-helicities, we make use of transport equation (3.12) with $\mathbf{R} = 0$, then

$$n_\alpha \frac{D_\alpha}{Dt}\left(\frac{\mathbf{P}_\alpha \cdot \Omega_\alpha}{n_\alpha}\right) = \nabla \cdot [(\mathbf{u}_\alpha \cdot \mathbf{P}_\alpha - \frac{m_\alpha u_\alpha^2}{2} - q_\alpha \phi - h_\alpha)\Omega_\alpha]. \tag{3.19}$$

Integrating over volume of entire system and using $D_\alpha(n_\alpha dv)/Dt = 0$, we get

$$\int \frac{\partial}{\partial t}(\mathbf{P}_\alpha \cdot \Omega_\alpha) + \mathbf{u}_\alpha \cdot \nabla(\mathbf{P}_\alpha \cdot \Omega_\alpha) dv = \int \nabla \cdot (\mathrm{u}_\alpha \cdot \mathbf{P}_\alpha - \frac{m_\alpha u_\alpha^2}{2} - q_\alpha \phi - h_\alpha)\Omega_\alpha dv. \tag{3.20}$$

Applying identity $\nabla \cdot (f\mathbf{u}_\alpha) = f\nabla \cdot \mathrm{u}_\alpha + \mathrm{u}_\alpha \cdot \nabla f$ and the Gauss's theorem, the above equation reads as

$$\int \frac{\partial}{\partial t}(\mathbf{P}_\alpha \cdot \Omega_\alpha) dv + \int (\mathbf{P}_\alpha \cdot \Omega_\alpha)\mathrm{u}_\alpha \cdot \mathbf{n} ds = \int (\mathrm{u}_\alpha \cdot \mathbf{P}_\alpha - \frac{m_\alpha u_\alpha^2}{2} - q_\alpha \phi - h_\alpha)\Omega_\alpha \cdot \mathrm{n} ds. \tag{3.21}$$

Applying boundary conditions, we get

$$\int \frac{\partial}{\partial t}(\mathbf{P}_\alpha \cdot \Omega_\alpha) dv = 0. \tag{3.22}$$

$$\int \mathbf{P}_\alpha \cdot \Omega_\alpha dv = \text{constt.} \tag{3.23}$$

This shows that self-helicity is globally invariant.

Having established the local and global invariance of self-helicities, relaxed states can be found by energy minimization principle. Next section will address this problem.

3.3 Relaxed State

Energy minimization is an approach to find the relaxed states. This minimizes the organized energy form i.e., magnetofluid energy W_{mf} rather than the total energy (which is conserved in a closed system). The minimum energy state is found by solving the constrained variational principle [6, 10, 32, 65]

$$\delta W_{mf} - \lambda_i \delta H_i - \lambda_e \delta H_e = 0, \tag{3.24}$$

where λ_i and λ_e are Lagrange multipliers associated with ion and electron self-helicities respectively. Above equation can be written as

$$\delta W_{mf} - \sum \lambda_\alpha \delta H_\alpha = 0. \tag{3.25}$$

First consider magnetofluid energy term

$$\delta W_{mf} = \int_v dv (\sum \frac{1}{2} m_\alpha n_\alpha \mathrm{u}_\alpha \cdot \delta \mathrm{u}_\alpha + \frac{\mathbf{B} \cdot \delta \mathbf{B}}{4\pi}). \tag{3.26}$$

Using identity, replacing $\mathbf{A}$ in favor of P_α and eliminating surface integrals due to boundary conditions, expression for variation in magnetofluid energy becomes

$$\delta W_{mf} = \int_v dv \sum \frac{\mathrm{j}_\alpha}{q_\alpha} \cdot \delta \mathrm{P}_\alpha. \tag{3.27}$$

Now consider

$$\lambda_\alpha \delta H_\alpha = (\frac{c^2}{8\pi q_\alpha^2}) \lambda_\alpha \int_v dv (\delta \mathrm{P}_\alpha \cdot \Omega_\alpha + \mathrm{P}_\alpha \cdot \delta \Omega_\alpha). \tag{3.28}$$

Using identity $\nabla \cdot (\mathrm{P}_\alpha \times \delta \mathrm{P}_\alpha) = \delta \mathrm{P}_\alpha \cdot (\nabla \times \mathrm{P}_\alpha) - \mathrm{P}_\alpha \cdot (\nabla \times \mathrm{P}_\alpha)$ and neglecting surface integrals, then

$$\lambda_\alpha \delta H_\alpha = \frac{c^2}{4\pi q_\alpha^2} \int_v \sum \lambda_\alpha (\delta \mathrm{P}_\alpha \cdot \Omega_\alpha) dv. \tag{3.29}$$

$$\delta W_{mf} - \sum \lambda_\alpha \delta H_\alpha = \int_v dv \sum \left(\frac{\mathrm{j}_\alpha}{q_\alpha} - \frac{c^2}{4\pi q_\alpha^2} \lambda_\alpha \Omega_\alpha \right) \cdot \delta \mathbf{P}_\alpha. \tag{3.30}$$

For any arbitrary value of $\delta \mathbf{P}_\alpha$, $\delta W_{mf} - \sum \lambda_\alpha \delta H_\alpha = 0$ when

$$\lambda_\alpha \Omega_\alpha = \frac{4\pi q_\alpha}{c^2} \mathbf{j}_\alpha. \tag{3.31}$$

It represents the relaxed state of α-species for the case of two fluid plasma when the self-helicity is considered to be an invariant of the system. Let us view some of its limiting conditions. Putting value of $\mathbf{\Omega}_\alpha$ in equation (3.31), we get

$$\lambda_\alpha (m_\alpha \nabla \times \mathbf{u}_\alpha + \frac{q_\alpha}{c} \nabla \times \mathbf{A}) = \frac{2\pi q_\alpha}{c^2} \mathbf{j}_\alpha. \tag{3.32}$$

We now discuss two specific cases:

(1) For massless electron ($\alpha = e$, $m_e = 0$), we get

$$\begin{aligned} \lambda_e \mathbf{B} &= \frac{4\pi}{c} \mathbf{j}_e, \\ \mathbf{j}_c &\propto \lambda_e \mathbf{B}. \end{aligned} \tag{3.33}$$

Thus in the absence of ion currents ($\mathbf{j} = \mathbf{j}_e$), the equilibrium is force-free as in MHD theory.

(2) For ions ($\alpha = i$), from equation (3.31), we have

$$\mathbf{u}_i \times \mathbf{\Omega}_i = 0, \tag{3.34}$$

and from the sum of species equation of motion for negligible mass of electrons, we get

$$\frac{\nabla p}{n} + m_i \nabla u_i^2/2 = \mathbf{u}_i \times \mathbf{\Omega}_i. \tag{3.35}$$

Using equations (3.34) and (3.35), we get the Bernoulli equation

$$\nabla p = -m_i n \nabla u_i^2/2, \tag{3.36}$$

where p is the sum of the electron and ion pressure. The above equation shows that finite pressure relaxed state can exist, but only with velocity shear (or more generally with $\nabla u_i^2 \neq 0$). Recently Mahajan and Yoshida [37] have also presented a very simple and novel model for

the relaxation of two species ideal magnetofluid. In their model, the relaxed state exhibits a significant pressure and sheared flow. The equilibrium solution is characterized by the double curl Beltrami functions. The solution is nothing but a linear sum of two single Beltrami functions. The Beltrami condition demanding alignment of vorticities and flows becomes a system of simultaneous equations in the magnetic field and the flow velocity for the case of two fluid plasma. Combining these equations yields the double curl Beltrami equation. In the following section, we will address this model.

3.4 Mahajan-Yoshida Model

The two-fluid model for the macroscopic dynamics of a plasma differentiates between the electron and ion velocities. Denoting the electron (ion) flow velocity by $\mathbf{V}_e$ ($\mathbf{V}_i$), the macroscopic evaluation equations become

$$\frac{\partial}{\partial t}\mathbf{V}_e + (\mathbf{V}_e \cdot \nabla)\mathbf{V}_e = \frac{-e}{m}(\mathbf{E} + \mathbf{V}_e \times \mathbf{B}) - \frac{1}{mn}\nabla p_e, \tag{3.37}$$

$$\frac{\partial}{\partial t}\mathbf{V}_i + (\mathbf{V}_i \cdot \nabla)\mathbf{V}_i = \frac{e}{M}(\mathbf{E} + \mathbf{V}_i \times \mathbf{B}) - \frac{1}{Mn}\nabla p_i, \tag{3.38}$$

where $\mathbf{E}$ is the electric field, p_e and p_i are the electron and the ion pressures respectively, e is the elementary charge, n is the number density of both electrons and ions (considering a quasineutral plasma with singly charged ions), m and M are the electron and ion mass respectively. In the electron equation, the inertial terms (left-hand side of (3.37)) can be neglected because of their small mass ($m \ll M$). Therefore, (3.37) reduces to

$$\mathbf{E} + \mathbf{V}_e \times \mathbf{B} + \frac{1}{en}\nabla p_e = 0. \tag{3.39}$$

When electron mass is neglected, $\mathbf{V}_i = \mathbf{V}$, the fluid velocity. We introduce the following set of dimensionless variables,

$$\begin{cases} \mathbf{x} = \lambda_i \hat{\mathbf{x}}, \quad \mathbf{B} = B_0 \hat{\mathbf{B}}, \\ t = (\lambda_i / V_A)\hat{t}, \quad p = (B_0^2/\mu_0)\hat{p}, \quad \mathbf{V} = V_A \hat{\mathbf{V}}, \\ \mathbf{A} = (\lambda_i B_0)\hat{\mathbf{A}}, \quad \phi = (V_A \lambda_i B_0)\hat{\phi}, \end{cases} \tag{3.40}$$

where the ion skin-depth

$$\lambda_i = \frac{c}{\omega_{pi}} = \frac{V_A}{\omega_{ci}} = \sqrt{\frac{M}{\mu_0 n e^2}} \tag{3.41}$$

is a characteristic length scale of the system, and the Alfvén speed is given by $V_A = B_0/\sqrt{\mu_0 M n}$ (where n is assumed to be constant) with B_0 as an appropriate measure of the magnetic field. Writing $\hat{\mathbf{E}} = -\partial\hat{\mathbf{A}}/\partial\hat{t} - \hat{\nabla}\hat{\phi}$, the dimensionless electrons and ions equation of motion reads

$$\frac{\partial\hat{\mathbf{A}}}{\partial\hat{t}} = (\hat{\mathbf{V}} - \hat{\nabla}\times\hat{\mathbf{B}})\times\hat{\mathbf{B}} - \hat{\nabla}(-\hat{\phi} + \hat{p_e}), \tag{3.42}$$

$$\frac{\partial}{\partial\hat{t}}(\hat{\mathbf{V}} + \hat{\mathbf{A}}) = \hat{\mathbf{V}}\times(\hat{\mathbf{B}} + \hat{\nabla}\times\hat{\mathbf{V}}) - \hat{\nabla}(\hat{V^2}/2 + \hat{p_i} + \hat{\phi}). \tag{3.43}$$

In what follows, hat will be dropped for simpler notation. Taking the curl of above equations, it can be cast in a revealing symmetric form

$$\frac{\partial\omega_j}{\partial t} - \nabla\times(\mathbf{U}_j\times\omega_j) = 0 \qquad (j = 1,2) \tag{3.44}$$

in terms of a pair of generalized vorticities

$$\begin{aligned} \omega_1 &= \mathbf{B}, \quad \omega_2 = \mathbf{B} + \nabla\times\mathbf{V}, \\ \mathbf{U}_1 &= \mathbf{V} - \nabla\times\mathbf{B}, \quad \mathbf{U}_2 = \mathbf{V}. \end{aligned}$$

The simplest equilibrium solution to (3.44) is given by the "Beltrami conditions"

$$\mathbf{U}_j = \mu_j\omega_j \qquad (j = 1,2), \tag{3.45}$$

which implies the alignment of vorticities and the corresponding flows. Writing $a = 1/\mu_1$ and $b = 1/\mu_2$, and assuming that a and b are constants, the Beltrami conditions (3.45) read as a system of simultaneous linear equations in $\mathbf{B}$ and $\mathbf{V}$

$$\mathbf{B} = a(\mathbf{V} - \nabla\times\mathbf{B}), \tag{3.46}$$

$$\mathbf{B} + \nabla\times\mathbf{V} = b\mathbf{V}. \tag{3.47}$$

These equations have a simple and significant connotation; the electron flow $(\mathbf{V} - \nabla \times \mathbf{B})$ parallels the magnetic field $\mathbf{B}$, while the ion flow $\mathbf{V}$ follows the "generalized magnetic field" $(\mathbf{B} + \nabla \times \mathbf{V})$. This generalized magnetic field contains the Coriolis' force induced by the ion inertia effect on a circulating flow.

Combining (3.46) and (3.47), following second order partial differential equation is obtained as

$$\nabla \times (\nabla \times \mathbf{B}) - \alpha_1 \nabla \times \mathbf{B} + \alpha_2 \mathbf{B} = 0, \tag{3.48}$$

where

$$\alpha_1 = b - 1/a, \quad \alpha_2 = 1 - b/a.$$

The double curl Beltrami equation (3.48) encompasses a wide class of steady-state equation of mathematical physics. Writing $\alpha_1 = \lambda_+ + \lambda_-$, and $\alpha_2 = \lambda_+ \lambda_-$, we can express the above as

$$(\nabla \times -\lambda_+)\nabla \times \mathbf{B} - \lambda_-(\nabla \times -\lambda_+)\mathbf{B} = 0,$$

$$(\nabla \times -\lambda_+)(\nabla \times \mathbf{B} - \lambda_- \mathbf{B}) = 0,$$

$$(\nabla \times -\lambda_+)(\nabla \times -\lambda_-)\mathbf{B} = 0,$$

or

$$(\mathrm{curl} - \lambda_+)(\mathrm{curl} - \lambda_-)\mathbf{B} = 0, \tag{3.49}$$

where

$$\lambda_\pm = \frac{1}{2}\left[\alpha_1 \pm (\alpha_1^2 - 4\alpha_2)^{1/2}\right]. \tag{3.50}$$

Since the operators (curl - $\lambda_\pm$) commute, the general solution to the "double-curl Beltrami equation" (3.48) is given by a linear combination of the two Beltrami fields. Let $\mathbf{G}_\pm$ be the Beltrami field such that

$$\begin{cases} (\mathrm{curl} - \lambda_\pm)\mathbf{G}_\pm = 0, & \\ \mathbf{n} \cdot \mathbf{G}_\pm = 0 & \text{(on the surface).} \end{cases} \tag{3.51}$$

Then, the general solution is

$$\mathbf{B} = c_+\mathbf{G}_+ + c_-\mathbf{G}_-, \tag{3.52}$$

where c_+, c_- are arbitrary constants. The corresponding ion flow as in (3.46) is given by

$$\mathbf{V} = \left(\frac{1}{a} + \lambda_+\right) c_+\mathbf{G}_+ + \left(\frac{1}{a} + \lambda_-\right) c_-\mathbf{G}_-. \tag{3.53}$$

In the next subsection, we will discuss some general features of the double curl Beltrami system.

3.4.1 General Properties of Double Curl Beltrami Field

Now we discuss the constraints on the eigenvalues $\lambda_\pm$ characterizing the field and consider the following cases:

- When $|\alpha_1|^2 \gg 4\alpha_2$, then the eigenvalues of the curl operator would have real values and we have

  $$\lambda_\pm = \frac{1}{2}\left[\alpha_1 \pm \alpha_1\right],$$

  Let us consider the following two cases:

  (i) When $b > 1/a$, then

  $$\lambda_+ \simeq \; b - (1/a) \qquad \text{and}$$
  $$\lambda_- \simeq \; a - b/(ab-1).$$

  (ii) When $1/a > b$, then

  $$\lambda_+ \simeq \; a - b/(ab-1) \quad \text{and}$$
  $$\lambda_- \simeq \; b - (1/a).$$

  For the above cases $\lambda_\pm$ are always real as shown by colored regions in figure (3-1). In the first case, we are concerned with points in the red colored region; in the second the green colored region.

- When $|b + 1/a| << 2$, complex eigenvalues are obtained and this corresponds to clear region of the figure (3-1).

- When $|b + 1/a| \simeq \pm 2$, then degenerate eigenvalues ($\lambda_+ = \lambda_-$) are obtained and

$$\lambda_\pm = \frac{1}{2}(b - \frac{1}{a}).$$

The blue colored line that separate the colored regions from clear one represent the degenerate values of $\lambda_\pm$.

- The conventional single Beltrami field, which describes paramagnetic fields, can be also achieved as a special case when $\alpha_1 = 0$ and $\alpha_2 < 0$. For this case λ_+ and λ_- have same value but opposite sign and are real. The value of b/a must be greater than unity and $b = 1/a$. These values are shown by a line inside the colored regions (real values).

- On the other hand, when $\alpha_1 = 0$, $\alpha_2 > 0$ or equivalently when $b = 1/a$ and $b/a < 1$, then $\lambda_+ = -\lambda_-$ and both of the scale parameters $\lambda_\pm$ are pure imaginary. Under these conditions, (3.48) resembles London's equation of superconductivity with its well known fully diamagnetic solutions. In this version of the London's equation, the characteristic shielding length for the magnetic field is the ion skin depth c/ω_{pi}, instead of the usual electron skin depth c/ω_{pe}, because it is the ion dynamics that brings about the coupling of the magnetic field with the collective motion of the medium. The values of $\lambda_\pm$ become purely imaginary on the portions of the trajectory, lying in the complex domain.

- The eigenvalues λ_+ and λ_- vanish when $a = b = \pm 1$. If $a = 1$ and $b = -1$ or vice versa, eigenvalues become complex.

- When $a = b$, $\alpha_2 = 0$, so that one of the scale parameters $\lambda_\pm$ is zero and the other equates to α_1 as shown by a straight diagonal line in the figure.

The double curl Beltrami solution leads to magnetic field and flow velocity structures far richer as compared to constant-λ Beltrami-Taylor system. In the next section, we will describe the characteristic of this formulation to confine a finite-pressure plasma.

3.4.2 Bernoulli Conditions

To show that the relaxed states obtained by this formalism permit magnetic confinement of a finite-pressure magnetofluid, we proceed as follows:

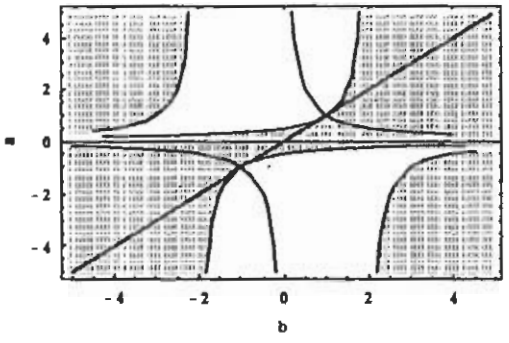

Figure 3-1: Character of eigenvalues, λ_+ and λ_- as a function of the Beltrami parameters, a and b.

Substituting Beltrami conditions as given in equations (3.46) - (3.47) in the steady state conditions of equations (3.42) - (3.43); we get a set of generalized "Bernoulli conditions"

$$V^2/2 + p_i + \phi = \text{constt.}, \tag{3.54}$$

$$p_e - \phi = \text{constt.} \tag{3.55}$$

This suggests a mechanism for creating pressure gradients in the relaxed state. We note that the constancy of the energy density (the sum of the potential and the kinetic energy) implied in equations (3.54) - (3.55) refers to the directions perpendicular, as well as parallel, to the streamlines of $\mathbf{V}$ and $\mathbf{V}_e$. This is an essential difference from the conventional Bernoulli condition.

It might appear that the Beltrami-Bernoulli states are very special and may be generally inaccessible. These conditions, however, follow from the concept of relaxed states. Indeed, the Bernoulli conditions describe homogeneous distributions of the energy density. The pressure gradients in the relaxed state equilibria maintained by the Bernoulli effect have been shown by Turner [32] and Steinhauer and Ishida [35, 36]. Existence of finite pressure in the relaxed state has been already studied by Sudan [31], Hameiri and Hammer [66] and Finn and Antonsen [67].

Adding (3.54) and (3.55) yields

$$\frac{1}{2}\beta + \frac{1}{2}V^2 = \text{constt.} \tag{3.56}$$

where β is the standard beta ratio. Equation (3.56) reveals that an appropriate ion sheared velocity field can sustain a desired pressure gradient. When the magnetic field and the flow have comparable magnitudes (in the Alfvén normalized units), the equilibrium can have a large beta value. Equations (3.48) and (3.56) can serve as a basis for designing a highly effective plasma confinement machine.

The set of equations (3.46) - (3.47) can also be obtained by using the variational principle. The double curl Beltrami system is characterized by two bilinear constants of motion, the usual total magnetic helicity $H_1 = -\frac{1}{2}\int \mathrm{A}\cdot\mathrm{B}dv$, and the generalized helicity $H_2 = \frac{1}{2}\int(\mathrm{A}+\mathrm{V})\cdot(\mathrm{B}+\nabla\times\mathrm{V})dv$. For these constrained helicities to describe the relaxed state, they must be invariant of the system. In the following section, we shall address this problem.

3.5 Invariance of Helicities of Double Curl Beltrami System

In this section, we will show that helicities H_1 and H_2 are constant of motion and behaves as invariant. First we show the invariance of H_1. To evaluate the time derivative of H_1, we need the expressions for $\partial\mathrm{A}/\partial t$ and $\partial\mathrm{B}/\partial t$. From equation (3.42), we have

$$\frac{\partial \mathrm{A}}{\partial t} = (\mathrm{V} - \nabla\times\mathrm{B})\times\mathrm{B} + \nabla S, \tag{3.57}$$

where $S = \phi - p_e$ is a scalar function. Taking curl of above equation, we get

$$\frac{\partial \mathrm{B}}{\partial t} = \nabla\times[(\mathrm{V} - \nabla\times\mathrm{B})\times\mathrm{B}]. \tag{3.58}$$

The time derivative of the dot product of A and B is given by

$$\frac{d}{dt}(\mathrm{A}\cdot\mathrm{B}) = \frac{\partial \mathrm{A}}{\partial t}\cdot\mathrm{B} + \mathrm{A}\cdot\frac{\partial \mathrm{B}}{\partial t} + (\mathrm{V}\cdot\nabla)(\mathrm{A}\cdot\mathrm{B}).$$

Using the equations (3.57) and (3.58), the above relation becomes

$$\begin{aligned}\frac{d}{dt}(\mathbf{A}\cdot\mathbf{B}) &= \nabla\cdot(S\mathbf{B})+(\mathbf{V}-\nabla\times\mathbf{B})\times\mathbf{B}\cdot\mathbf{B}\\ &\quad+\mathbf{A}\cdot\nabla\times[(\mathbf{V}-\nabla\times\mathbf{B})\times\mathbf{B}]+(\mathbf{V}\cdot\nabla)(\mathbf{A}\cdot\mathbf{B}).\end{aligned}$$

The second term on right-hand side vanishes identically. Simplifying the above equation using the identities

$$\mathbf{A}\cdot\nabla\times(\mathbf{V}\times\mathbf{B})=\mathbf{V}\times\mathbf{B}\cdot\mathbf{B}-\nabla\cdot[\mathbf{A}\times(\mathbf{V}\times\mathbf{B})],$$

$$\mathbf{A}\cdot\nabla\times[(\nabla\times\mathbf{B})\times\mathbf{B}]=(\nabla\times\mathbf{B})\times\mathbf{B}\cdot\nabla\times\mathbf{A}-\nabla\cdot[\mathbf{A}\times((\nabla\times\mathbf{B})\times\mathbf{B})],$$

and recognizing $\nabla\cdot\mathbf{B}=0$, we obtain

$$\begin{aligned}\frac{d}{dt}(\mathbf{A}\cdot\mathbf{B}) &= \nabla\cdot(S\mathbf{B})-\nabla\cdot[(\mathbf{A}\cdot\mathbf{B})\mathbf{V}]+\nabla\cdot[(\mathbf{A}\cdot\mathbf{V})\mathbf{B}]\\ &\quad+\nabla\cdot[(\mathbf{A}\cdot\mathbf{B})(\nabla\times\mathbf{B})]-\nabla\cdot[(\mathbf{A}\cdot\nabla\times\mathbf{B})\mathbf{B}]\\ &\quad+\nabla\cdot[(\mathbf{A}\cdot\mathbf{B})\mathbf{V}].\end{aligned}$$

Taking the volume integral of above equation, we obtain

$$\frac{d}{dt}\int_v \mathbf{A}\cdot\mathbf{B}dv=0. \tag{3.59}$$

In obtaining the above result, we have used the boundary conditions that the normal components of $\mathbf{V}$, $\mathbf{B}$ and $\nabla\times\mathbf{B}$ vanish at the surface. Equation (3.59) shows that helicity $H_1=-\frac{1}{2}\int_v \mathbf{A}\cdot\mathbf{B}dv$ is a constant.

To calculate the time derivative of H_2, let us take $\mathbf{P}=\mathbf{A}+\mathbf{V}$ and $\Omega=\nabla\times(\mathbf{A}+\mathbf{V})$. From equation (3.43), we have

$$\frac{\partial\mathbf{P}}{\partial t}=\mathbf{V}\times(\mathbf{B}+\nabla\times\mathbf{V})-\nabla S', \tag{3.60}$$

where $S'=\mathbf{V}^2+\phi+p_i$ represents a scalar function. Curl of above equation yields

$$\frac{\partial\Omega}{\partial t}=\nabla\times[\mathbf{V}\times(\mathbf{B}+\nabla\times\mathbf{V})]. \tag{3.61}$$

Time derivative of the scalar product of P and Ω reads as

$$\frac{d}{dt}(\mathbf{P}\cdot\Omega) = \frac{\partial \mathbf{P}}{\partial t}\cdot\Omega + \mathbf{P}\cdot\frac{\partial \Omega}{\partial t} + (\mathbf{V}\cdot\nabla)(\mathbf{P}\cdot\Omega)$$

Making use of vector identities and after simplification, we are left with

$$\frac{d}{dt}(\mathbf{P}\cdot\Omega) = -\nabla\cdot(S'\mathbf{B}) - \nabla\cdot(\mathbf{P}\times\mathbf{D}) + \nabla[(\mathbf{P}\cdot\Omega)\mathbf{V}], \tag{3.62}$$

where

$$\begin{aligned}
\mathbf{D} &= \mathbf{V}\times(\mathbf{B}+\nabla\times\mathbf{V}) \qquad \text{and} \\
\mathbf{P}\times\mathbf{D} &= (\mathbf{A}\cdot\mathbf{B})\mathbf{V} - (\mathbf{A}\cdot\mathbf{V})\mathbf{B} + (\mathbf{A}\cdot\nabla\times\mathbf{V})\mathbf{V} \\
&\quad -(\mathbf{A}\cdot\mathbf{V})\nabla\times\mathbf{V} + (\mathbf{V}\cdot\mathbf{B})\mathbf{V} - (\mathbf{V}\cdot\mathbf{V})\mathbf{B}.
\end{aligned}$$

Taking volume integral of equation (3.62), we get

$$\int_v \frac{d}{dt}(\mathbf{P}\cdot\Omega)dv = -\int_v \nabla\cdot(S\mathbf{B})dv - \int_v \nabla\cdot(\mathbf{P}\times\mathbf{D})dv + \int_v \nabla\cdot[(\mathbf{P}\cdot\Omega)\mathbf{V}]\,dv.$$

Using divergence theorem, we get

$$\int_v \frac{d}{dt}(\mathbf{P}\cdot\Omega)dv = -\int_s \mathbf{n}\cdot(S\mathbf{B})ds - \int_s \mathbf{n}\cdot(\mathbf{P}\times\mathbf{D})ds + \int_s \mathbf{n}\cdot\mathbf{V}ds. \tag{3.63}$$

For the boundary conditions that $\mathbf{n}\cdot\mathbf{V} = \mathbf{n}\cdot\mathbf{B} = \mathbf{n}\cdot\nabla\times\mathbf{V} = \mathbf{n}\cdot\nabla\times\mathbf{B} = 0$ on the surface, the right-hand side of equation (3.63) vanishes and we have

$$\int_v \frac{d}{dt}(\mathbf{P}\cdot\Omega)dv = 0.$$

This shows that the generalized helicity $H_2 = \frac{1}{2}\int(\mathbf{A}+\mathbf{V})\cdot(\mathbf{B}+\nabla\times\mathbf{V})dv$ also behaves as an invariant of double curl Beltrami system. Having established the invariance of helicities, in the next section we shall describe the variational principle to get the relaxed states of flows and fields for the system.

3.6 Variational Principle for Double Curl Beltrami System

When dissipation effects are present, such as resistivity and viscosity, the total energy, kinetic plus magnetic, decays more readily than do the constrained helicities. To derive the Euler equation, whose solutions specify the flow velocity and magnetic field configuration of the relaxed minimum energy state of the double curl Beltrami system, we must solve the variational problem

$$\delta(\mu_1 H_1 + \mu_2 H_2 - W) = 0, \tag{3.64}$$

in which μ_1 and μ_2 play the role of Lagrange undetermined multipliers associated with usual magnetic helicity H_1 and the generalized helicity H_2. Let us first consider the variation of magnetofluid energy

$$\begin{aligned} \delta W &= \delta \int \frac{1}{2}(\mathbf{B}^2 + \mathbf{V}^2) dv, \\ &= \int (\mathbf{B} \cdot \delta\mathbf{B} + \mathbf{V} \cdot \delta\mathbf{V}) dv. \end{aligned}$$

Replace $\delta\mathbf{B}$ with $\nabla \times \delta\mathbf{A}$, use the identity $\nabla \cdot (\mathbf{B} \times \delta\mathbf{A}) = \delta\mathbf{A} \cdot (\nabla \times \mathbf{B}) - \mathbf{B} \cdot \nabla \times \delta\mathbf{A}$, and eliminate the surface integral due to boundary condition. Then we get

$$\delta W = \int (\delta\mathbf{A} \cdot \nabla \times \mathbf{B} + \mathbf{V} \cdot \delta\mathbf{V}) dv. \tag{3.65}$$

Next, consider the variation of H_1,

$$\delta H_1 = -\frac{1}{2} \int \delta(\mathbf{A} \cdot \mathbf{B}) dv.$$

Replacing $\delta\mathbf{B}$ with $\nabla \times \delta\mathbf{A}$ and implementing the boundary condition that at the surface $\mathbf{n} \times \delta\mathbf{A} = 0$, get

$$\delta H_1 = -\int \delta\mathbf{A} \cdot \mathbf{B} dv. \tag{3.66}$$

And the variation of H_2 is

$$\delta H_2 = \frac{1}{2} \int \delta[(\mathbf{A} + \mathbf{V}) \cdot (\mathbf{B} + \nabla \times \mathbf{V})]\, dv.$$

Similarly, replacing $\delta\mathbf{B}$ in favor of $\nabla \times \delta\mathbf{A}$, using identities and neglecting the contribution of surface integral due to boundary conditions that at the surface $\mathbf{n} \times \mathbf{A} = 0$ and $\mathbf{n} \cdot \mathbf{V} = 0$, we get

$$\delta H_2 = \int (\delta\mathbf{A} \cdot \mathbf{B} + \delta\mathbf{A} \cdot \nabla \times \mathbf{V} + \delta\mathbf{V} \cdot \mathbf{B} + \delta\mathbf{V} \cdot \nabla \times \mathbf{V}) dv. \tag{3.67}$$

Putting values of (3.65), (3.66) and (3.67) in (3.64) and taking the independent variations of $\delta\mathbf{A}$ and $\delta\mathbf{V}$, we get

$$\mu_2\mathbf{B} + \mu_2\nabla \times \mathbf{V} - \mu_1\mathbf{B} - \nabla \times \mathbf{B} = 0, \tag{3.68}$$

$$\mu_2\mathbf{B} + \mu_2\nabla \times \mathbf{V} - \mathbf{V} = 0. \tag{3.69}$$

Using equation (3.69) in (3.68), we get

$$\mathbf{V} - \mu_1\mathbf{B} - \nabla \times \mathbf{B} = 0.$$

Taking $1/\mu_1 = a$ and $1/\mu_2 = b$, the above equations become

$$\mathbf{B} = a(\mathbf{V} - \nabla \times \mathbf{B}), \tag{3.70}$$

$$\mathbf{B} + \nabla \times \mathbf{V} = b\mathbf{V}. \tag{3.71}$$

Combining above equations yield the double curl Beltrami equation (3.48) - the relaxed state of multifluid plasma.

The detailed description of two different relaxation models as given in previous sections show that both the models reveal the relaxed state with a strong flow and finite pressure. In one model, presented by Steinhauer and Ishida, self helicity conservation of each species leads to the relaxed state. In the other, presented by Mahajan and Yoshida, relaxed state is characterized by double curl Beltrami fields. Comparison of these two relaxed states is given in the next section.

3.7 Double Curl Beltrami and Self-helicities

The relaxed state for two fluid plasma using the concept of self helicity derived in the Steinhauer-Ishida model as given in equation (3.32) can be written as

$$\lambda_\alpha(m_\alpha \nabla \times \mathbf{u}_\alpha + \frac{q_e}{c}\nabla \times \mathbf{A}) = \frac{4\pi q_\alpha}{c^2}\mathbf{j}_\alpha. \tag{3.72}$$

Multiplying above equation by $n_\alpha q_\alpha$, we get

$$\lambda_\alpha m_\alpha \nabla \times n_\alpha q_\alpha \mathbf{u}_\alpha + \frac{\lambda_\alpha n_\alpha q_\alpha^2}{c}\nabla \times \mathbf{A} = \frac{4\pi n_\alpha q_\alpha^2}{c^2}\mathbf{j}_\alpha. \tag{3.73}$$

After simplification, we get

$$\nabla \times (\nabla \times \mathbf{B}) - \alpha_1 \nabla \times \mathbf{B} + \alpha_2 \mathbf{B} = 0, \tag{3.74}$$

where $\alpha_1 = 4\pi n_\alpha q_\alpha^2/\lambda_\alpha m_\alpha c^2$, and $\alpha_2 = 4\pi n_\alpha q_\alpha^2/m_\alpha c^2$ are constants. This is the relaxed state equation of Steinhauer-Ishida model for two species plasma using self-helicity as system's invariant. This is nothing but very similar to relaxed state for the two fluid plasma given by Mahajan and Yoshida [37] as described in equation (3.48).

Finally, we can make a catalog of the known relaxed state equilibria and also point out how one may arrive at them. In figure (3-2), we may see a hierarchy determined by the increasing complexity of the final state. In supplying a magnetic field, current, and flow to the plasma, the energy of the system rises successively with the harmonic, the first, and the second Beltrami fields. These energy levels are explained as follows. Suppose that a plasma is produced in an external magnetic field (harmonic field). In the absence of a drive, such a plasma will disappear and the system will relax into the pure harmonic magnetic field ($\nabla \times \mathbf{B} = 0$). When a drive in the form of a plasma current is added, it sustains the total helicity, and the plasma relaxes into the Taylor state corresponding to the single Beltrami magnetic field. When a strong flow exists in addition to the current in a two component plasma, the system must conserve two distinct helicities and the self organized state becomes qualitatively different from the Taylor relaxed state. The new states represent a "singular perturbation" to the MHD accessible states because the two-fluid effect induces a coupling among the flow, magnetic field, electric field,

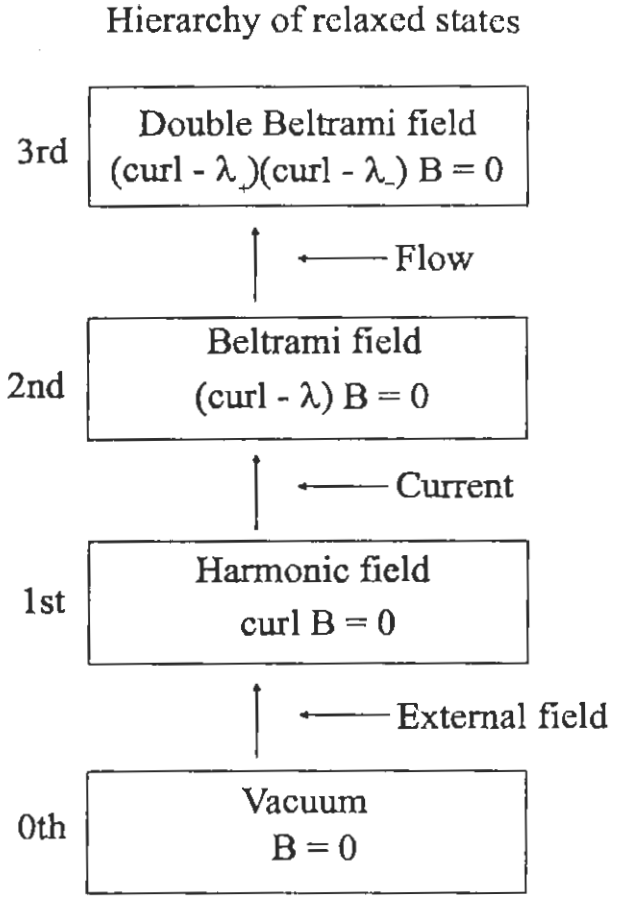

Figure 3-2: Hierarchy of relaxed states. The absolute minimum energy state is the vacuum. On supplying a magnetic field, current, and flow to the plasma, the energy of the system rises successively with the harmonic, the first, and the second Beltrami fields.

and the pressure. To access these states one must also maintain the second helicity invariant by driving and sustaining an appropriate flow. It is equivalent to giving an internal electric field or applying a steep gradient in pressure, because these fields are tightly coupled. As the final state becomes more and more complex, greater and greater care is needed for its creation and maintenance. However, if all the requirements are met, the more complex states can display a tremendously variegated and rich structure in field variations.

Chapter 4

Analytical Solutions in Cylindrical Geometry

A general solenoidal (divergence-free) vector field, such as a magnetic field or the velocity field of an incompressible flow, can be decomposed into an orthogonal sum of Beltrami fields (eigenfunctions of the curl operator) [68]. In the dynamical evolution of a general plasma, the nonlinearities in the equations of motion will necessarily induce couplings among the constituent Beltrami fields (into which the initial field may be composed), making the resultant dynamics rather complicated. It is remarkable, however, that in the single fluid MHD, the energy of the system tends to condensate into a single Beltrami magnetic field, leading to a self-organized, force-free equilibrium - the well-known Taylor relaxed state. It is equally remarkable that a more general equilibrium, a relaxed state described by a pair of different Beltrami fields, is available even in a two fluid description of a plasma. As we have seen in the last chapter, the double Beltrami fields are a well-defined combination of the magnetic and flow-velocity fields. The essential new physics is due to the Hall term that relates the kinematic and the magnetic aspects of a magnetofluid. The adequate formulation of the plasma dynamics based on the double Beltrami fields, despite its simple mathematical structure, yields a far richer set of equilibrium solutions than conventional single Beltrami fields. The set of new relaxed states includes a variety of plasma states and explains interesting phenomena. It opens up the possibility of experimenting with altogether different configurations, some of which may lead to

a novel regime of high-pressure plasma confinement. In the next section, we would apply the double curl Beltrami systems to simple one-dimensional cylindrical geometries. The cylinder is taken to be a limiting case of large aspect ratio torus.

4.1 Cylindrical Plasma System

4.1.1 Combination of Taylor States

The double Beltrami field is given by a linear combination of two different Beltrami fields (see (3.54)). In a cylindrical geometry (r, θ, z), the Beltrami field can be expressed in terms of Bessel functions as given by the Chandrasekhar-Kendal function (Sec. (2.3.1)). To obtain the axisymmetric solution ($\partial/\partial\theta = 0$) for Beltrami field that is homogeneous along z-axis ($\partial/\partial z = 0$), we consider

$$\nabla \times \mathbf{B} = \lambda \mathbf{B}. \tag{4.1}$$

The components of the above equation give

$$B_r = 0, \tag{4.2}$$

$$\frac{\partial^2 B_\theta}{\partial r^2} + \frac{1}{r}\frac{\partial B_\theta}{\partial r} + \lambda^2\left(1 - \frac{1}{\lambda^2 r^2}\right) B_\theta = 0, \tag{4.3}$$

$$\frac{\partial^2 B_z}{\partial r^2} + \frac{1}{r}\frac{\partial B_z}{\partial r} + \lambda^2 B_z = 0. \tag{4.4}$$

Equations (4.3) and (4.4) are the Bessel equations of first and zero order respectively. Therefore, the general solution of (4.1) can be written as

$$\mathbf{B} = \begin{pmatrix} 0 \\ CJ_1(\lambda_+ r) \\ CJ_0(\lambda_+ r) \end{pmatrix},$$

where C is a constant and can be evaluated by using the boundary conditions.

The double Beltrami field is a linear combination of two Beltrami fields, therefore, the

general solution of equation (3.49) reads

$$\mathbf{B} = \begin{pmatrix} 0 \\ C_1 J_1(\lambda_+ r) \\ C_1 J_0(\lambda_+ r) \end{pmatrix} + \begin{pmatrix} 0 \\ C_2 J_1(\lambda_- r) \\ C_2 J_0(\lambda_- r) \end{pmatrix}, \tag{4.5}$$

and

$$\nabla \times \mathbf{B} = \lambda_+ \begin{pmatrix} 0 \\ C_1 J_1(\lambda_+ r) \\ C_1 J_0(\lambda_+ r) \end{pmatrix} + \lambda_- \begin{pmatrix} 0 \\ C_2 J_1(\lambda_- r) \\ C_2 J_0(\lambda_- r) \end{pmatrix}. \tag{4.6}$$

Applying boundary conditions, values of constants C_1 and C_2 can be evaluated. Under boundary conditions $|(\nabla \times \mathbf{B})_z|_{r=0} = g$ and $|\mathbf{B}_z|_{r=0} = s$, we get

$$C_1 = \frac{s - \lambda_- g}{\lambda_+ - \lambda_-}, \tag{4.7}$$

$$C_2 = \frac{\lambda_+ g - s}{\lambda_+ - \lambda_-}. \tag{4.8}$$

The values of V_z and V_θ can be obtained using equations (3.46) and (3.47), and are given by

$$V_{z(t)} = (\frac{1}{a} + \lambda_+) C_1 J_0(\lambda_+ r) + (\frac{1}{a} + \lambda_-) C_2 J_0(\lambda_- r), \tag{4.9}$$

$$V_{\theta(p)} = (\frac{1}{a} + \lambda_+) C_1 J_1(\lambda_+ r) + (\frac{1}{a} + \lambda_-) C_2 J_1(\lambda_- r), \tag{4.10}$$

where the subscripts t and p represent the toroidal and poloidal velocities respectively.

The Taylor's relaxed states being force-free states are characterized by large values of currents parallel to the magnetic field. In plasma relaxation, helicity is to remain conserved. The well-known helicity balance equation for a fixed gauge [69] can be obtained as follows:

$$\frac{\partial}{\partial t} \int_v \mathbf{A} \cdot \mathbf{B} dv = \int_v \left(\mathbf{A} \cdot \frac{\partial \mathbf{B}}{\partial t} + \frac{\partial \mathbf{A}}{\partial t} \cdot \mathbf{B} \right) dv. \tag{4.11}$$

$$\begin{aligned} \frac{\partial \mathbf{B}}{\partial t} &= -\nabla \times \mathbf{E} \\ &= -\nabla \times \left[-\nabla \phi - \frac{\partial \mathbf{A}}{\partial t} \right] \end{aligned}$$

$$\frac{\partial \mathbf{B}}{\partial t} = \nabla \times \frac{\partial \mathbf{A}}{\partial t}. \tag{4.12}$$

and

$$\begin{aligned} \frac{\partial \mathbf{A}}{\partial t} &= -\mathbf{E} - \nabla\phi \\ &= \mathbf{V} \times \mathbf{B} - \eta \mathbf{j} - \nabla\phi. \end{aligned} \tag{4.13}$$

Putting equations (4.12) and (4.13) in (4.11), we get

$$\frac{\partial}{\partial t} \int_v \mathbf{A} \cdot \mathbf{B} dv = \int_v \left(\mathbf{A} \cdot \nabla \times \frac{\partial \mathbf{A}}{\partial t} - \nabla\phi \cdot \mathbf{B} - \eta \mathbf{j} \cdot \mathbf{B} \right) dv. \tag{4.14}$$

Using the identity

$$\nabla \cdot \left(\mathbf{A} \times \frac{\partial \mathbf{A}}{\partial t} \right) = \frac{\partial \mathbf{A}}{\partial t} \cdot \nabla \times \mathbf{A} - \mathbf{A} \cdot \nabla \times \frac{\partial \mathbf{A}}{\partial t},$$

equation (4.14) becomes

$$\begin{aligned} \frac{\partial}{\partial t} \int_v \mathbf{A} \cdot \mathbf{B} dv &= -\int_s \mathbf{n} \cdot \left[(-\partial_t \mathbf{A}) \times \mathbf{A} + 2\mathbf{B}\varphi \right] ds \\ &\quad -2 \int_v \eta \mathbf{j} \cdot \mathbf{B} dv, \end{aligned} \tag{4.15}$$

where v is a fixed volume, $\mathbf{n}$ is the outward unit normal vector onto the boundary s, and φ is the electrostatic potential. The first term of the right-hand side represents the helicity flux, while the second one, the helicity dissipation by the parallel resistivity. Since the dissipation of the helicity is caused by the parallel current, the helicity is a quantity that is primarily related to parallel currents. In a sustained equilibrium, to compensate for the helicity dissipation there should be a balanced helicity flux.

Most of the magnetic configurations with currents parallel to the magnetic field intended for confinement of plasmas for fusion require means for current drive [64]. The concepts of helicity transport has attracted interest because of its relation with the driving mechanisms of plasma current. Most often, this drive is accomplished inductively in such a manner that steady operation, which may be desirable from an engineering point of view for fusion reactors, is not possible. Moreover, parallel current density provides a free energy source for current-driven

instabilities. Large amount of parallel flows are more likely to generate shock waves in plasmas and can cause destabilization. In open end plasma devices, large parallel components of flow and current at the ends are also not useful for confinement purposes.

On the other hand, the perpendicular currents in plasmas don't need an external drive for transport and can be sustained by pressure gradients or electric field drifts, and are useful for steady operation. For such considerations, it is quite indispensable to investigate the parallel and perpendicular components of fields. In the next section, we will derive expressions for the components of flow and current in order to visualize more realistic picture of this extended relaxed model.

4.1.2 Components of Flow and Current

To obtain parallel components of flow and current, we use equation (3.46) by taking $\nabla \times \mathbf{B} = \mathbf{j}$, such that

$$\mathbf{B} = a\mathbf{V} - a\mathbf{j}. \tag{4.16}$$

Taking the dot product of above equation with $\mathbf{B} = \mathbf{b}B$, where $\mathbf{b}$ is a unit vector pointing in the direction of $\mathbf{B}$ and using $\mathbf{V} = \mathbf{b}V_{\parallel} + \mathbf{V}_{\perp}$ and $\mathbf{j} = \mathbf{b}j_{\parallel} + \mathbf{j}_{\perp}$, we obtain

$$j_{\parallel} = V_{\parallel} - B/a, \tag{4.17}$$

where $\parallel$ and $\perp$ refer to the direction of $\mathbf{B}$. Making use of the relation $V_{\parallel} = \mathbf{b} \cdot \mathbf{V}$, we obtain

$$V_{\parallel} = \frac{B_z V_z + B_\theta V_\theta}{(B_z^2 + B_\theta^2)^{1/2}}. \tag{4.18}$$

Putting values of $V_{\parallel}$ and $B = (B_z^2 + B_\theta^2)^{1/2}$ in equation (4.17), the expression for the electron current $j_{\parallel}$ becomes

$$j_{\parallel} = \frac{B_z V_z + B_\theta V_\theta}{(B_z^2 + B_\theta^2)^{1/2}} - \frac{(B_z^2 + B_\theta^2)^{1/2}}{a}. \tag{4.19}$$

To evaluate the perpendicular components of flow and current, we take the cross-product of equation (4.16) with $\mathbf{B}$ and easily obtain that

$$\mathbf{V}_{\perp} = \mathbf{j}_{\perp}. \tag{4.20}$$

The magnitude of perpendicular components can be obtained by using the relation

$$V^2 = V_{\parallel}^2 + V_{\perp}^2. \tag{4.21}$$

Plugging the values of $V^2 = V_z^2 + V_\theta^2$ and $V_\parallel$ in the above equation, we get

$$V_\perp = \frac{B_z V_\theta - B_\theta V_z}{(B_z^2 + B_\theta^2)^{1/2}}. \tag{4.22}$$

Next subsection will address the radial variation of field, flows, and pressure for different scale parameters and boundary conditions.

4.2 Radial Profiles

Radial profiles of magnetic fields, flows, pressure and components of flows and currents for the case of a one dimensional simple cylindrical geometry are given in figures (4-1)-(4-4) for different boundary conditions and Beltrami parameters by using equations (4.5), (4.9), (4.10), (3.56), (4.17), (4.18) and (4.22). Subject to appropriate boundary conditions and Beltrami parameters, the double Beltrami formulation provide paramagnetic and diamagnetic structures as is evident from the following figures. The system size for all the following cases is taken to be $2\lambda_i$, where $\lambda_i = 0.072$ m for $n = 10^{19}$ m^{-3}, β at the edge $r = 2$ is taken to be zero and the velocities are measured in the units of central Alfvén speed.

Figure (4-1) shows the radial profiles of magnetic fields, velocities and components of flows and currents for the Beltrami parameters $a = -0.8$ and $b = -1.25$ with the boundary conditions of $B_z = g = 1$ and $j_z = s = 0.75$. The normalized eigenvalues of the curl operators are $\lambda_+ = 0.75$ and $\lambda_- = -0.75$. Fields show the paramagnetic behavior and are minimized at the edge. We have taken for this case $s = \lambda_+ g$ as a boundary condition which leads us to a single Beltrami system. $V_\perp$ and $j_\perp$ are zero and there exist only parallel components of current and flow. It indicates the emergence of force-free magnetic fields as considered by Taylor [10, 22] and Sudan [31] that exhibit only higher values of parallel components. This configuration produces very insignificant pressure confinement by the Bernoulli mechanism.

Figure (4-2) represents radial profiles of fields, flows, components of flow and current and

pressure for real values of $\lambda_{\pm}$. In this case, we have taken $B_z = 1$ and $j_z = 0.52$ as boundary conditions. The Beltrami parameters are $a = -1.8$ and $b = -1.5$ implying the eigenvalues of $\lambda_+ = -0.2349$ and $\lambda_- = -0.7096$. Fields and flows increase away from the center showing diamagnetism. Pressure is high at the center and decreases monotonically. $j_\parallel$ has higher value at $r \sim 0$, then decreases smoothly towards edge while $j_\perp = 0$ at $r = 0$ but increases smoothly and at the edge of plasma $j_\perp > j_\parallel$. On the other hand, $V_\parallel > V_\perp$ from $r \sim 0$ to $r \sim 0.1$, then $V_\perp$ dominates $V_\parallel$ until $r \sim 1.1$, after that $V_\parallel$ increases and at the boundary $V_\parallel > V_\perp$.

Figure (4-3) depicts the profiles for pure imaginary values of $\lambda_{\pm}$. For this case, we have taken values of Beltrami parameters $a = -2.5$ and $b = -0.4$ that make $\alpha_1 = 0$ and $\alpha_2 > 0$. The boundary values are $B_z = 1$ and $j_z = 0.42$. The eigenvalues normalized to λ_i are $\lambda_{\pm} = \pm 0.9165i$. For these parameters and boundary conditions, system reduces to London's equation and we can observe diamagnetic behavior as shown in figure (4-3). $j_\parallel$ remain constant throughout the system while $j_\perp$ increases sharply. Starting from $r \sim 0$ to $r \sim 0.8$, $j_\parallel > j_\perp$ and after that $j_\perp$ dominates $j_\parallel$ whereas $V_\perp$ is almost greater than $V_\parallel$ throughout the system.

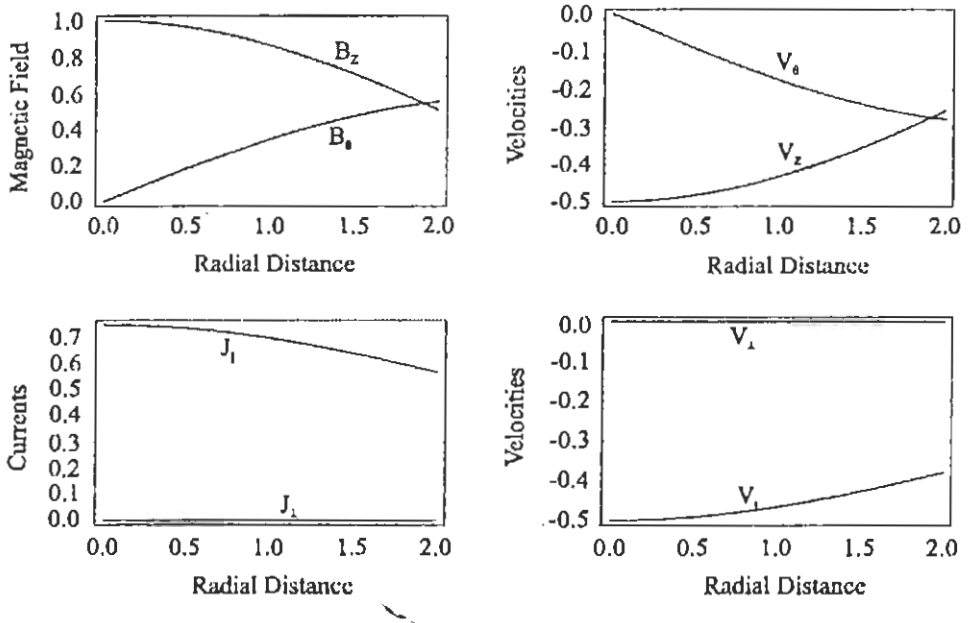

Figure 4-1: Radial profiles of B_z, B_θ, V_z, V_θ, $j_\parallel$, $j_\perp$, $V_\parallel$, $V_\perp$ for the Beltrami parameters $a = -0.8$ and $b = -1.25$. The eigenvalues are $\lambda_{\pm} = \pm 0.75$.

pressure for real values of $\lambda_{\pm}$. In this case, we have taken $B_z = 1$ and $j_z = 0.52$ as boundary conditions. The Beltrami parameters are $a = -1.8$ and $b = -1.5$ implying the eigenvalues of $\lambda_+ = -0.2349$ and $\lambda_- = -0.7096$. Fields and flows increase away from the center showing diamagnetism. Pressure is high at the center and decreases monotonically. $j_{\parallel}$ has higher value at $r \sim 0$, then decreases smoothly towards edge while $j_{\perp} = 0$ at $r = 0$ but increases smoothly and at the edge of plasma $j_{\perp} > j_{\parallel}$. On the other hand, $V_{\parallel} > V_{\perp}$ from $r \sim 0$ to $r \sim 0.1$, then $V_{\perp}$ dominates $V_{\parallel}$ until $r \sim 1.1$, after that $V_{\parallel}$ increases and at the boundary $V_{\parallel} > V_{\perp}$.

Figure (4-3) depicts the profiles for pure imaginary values of $\lambda_{\pm}$. For this case, we have taken values of Beltrami parameters $a = -2.5$ and $b = -0.4$ that make $\alpha_1 = 0$ and $\alpha_2 > 0$. The boundary values are $B_z = 1$ and $j_z = 0.42$. The eigenvalues normalized to λ_i are $\lambda_{\pm} = \pm 0.9165i$. For these parameters and boundary conditions, system reduces to London's equation and we can observe diamagnetic behavior as shown in figure (4-3). $j_{\parallel}$ remain constant throughout the system while $j_{\perp}$ increases sharply. Starting from $r \sim 0$ to $r \sim 0.8$, $j_{\parallel} > j_{\perp}$ and after that $j_{\perp}$ dominates $j_{\parallel}$ whereas $V_{\perp}$ is almost greater than $V_{\parallel}$ throughout the system.

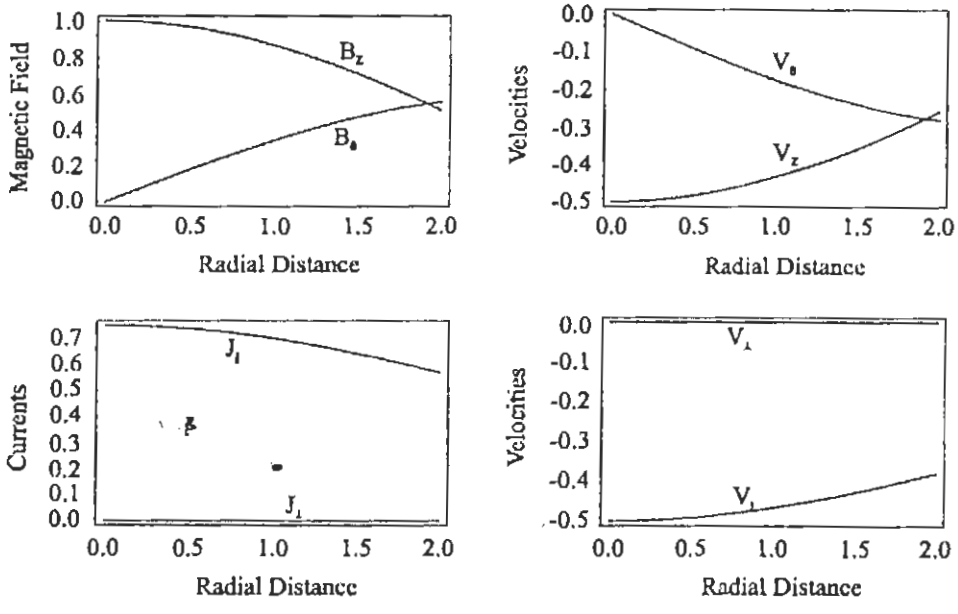

Figure 4-1: Radial profiles of B_z, B_θ, V_z, V_θ, $j_{\parallel}$, $j_{\perp}$, $V_{\parallel}$, $V_{\perp}$ for the Beltrami parameters $a = -0.8$ and $b = -1.25$. The eigenvalues are $\lambda_{\pm} = \pm 0.75$.

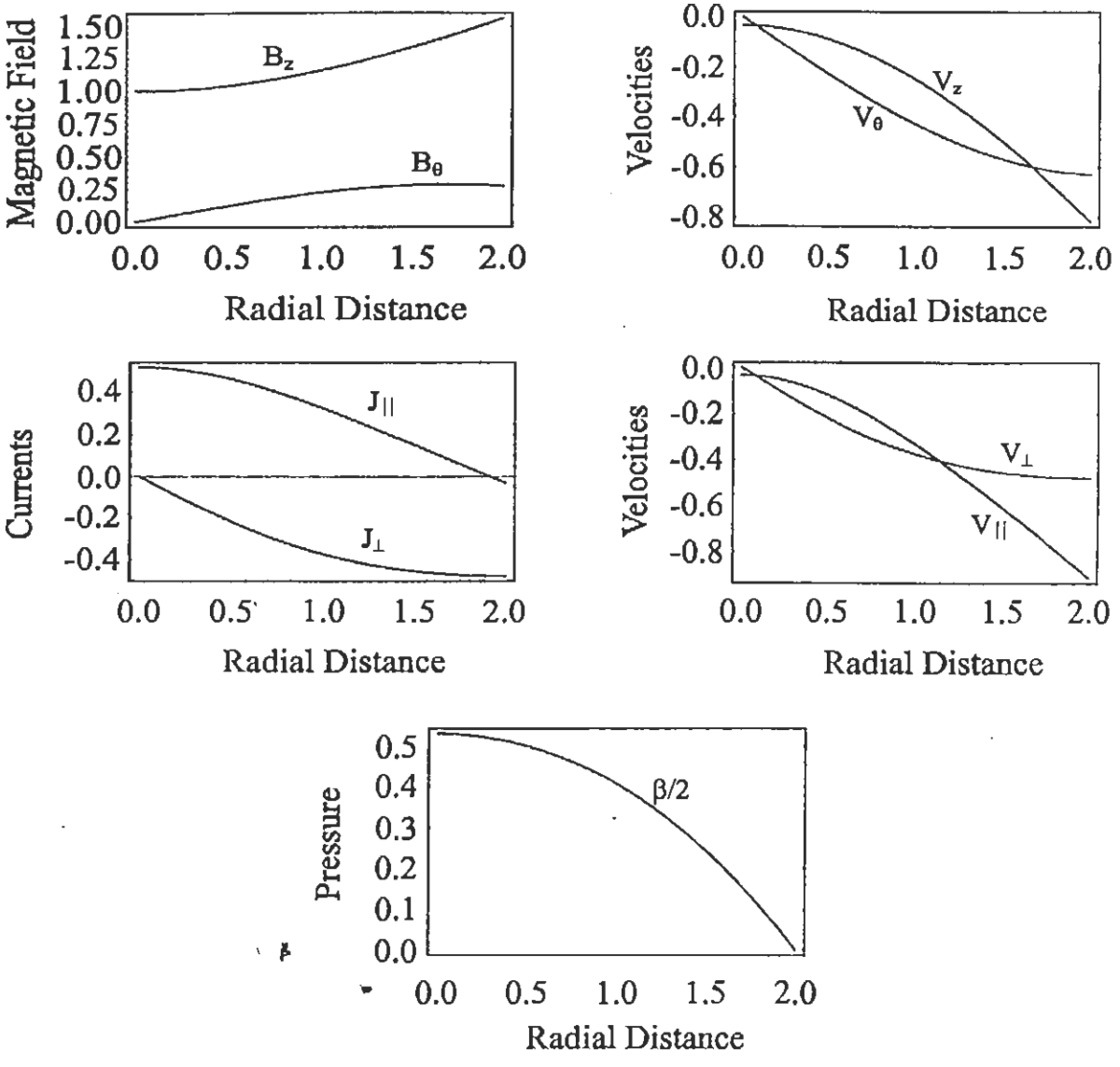

Figure 4-2: Radial profiles of B_z, B_θ, V_z, V_θ, $j_{||}$, $j_\perp$, $V_{||}$, $V_\perp$ and $\beta/2$ for the Beltrami parameters $a = -1.8$ and $b = -1.5$. The corresponding eigenvalues are $\lambda_+ = -0.2349$ and $\lambda_- = -0.7096$.

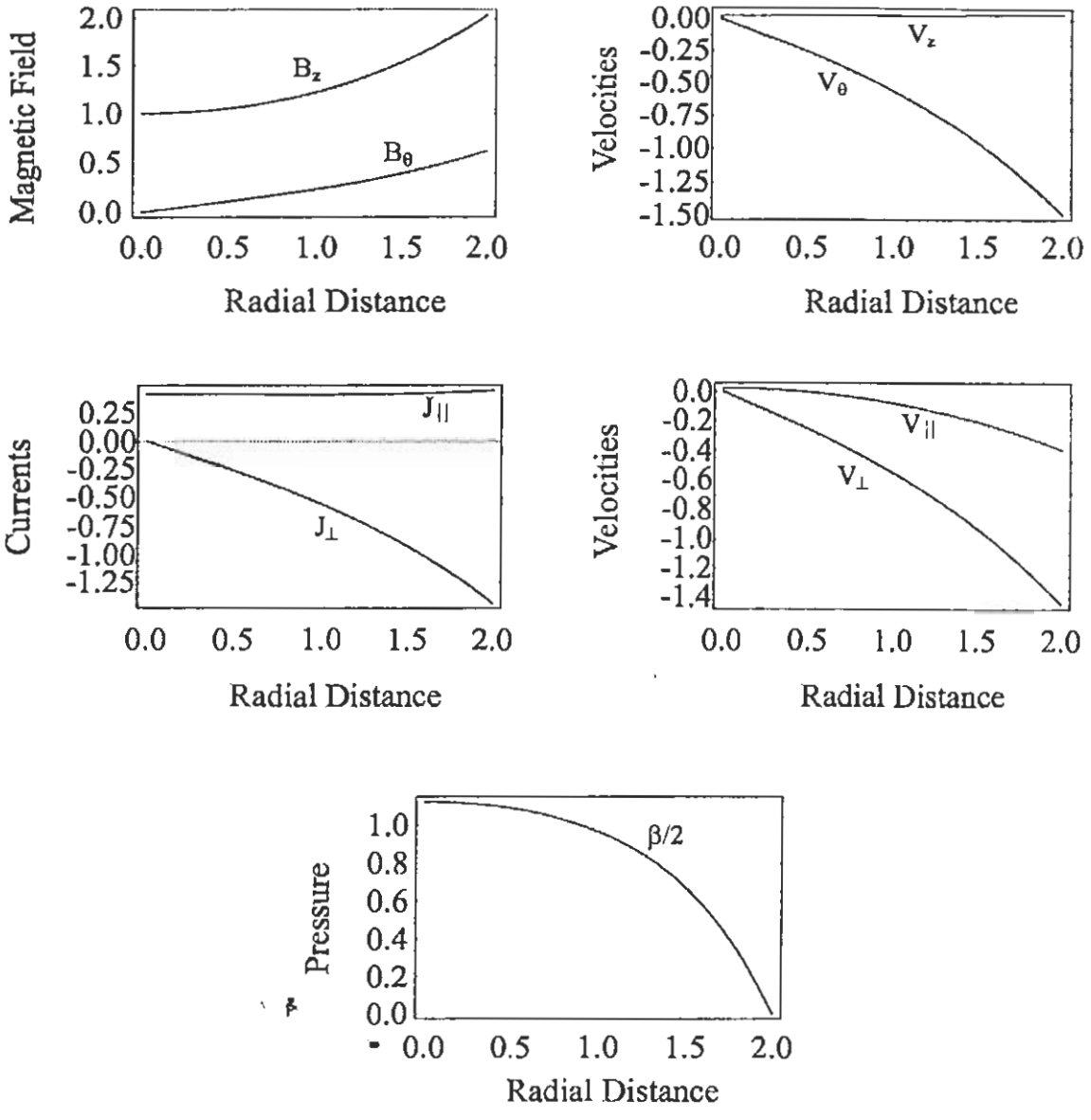

Figure 4-3: Radial profiles of B_z, B_θ, V_z, V_θ, $j_{||}$, $j_\perp$, $V_{||}$, $V_\perp$ and $\beta/2$ for the Beltrami parameters $a = -2.5$ and $b = -0.4$. The imaginary eigenvalues normalized to λ_i are $\lambda_\pm = \pm 0.9165i$.

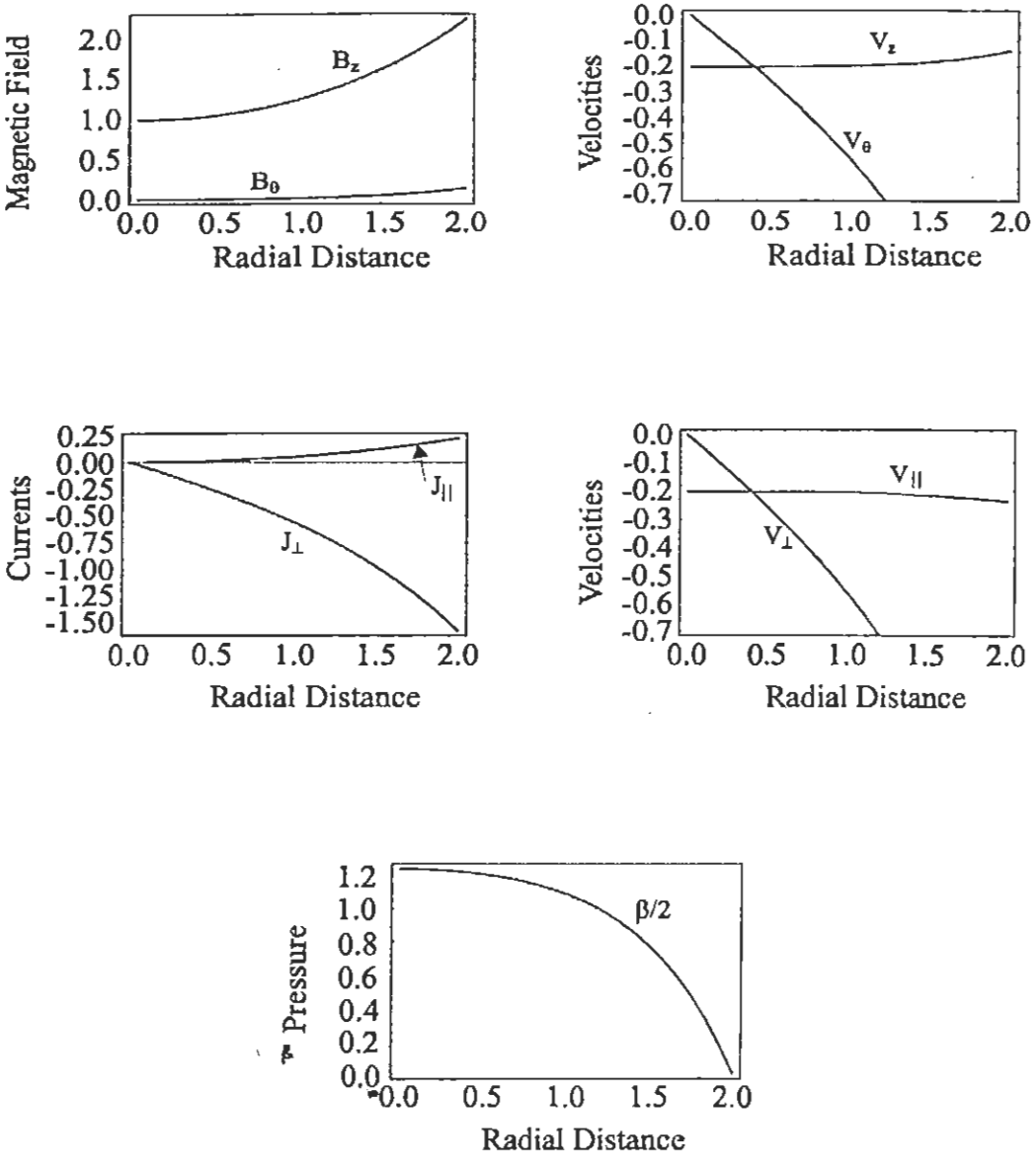

Figure 4-4: Radial profiles of B_z, B_θ, V_z, V_θ, $j_{||}$, $j_\perp$, $V_{||}$, $V_\perp$ and $\beta/2$ for the Beltrami parameters $a = -4.9$ and $b = 0$. The eigenvalues normalized to λ_i are complex conjugate pair $\lambda_\pm = 0.102 \pm 0.9948i$.

In figure (4-4), the eigenvalues λ_+ and λ_- are complex conjugate. The Beltrami parameters are taken as $a = -4.9$ and $b = 0$ implying $\lambda_\pm = 0.102 \pm 0.9948i$. The boundary conditions are $B_z = 1$ and $j_z = 0$. Due to complex nature of the eigenvalues $(\lambda_\pm)$,of the curl operator, Bessel functions of 2nd kind are introduced in the system that always increase away from the center. Therefore, in this case also, the magnetic fields and flows show diamagnetism i.e., field and flows are minimum at the center and increase towards edge of the plasma. $j_\parallel$ varies from 0 to 0.23 whereas $V_\parallel$ changes its value from 0.204 to 0.214 in the system. For this case magnetic field becomes proportional to vorticity of flow because of $b = 0$. In figures (4-3)-(4-4), the eigenvalues of the curl operator $\lambda_\pm$ are taken as complex but the corresponding fields and flows come out to be real.

We observe by analyzing figures (4-1)-(4-4) that double Beltrami fields have a potential to change from paramagnetic state to diamagnetic state or vice versa depending on different Beltrami parameters. From figures (4-3)-(4-4), we notice the following:

(1) The magnetic fields increase away from the center.

(2) The magnitude of the velocity field normalized to Alfvén speed is sizable and increases monotonically.

(3) These configuration through Bernoulli mechanism produce excellent pressure confinement with a central $\beta > 1$. Since for the plasma confinement through Bernoulli mechanism, the velocity fields must increase away from the center and this is possible due to retaining the term proportional to $\mathbf{j} \sim \nabla \times \mathbf{B}$ in the evolution equations.

We know that parallel current density $j_\parallel$ being current due to electrons does not have any contribution to gradient in pressure and in case of a single Beltrami system (Taylor's relaxed state), there exist only very large values of $j_\parallel$ indicating zero β which is undesirable for fusion concept. For the simple cylindrical geometry, the parallel components of flow at the center of the plasma $r = 0$ can be evaluated by using equation (4.18). From equation (4.18), we get

$$\left|V_\parallel\right|_{r=0} = \left(\frac{1}{a} + \lambda_+\right) C_1 + \left(\frac{1}{a} + \lambda_-\right) C_2. \tag{4.23}$$

Putting the values of constants C_1 and C_2 from equations (4.7) and (4.8) respectively, the above

equation becomes

$$\left|V_{\parallel}\right|_{r=0} = s + \frac{g}{a}, \tag{4.24}$$

where $g = 1$ for the present case. Similarly, the parallel components of current density at the center, using equation (4.19), come out to be

$$\left|j_{\parallel}\right|_{r=0} = s. \tag{4.25}$$

We observe that the parallel components of flow and current are zero at the center if we take $j_z = s = -1/a$ and $j_z = s = 0$ respectively as boundary conditions at the center while the perpendicular components of flow and current are always zero at the center ($r = 0$). The components of flow and current for the radius other than $r = 0$ will have different values depending on different Beltrami parameters and boundary conditions.

We need finite β relaxed state and these are the perpendicular components which contribute to gradient in pressure and confinement of plasma. More importantly, these figures also show that double Beltrami formulation has a potential to create the relaxed states that sustain pressure gradients with large values of perpendicular components of flow and current density. It shows that double Beltrami states can exhibit diamagnetism and pressure confinement that is not allowed in a single Beltrami state. These highly compact diamagnetic structures with scale length of a few λ_i having strong plasma flow, being the states of lowest free energy, are expected to be MHD stable. Such relaxed states are considered to be useful regarding fusion concept and point to a possible new path in our quest for controlled thermonuclear fusion.

In this section, we have studied the radial profiles of magnetic fields, flows, β, components of current density and flow for a simple cylindrical plasma configuration taking only the toroidal magnetic field and current density as boundary conditions. Moreover, we have always taken $B_z = 1$ as boundary condition. In order to see the effect of different boundary values of B_z and to include the effect of poloidal field and current density as well, we examine an annular plasma configuration as described in the next section.

4.3 Internal Conductor Plasma System

For a cylindrical plasma having an internal conductor at its center carrying a current I and producing magnetic field in azimuthal direction, the general solution for the "*double curl Beltrami equation*" reads as

$$\mathbf{B} = \begin{pmatrix} 0 \\ P_1 J_1(\lambda_+ r) + P_2 Y_1(\lambda_+ r) \\ P_1 J_0(\lambda_+ r) + P_2 Y_0(\lambda_+ r) \end{pmatrix} + \begin{pmatrix} 0 \\ Q_1 J_1(\lambda_- r) + Q_2 Y_1(\lambda_- r) \\ Q_1 J_0(\lambda_- r) + Q_2 Y_0(\lambda_- r) \end{pmatrix}, \tag{4.26}$$

where J's and Y's are Bessel functions of Ist and 2nd kind respectively with the subscripts indicating their orders. C's and D's are constants and can be evaluated by using boundary conditions. Applying boundary values at the conductor radius d i.e., $|(\nabla \times \mathbf{B})_z|_{r=d} = j_z = s$, $|(\nabla \times \mathbf{B})_\theta|_{r=d} = j_\theta = k$ and $|\mathbf{B}_z|_{r=d} = g$, $|\mathbf{B}_\theta|_{r=d} = h$, values of constants come out to be as follows:

$$\begin{aligned}
P_1 &= \frac{(s-\lambda_- g)Y_1(\lambda_+ d) - (k-\lambda_- h)Y_0(\lambda_+ d)}{(\lambda_+ - \lambda_-)(Y_1(\lambda_+ d)J_0(\lambda_+ d) - J_1(\lambda_+ d)Y_0(\lambda_+ d))}, \\
P_2 &= \frac{(k-\lambda_- h)J_0(\lambda_+ d) - (s-\lambda_- g)J_1(\lambda_+ d)}{(\lambda_+ - \lambda_-)(Y_1(\lambda_+ d)J_0(\lambda_+ d) - J_1(\lambda_+ d)Y_0(\lambda_+ d))}, \\
Q_1 &= \frac{(\lambda_+ g - s)Y_1(\lambda_- d) - (\lambda_+ h - k)Y_0(\lambda_- d)}{(\lambda_+ - \lambda_-)(Y_1(\lambda_- d)J_0(\lambda_- d) - J_1(\lambda_- d)Y_0(\lambda_- d))}, \\
Q_2 &= \frac{(\lambda_+ h - k)J_0(\lambda_- d) - (\lambda_+ g - s)J_1(\lambda_- d)}{(\lambda_+ - \lambda_-)(Y_1(\lambda_- d)J_0(\lambda_- d) - J_1(\lambda_- d)Y_0(\lambda_- d))}.
\end{aligned} \tag{4.27}$$

Using the Wronskian relation [70],

$$J_{m+1}(z)Y_m(z) - Y_{m+1}(z)J_m(z) = 2/\pi z, \tag{4.28}$$

we can cast the values of constants as,

$$P_1 = \frac{\pi \lambda_+ d}{2(\lambda_- - \lambda_+)} \left[(s-\lambda_- g)Y_1(\lambda_+ d) - (k-\lambda_- h)Y_0(\lambda_+ d)\right],$$

$$P_2 = \frac{\pi \lambda_+ d}{2(\lambda_- - \lambda_+)} \left[(k-\lambda_- h)J_0(\lambda_+ d) - (s-\lambda_- g)J_1(\lambda_+ d)\right],$$

$$Q_1 = \frac{\pi\lambda_- d}{2(\lambda_- - \lambda_+)}\left[(\lambda_+ g - s)Y_1(\lambda_- d) - (\lambda_+ h - k)Y_0(\lambda_- d)\right],$$

and

$$Q_2 = \frac{\pi\lambda_- d}{2(\lambda_- - \lambda_+)}\left[(\lambda_+ h - k)J_0(\lambda_- d) - (\lambda_+ g - s)J_1(\lambda_- d)\right]. \tag{4.29}$$

Using relation (3.46), expressions for V_z and V_θ are given by

$$V_z = (\frac{1}{a} + \lambda_+)\left(P_1 J_0(\lambda_+ r) + P_2 Y_0(\lambda_+ r)\right) + (\frac{1}{a} + \lambda_-)\left(Q_1 J_0(\lambda_- r) + Q_2 Y_0(\lambda_- r)\right), \tag{4.30}$$

$$V_\theta = (\frac{1}{a} + \lambda_+)\left(P_1 J_1(\lambda_+ r) + P_2 Y_1(\lambda_+ r)\right) + (\frac{1}{a} + \lambda_-)\left(Q_1 J_1(\lambda_- r) + Q_2 Y_1(\lambda_- r)\right). \tag{4.31}$$

Pressure can be obtained by the help of a generalized Bernoulli condition as described in equation (3.56).

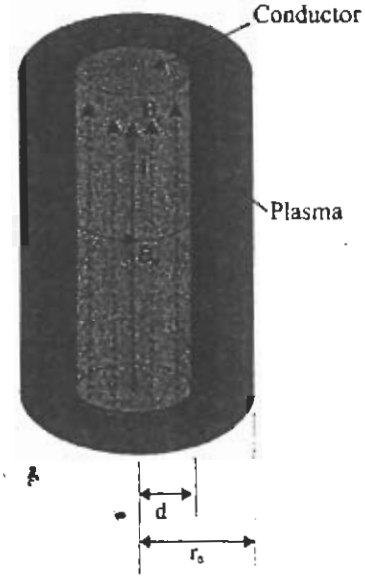

Figure 4-5: A schematic representation of Internal-conductor Plasma configuration.

4.3.1 Radial Profiles

Figures (4-6)-(4-10) show the radial plots of fields, velocity components, and the current density components for one dimensional annular plasma configuration. The size of the system is taken to be $3\lambda_i$, where $\lambda_i = 7.2 \times 10^{-2}$ m for $n = 10^{19}$ m^{-3}, β at the edge $r = 3$ is taken to be zero

and the velocities are measured in the units of central Alfvén speed.

Under the boundary conditions $s = \lambda_- g$ and $k = \lambda_- h$ or $s = \lambda_+ g$ and $k = \lambda_+ h$, the system is characterized by λ_- and λ_+, respectively, and smooth profiles for magnetic fields and velocities could be obtained. For this case, the system is reduced to single curl Beltrami and we can see a glimpse of relaxed state with insignificant pressure but with nonzero flows as depicted in figure (4-6). The boundary conditions for this case are taken as $g = 1.00$, $h = 0.10$, $s = 0.025$ and $k = 0.002$, whereas, the Beltrami parameters are a=2.3 and b=2.2.

For the boundary value $k = \lambda_+ h$, the poloidal components of magnetic field and current follow the Beltrami condition. We get a very small value of β at the boundary of the internal conductor and as we move away from the conductor we observe higher pressure that goes to zero at the outer edge of the plasma. The hollow pressure profile is obtained and can easily be controlled by changing the value of current in the conductor. Parallel components can be minimized to a greater extent as compared to the perpendicular components. It depicts the importance of introducing internal conductor at the center of the plasma. The poloidal magnetic field thus produced behaves as a controlling parameter of the system. Minimization of pressure to zero at the conductor radius for boundary values of $g = 1.00$, $h = 0.85$, $s = 0.25$, $k = 2.098$ and Beltrami parameters $a = -1.7$ and $b = 3.00$ is depicted in figure (4-7). It is evident from the figure that with the help of internal conductor, it is possible to maintain zero pressures both at the inner and outer edge of the plasma with diamagnetic structure of fields showing that double curl Beltrami effect is prominent in the system. In this case, $\beta = 0$ at $r = 1$, and it increases to a maximum value of ~ 1.7 at $r \sim 1.73$, and then decreases to zero at the edge of the plasma. Radial profiles for $j_\parallel$ and $j_\perp$ show that from $r \sim 1.7$ to 2.2, the magnitude of $j_\perp$ is more than $j_\parallel$. At the initial stage and from $r \sim 2.2$, magnitude of $j_\parallel$ is more than $j_\perp$. The magnitude of $V_\perp$ is more than $V_\parallel$ at $r = 1$, whereas, at the edge $V_\parallel > V_\perp$ and at $r \sim 1.73$, the magnitude of $V_\parallel$ decreases and $V_\perp$ increases.

In order to highlight the key role played by double curl term $\nabla \times (\nabla \times \mathbf{B})$, three specific cases are presented. In the first case (Fig. (4-8)), scale parameters $\lambda_\pm$ are real, while in the second case (Fig. (4-9)), they are assumed purely imaginary, and, in the third case (Fig. (4-10)) $\lambda_\pm$ are taken as a complex conjugate of one another. It is evident from figure (4-8), we get hollow profile of pressure that is maximum at $r \sim 1.68$. The radial profiles of parallel and

perpendicular components of current show that $j_\perp > j_\parallel$ at $r = 1$ but at the plasma edge $j_\parallel > j_\perp$. For $r \sim 1.68$, wherein β is maximum, we found that $V_\perp = j_\perp = 0$ but $V_\parallel = 0.078$ and $j_\parallel = 0.091$. Regarding flow components, $V_\perp > V_\parallel$ at the conductor's radius but $V_\perp < V_\parallel$ at the edge of the plasma. The boundary conditions for this case are taken to be $g = 1.00$, $h = 0.10$, $s = 0.15$, $k = 0.54$ and the Beltrami parameters are $a = 4.9$, $b = 1.8$ implying $\lambda_+ = 0.8619$ and $\lambda_- = 0.734$.

Figure (4-9) shows that the magnetic field and velocities increase away from the center and the plasma β at $r = 1$ is 2.27 which attains its maximum value ~ 2.4 at $r = 1.36$, and then decreases monotonically. The perpendicular components of flow and current decrease until $r = 1.36$ to zero value and afterwards increase sharply. On the other hand, $V_\parallel$ changes from 0.02 to 0.19 and $j_\parallel$ from 0.17 to 0.20 in the system. It shows that parallel components are almost constant throughout the system. For this configuration, we have taken $a = -5.0$ and $b = -0.20$ such that $\lambda_\pm = \pm 0.9798i$. Under these parameters, double curl Beltrami equation reduces to London's equation of superconductivity and consequently diamagnetic structures are obtained. The boundary conditions for this case at conductor's radius $r = 1$ are taken to be $g = 0.95$, $h = 0.12$, $s = 0.12$, and $k = 0.40$.

Figure (4-10) shows that the radial plots for the complex conjugate pair of scale parameters $\lambda_\pm = 0.1 \pm 0.995i$ and Beltrami parameters of $a = -5.0$ and $b = 0.0$. The boundary conditions are $g = 0.95$, $h = 0.10$, $s = 0.15$, and $k = 0.54$. For this case, we also get diamagnetic structures because of the complex nature of the eigenvalues that introduce modified Bessel functions in the system that always increase away from the center $r = 0$. At $r = 1$, $\beta = 1.55$ and it becomes maximum at $r = 1.48$ attaining a value of 1.8. From $r = 1.48$, β start decreasing and becomes zero at $r = 3$. At $r = 1.48$, $V_\perp = j_\perp = 0.0067$ and at the edge $V_\perp = j_\perp = 1.35$. The parallel component of current changes its value from 0.21 to 0.36 and parallel component of flow changes from 0.014 at $r = 1$ to 0.010 at $r = 3$. Although, the scale parameters in the above two cases shown in figures (4-9) and (4-10) are complex but fields and flows are real.

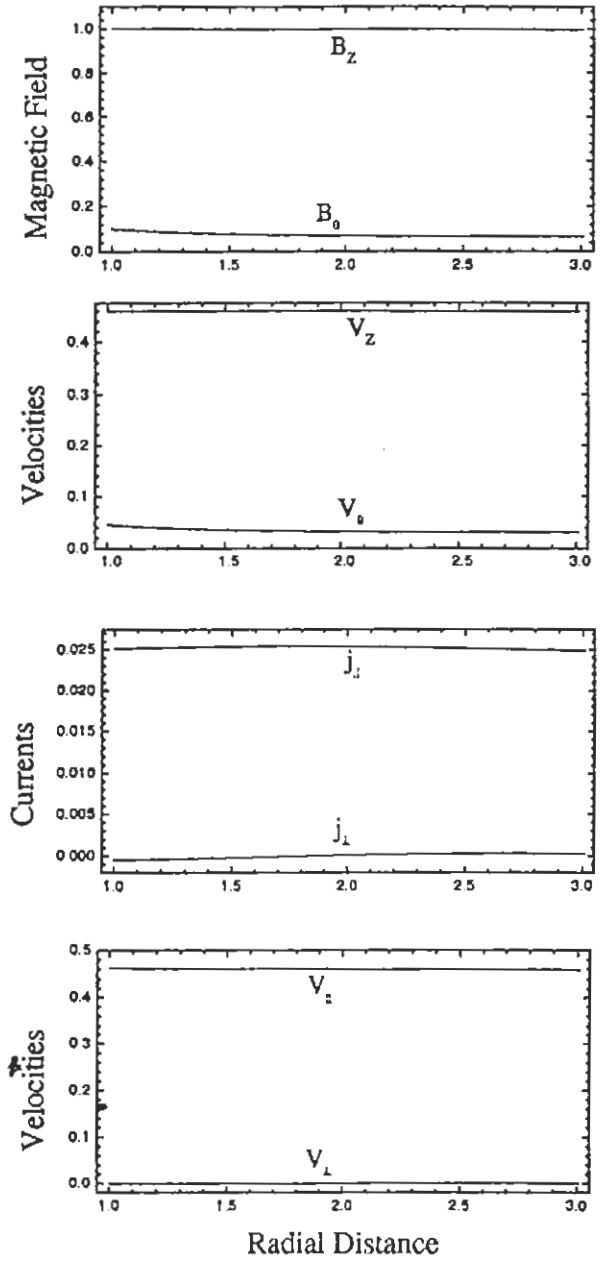

Figure 4-6: Radial profiles of B_z, B_θ, V_z, V_θ, $j_\parallel$, $j_\perp$, $V_\parallel$, and $V_\perp$ for the Beltrami parameters $a = 2.3$ and $b = 2.2$. The normalized eigenvalues are $\lambda_+ = 1.74$ and $\lambda_- = 0.025$ with $s = \lambda_- g$ and $k = \lambda_- h$. Velocities are measured in units of central Alfvén speed.

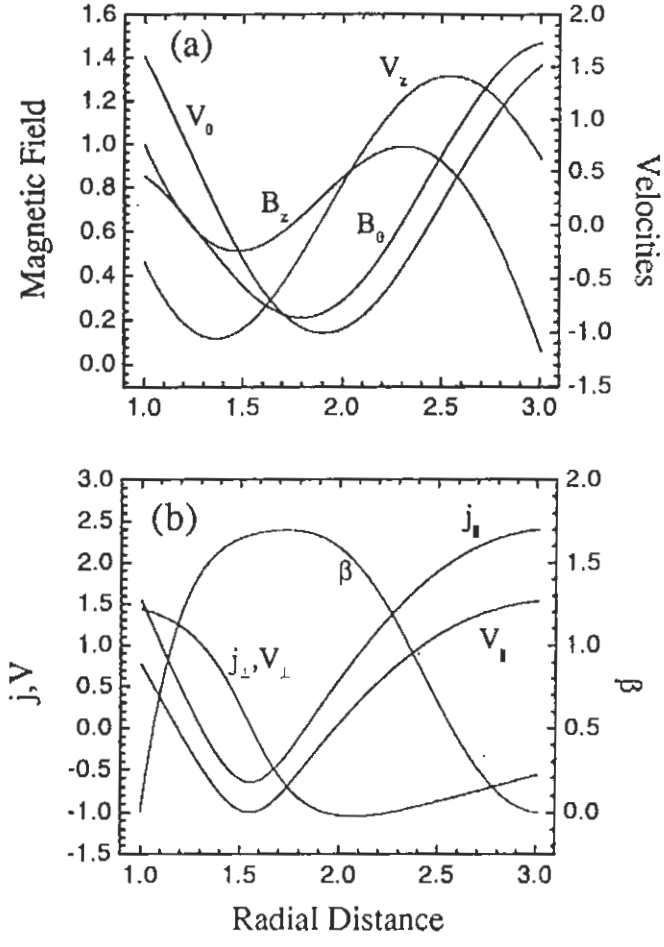

Figure 4-7: Radial profiles of (a) B_z, B_θ (left vertical axis) and V_z, V_θ (right vertical axis), and (b) $j_\parallel$, $j_\perp$, $V_\parallel$, $V_\perp$ (left vertical axis) and β (right vertical axis). Velocities are meaured in units of central Alfvén speed. The Beltrami parameters are $a = -1.7$ and $b = 3.0$. The corresponding normalized eigenvalues are $\lambda_+ = 2.468$ and $\lambda_- = 1.12$.

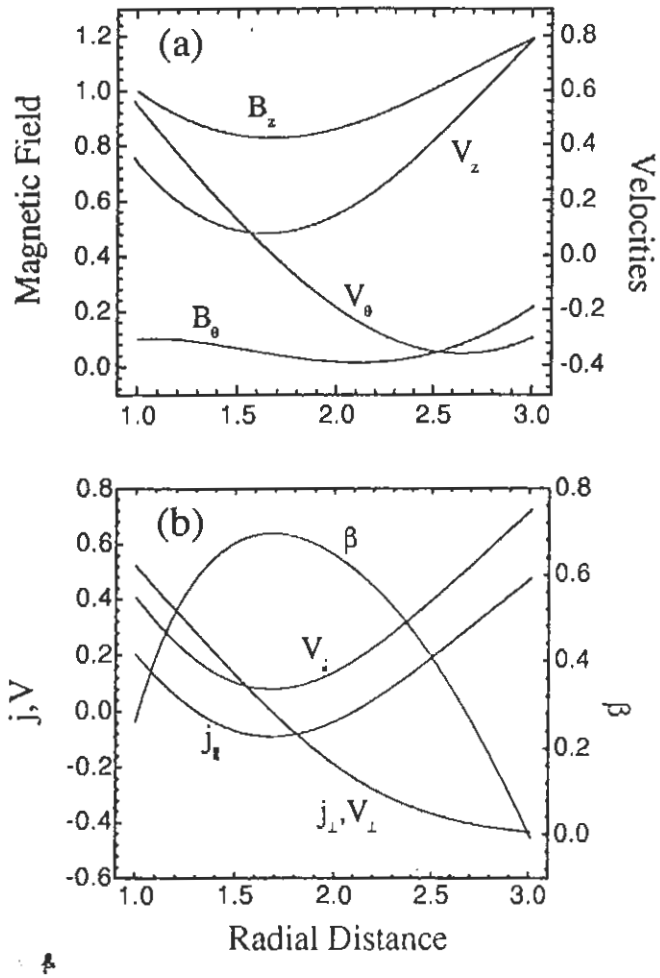

Figure 4-8: The same as in figure 2 but with Beltrami parameters $a = 4.9$ and $b = 1.8$, implying the normalized eigenvalues of $\lambda_+ = 0.8619$ and $\lambda_- = 0.734$.

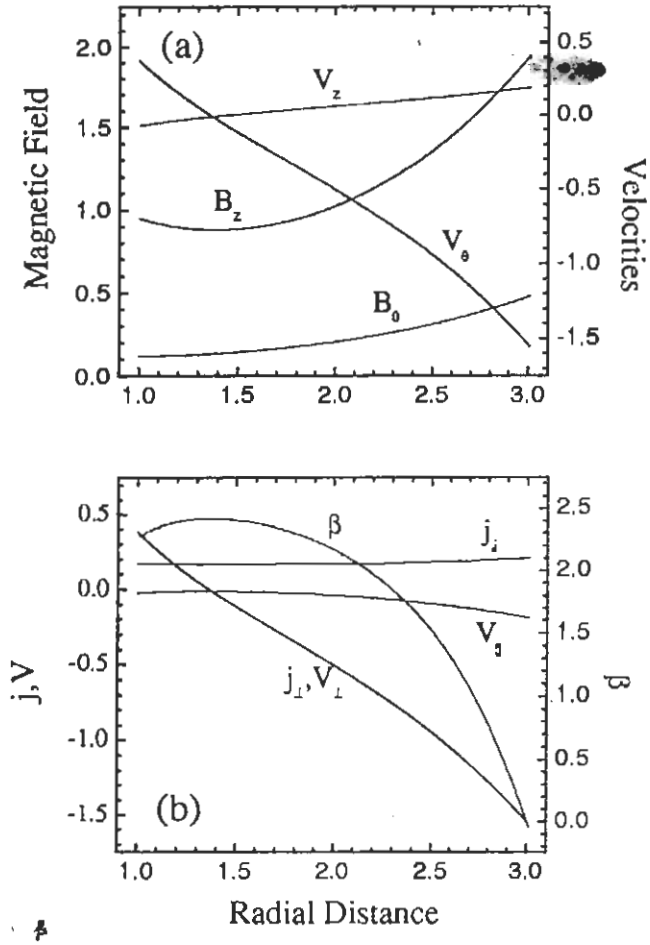

Figure 4-9: The same as in figure 3 but with Beltrami parameters $a = -5.0$ and $b = -0.20$, implying the normalized eigenvalues of $\lambda_\pm = \pm 0.9165i$.

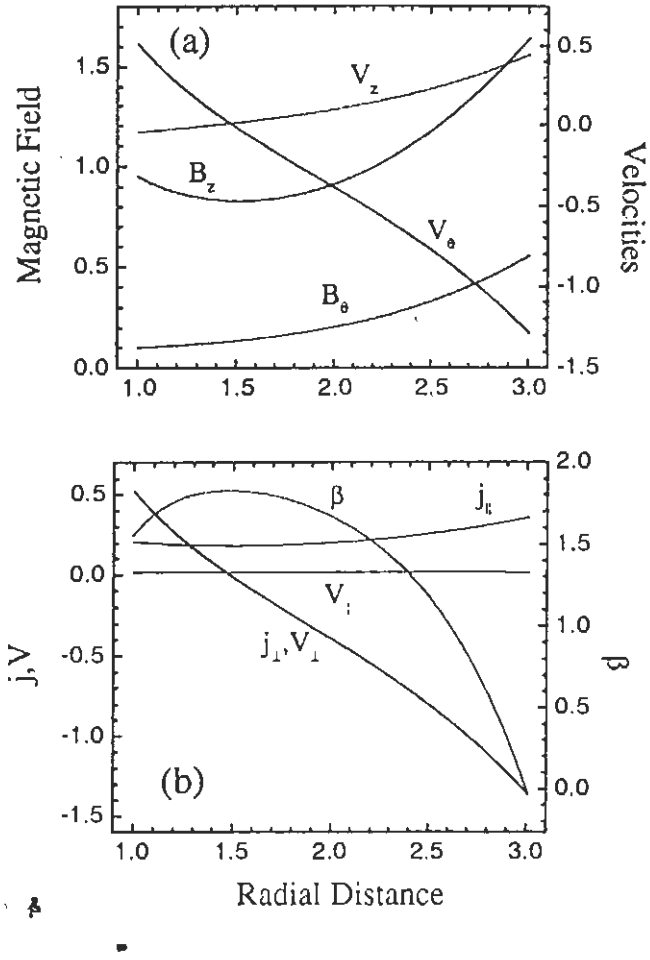

Figure 4-10: The same as in figure 4 but with Beltrami parameters $a = -5.0$ and $b = 0.0$. The normalized eigenvalues are complex conjugate pair $\lambda_\pm = 0.102 \pm 0.9948i$.

4.3.2 Optimization of β and Parallel Components of flow

To search for the appropriate parameters and boundary conditions for higher values of β, we have optimized the system for real values of scale parameters λ_+ and λ_-. Figure (4-11) shows a plot of maximum value of β versus $B_z(r=1)=g$, $B_\theta(r=1)=h$, $j_z(r=1)=s$ and $j_\theta(r=1)=k$ for constant values of $a=4.9$ and $b=1.8$. We have considered the absolute value of β. Curve "g" shows the maximum value of β for different values of g, keeping other parameters $h=0.10$, $s=0.15$ and $k=0.54$ as fixed. Curve labelled as "h" represent the maximum value of β for changing values of h and keeping $g=1.00$, $s=0.15$ and $k=0.05$ as fixed. Curve denoted by "s" depicts the maximum value of β for fixed values of $g=1.00$, $h=0.10$ and $k=0.54$ and varying the values of s. The maximum value of β for different values of k, for constant parameters $g=1.00$, $h=0.10$ and $s=0.15$ is shown by the curve labelled as "k". It is evident from figure (4-11) that maximum value of β can be achieved by choosing higher boundary values of g and smaller values of h, s, and k.

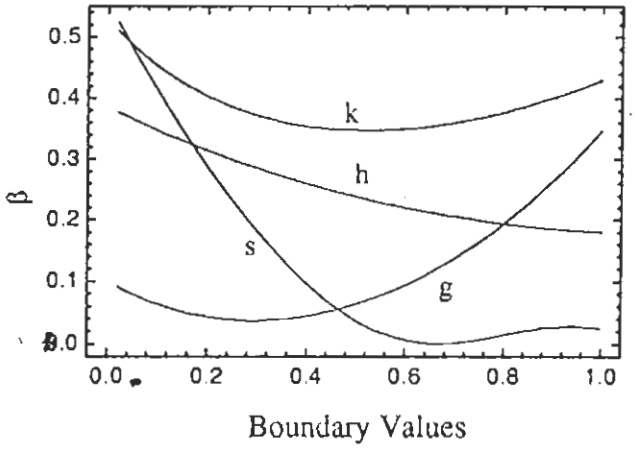

Figure 4-11: A radial profile of maximum β vs different boundary values for constant Beltrami parameters $a=4.9$ and $b=1.8$.

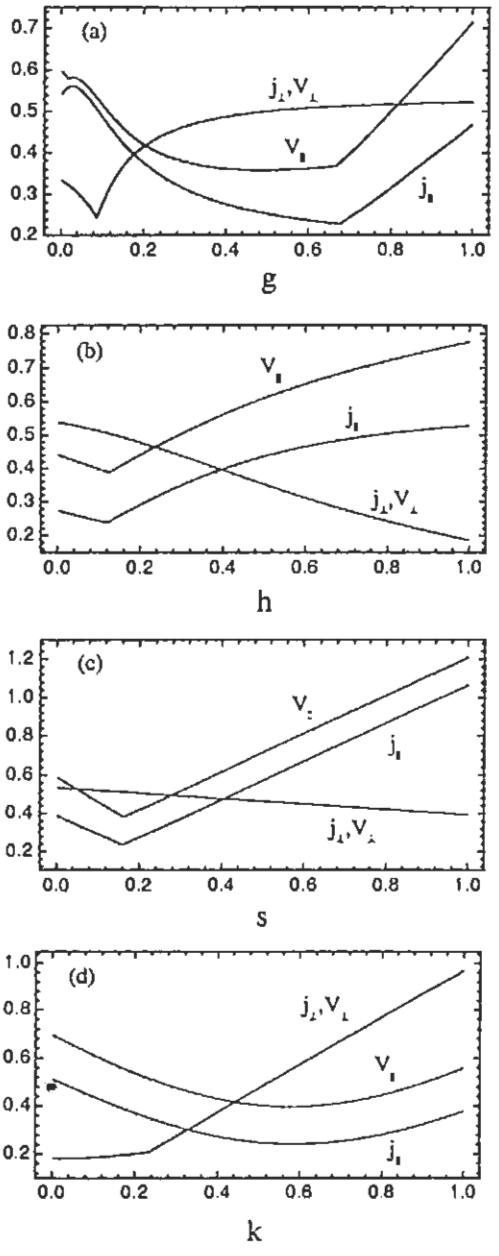

Figure 4-12: A radial graph of maximum values of parallel and perpendicular components vs boundary values for constant parameters $a = 4.9$ and $b = 1.8$.

In figure (4-12), maximum values of parallel and perpendicular components of flows and currents vs different values of boundary conditions g, h, s and k, for constant values of $a = 4.9$ and $b = 1.8$ are plotted. Figure (4-12 (a)), plot of parallel and perpendicular components of flow and current versus g, keeping other parameters $h = 0.10$, $s = 0.15$ and $k = 0.54$ as constant, indicate that for boundary value of g in between 0.21 and 0.84, parallel components have less values as compared to other components. In figure (4-12 (b)), maximum values of parallel and perpendicular components of flow and current for different values of h taking 0.7, 0.15 and 0.54 as values of g, s and k respectively as constant are shown. This figure depicts that for the boundary value of h lower than 0.24, perpendicular components of flows and currents are of higher values than that of parallel components. Figure (4-12 (c)) showing plot of said components vs different values of s for constant value of $g = 0.7$, $h = 0.10$ and $k = 0.54$ illustrates that perpendicular components have higher maximum values for s ranging from 0.04 and 0.28. Figure (4-12 (d)) shows the maximum values of perpendicular components of flows and currents for values of k greater than 0.44 are higher as compared to parallel components of flows and currents for constant values of $g = 0.7$, $h = 0.10$ and $s = 0.15$.

In the next section we would describe the comparison of two systems that is simple cylindrical and internal conductor plasma systems.

4.3.3 Comparison of Cylindrical and Annular Systems

• Introducing internal conductor at the center of simple plasma system converts it into an internal conductor plasma system. Physically the difference between the simple cylindrical plasma system and the internal conductor cylindrical plasma system is the internal conductor. The internal conductor produces azimuthal magnetic field whereas a simple cylinder produces no poloidal magnetic field at the center. Mathematically, solution of the two systems differ by Bessel function of second kind. In case of simple cylinder, solution consists of only Bessel functions of first kind because the Bessel function of second kind $Y_m(r)$ are infinite at the center of the cylinder where $r = 0$. When internal conductor of radius d is placed at the center, the solution consists of Bessel functions of both first and second kind. Therefore, mathematically, the difference between these systems are the Bessel function of second kind. The two systems become equivalent if $C_1 = P_1$, $C_2 = Q_1$ and P_2 and Q_2 are identically zero. $C_1 = P_1$, gives the

condition

$$2/\pi\lambda_+ d = \frac{k-\lambda_- h}{s-\lambda_- g} Y_0(\lambda_+ d) - Y_1(\lambda_+ d). \tag{4.32}$$

When $C_2 = Q_1$ gives

$$2/\pi\lambda_- d = \frac{\lambda_+ h - k}{\lambda_+ g - s} Y_0(\lambda_- d) - Y_1(\lambda_- d). \tag{4.33}$$

Further, $P_2 = 0$ yields

$$\frac{k-\lambda_- h}{s-\lambda_- g} = \frac{J_1(\lambda_+ d)}{J_0(\lambda_+ d)}, \tag{4.34}$$

and $Q_2 = 0$ give the result

$$\frac{k-\lambda_+ h}{s-\lambda_+ g} = \frac{J_1(\lambda_- d)}{J_0(\lambda_- d)}. \tag{4.35}$$

Plugging in the values of (4.34) in (4.32), we obtain

$$J_0(\lambda_+ d) = 1. \tag{4.36}$$

Throughout the space, $J_0(\lambda_+ d) = 1$ only if $\lambda_+ d = 0$.

For $\lambda_+ \neq 0$, we get $d = 0$. Similarly putting value of (4.35) into (4.33), we obtain $d = 0$ taking $\lambda_- \neq 0$. Hence we conclude that both the systems are identically the same under the above imposed conditions and there is no internal conductor due to $d = 0$.

• For a simple cylindrical plasma system, it is impossible to have $|j_\perp|$ and $|V_\perp|$ greater than $|j_\parallel|$ and $|V_\parallel|$ respectively throughout the system. For this system $|j_\perp|(r=0) = |V_\perp|(r=0) = 0$ whereas $|j_\parallel|(r=0) = s$ and $|V_\parallel|(r=0) = s + 1/a$. Hence the perpendicular components of both the current and the flows are always zero at the center of the simple cylindrical plasma system; whereas for the case of internal conductor system, the perpendicular components may have some finite values and for certain boundary conditions and scale parameters, could have higher values than the parallel components.

• For the internal conductor system, we have some extra boundary conditions and as a consequence of these extra degrees of freedom, we can control the whole system very effectively. Pressure inside the internal conductor system can be handled easily by varying the current in the internal conductor. Central pressure can be minimized at the radius of the internal conductor and hollow profile of pressure can be obtained very easily. On the other hand, simple cylindrical plasma system having fewer boundary conditions can not be controlled so effectively.

It is difficult using the simple cylindrical configuration to minimize the pressure at the center and edge simultaneously with a hollow profile of pressure.

The internal conductor plasma configuration based on double curl Beltrami equation has been studied and compared with the simple cylindrical plasma system. The system is optimized and for certain Beltrami parameters and boundary conditions, ultra-high β relaxed states can be obtained for small values of parallel components of flows and currents. The parallel current due to electrons does not seem to make any contribution to the gradient in pressure. This is in contrast with the case of single Beltrami system, wherein large values of $j_{\parallel}$ occur and thus only a very small β is achievable - a highly undesirable circumstance for fusion concept. On the other hand, perpendicular components of flow and current contribute substantially to the pressure gradient and play a paramount role in plasma confinement. Our numerical results based on double curl Beltrami treatment demonstrate the possibility of creating ultra-high β relaxed states with minimum values of parallel components of current and flows. Although a complete analysis of stability requires a detailed analytical as well as numerical study which is beyond the scope of the present work. The emergence of a hollow profile of β may improve the stability of the relaxed states. Specifically, the fall of β value towards the edge where the flow velocity increases may stabilize the ballooning modes [71, 72]. The minimization of parallel components of flow and current as shown in Figs. (4-9) and (4-10) may reduce the current driven instabilities in the plasma system. Minimization of parallel components is also very helpful in maintaining helicity as an invariant of the system. Our numerical results based on double curl Beltrami treatment give us values of $j_{\perp}$ and $V_{\perp}$ higher than that of parallel components throughout the system whereas for simple cylindrical system we can not sustain the dominance of perpendicular components throughout the system. The present analysis would be very useful to study different features of high-β relaxed states of the plasma using internal conductor plasma configuration.

Chapter 5

Catastrophic Change of Relaxed Equilibria

So far, the relaxed equilibrium based on double Beltrami fields using different boundary conditions and Beltrami parameters is studied. In this chapter, we will take into account the ideal invariants (helicities and energy) of the system to study the relaxed equilibria. The double Beltrami fields are characterized by four parameters (two amplitudes $c_{\pm}$ and two eigenvalues of the curl operator $\lambda_{\pm}$). A set of algebraic equations relating these parameters with the macroscopic constants of motion is derived and the system is analyzed to study the loss of equilibrium. This study is important to understand the relaxed equilibria in different fusion oriented devices and bears a potential relevance to the solar eruptive events which results mainly from a sudden release of energy. The solutions of Beltrami fields are widely used to model the magnetic fields of a solar active region, and such an example is presented in section (2.4). The solar eruptive events such as solar flares, eruptive prominences, and coronal mass ejections are associated with the catastrophic behavior of an equilibrium (termination of an equilibrium sequence), or an instability [73]. The loss of equilibrium is considered to be more appropriate to cause eruption in the solar corona rather than the onset of a linear instability. The catastrophe corresponding to bifurcation or loss of equilibrium has been followed by several authors to account for the triggering of eruptions in the corona [74]-[77]. The catastrophe is defined as a critical behavior in the equilibrium evolution characterized by a monotonically changing control parameter, which

in many cases corresponds only to an equilibrium bifurcation.

In order to study the catastrophic change of solutions permitted by double Beltrami (DB) fields, let us consider a quasi-equilibrium state of a structure associated with a slowly changing double Beltrami state. The parameter change is also assumed to be sufficiently slow so that at each stage, the system can find its local DB equilibrium (adiabatic evolution). The slow evolution is considered to conserve the dynamical invariants: the helicity h_1, the generalized helicity h_2, and the total (magnetic plus fluid) energy E. The problem of predicting catastrophe in the equilibrium evolution reduces to finding the range, if any, in which the slowly evolving structure may suffer a loss of equilibrium. The signature of the loss of equilibrium is quite easy to identify for the double Beltrami states. The slowly evolving structure may find itself in a state of no equilibrium in one of the following two ways:

(1) When roots of the quadratic equation, determining the length scales for the field variation, go from being real to complex. This imply a change in the topology of the magnetic and velocity fields where paramagnetic structures are changed to diamagnetic (see Fig. (3-1)).

(2) The amplitude of either of the two states ceases to be real.

In the next section, we will summarize the basic relations between the Beltrami parameters a, b and the eigenvalues of the curl operator $\lambda_{\pm}$.

5.1 Double Beltrami Fields

Let us suppose that the given structure corresponds to the equilibrium solution of the following vortex dynamic equation for the two-fluid system (see Sec. (3.4)),

$$\frac{\partial \omega_j}{\partial t} - \nabla \times (\mathbf{U}_j \times \omega_j) = 0, \tag{5.1}$$

where ω_j represents a pair of generalized vorticities $\omega_1 = \mathbf{B}$, $\omega_2 = \mathbf{B} + \nabla \times \mathbf{V}$, and $\mathbf{U}_j$ represent a pair of effective flows $\mathbf{U}_1 = \mathbf{V} - \nabla \times \mathbf{B}$, $\mathbf{U}_2 = \mathbf{V}$. The magnetic field $\mathbf{B}$ is the normalized magnetic field with some arbitrary B_0 and $\mathbf{V}$ is the normalized velocity with Alfvén speed. The simplest and perhaps the most fundamental equilibrium solution to (5.1) given by the "Beltrami

condition", leads to a system of simultaneous linear equation in $\mathbf{B}$ and $\mathbf{V}$ as

$$\mathbf{B} = a(\mathbf{V} - \nabla \times \mathbf{B}), \tag{5.2}$$

$$b\mathbf{V} = (\mathbf{B} + \nabla \times \mathbf{V}), \tag{5.3}$$

where a and b are constants. Combining (5.2) and (5.3) yields a second order partial differential equation either in $\mathbf{B}$ or $\mathbf{V}$ as

$$\nabla \times \nabla \times \mathbf{B} - (b - \tilde{a})\nabla \times \mathbf{B} + (1 - \tilde{a}b)\mathbf{B} = 0, \tag{5.4}$$

where $\tilde{a} = 1/a$. Equation (5.4) can also be written as

$$(\text{curl} - \lambda_+)(\text{curl-}\lambda_-)\mathbf{B} = 0, \tag{5.5}$$

where

$$\lambda_\pm = \frac{1}{2}\left[(b - \tilde{a}) \pm \sqrt{(b + \tilde{a})^2 - 4}\right]. \tag{5.6}$$

The Beltrami parameters a, b and the eigenvalues of the curl operator $\lambda_\pm$ also satisfy the following relations.

$$(\lambda_+ + \tilde{a})^{-1} = (\lambda_- + \tilde{a}), \tag{5.7}$$

$$\lambda_+ + \lambda_- = b - \tilde{a}, \tag{5.8}$$

$$\lambda_+\lambda_- = 1 - b\tilde{a}, \tag{5.9}$$

$$\tilde{a} = \frac{1}{2}\left[-(\lambda_+ + \lambda_-) \pm \sqrt{(\lambda_+ - \lambda_-)^2 + 4}\right], \tag{5.10}$$

$$b = \frac{1}{2}\left[(\lambda_+ + \lambda_-) \pm \sqrt{(\lambda_+ - \lambda_-)^2 + 4}\right]. \tag{5.11}$$

Since the operators $(\text{curl} - \lambda_\pm)$ commute, the general solution to the "double Beltrami equation" (5.5) is given by the linear combination of two Beltrami fields. Let $\mathbf{G}_\pm$ be the Beltrami field such that

$$\begin{cases} (\text{curl} - \lambda_\pm)\mathbf{G}_\pm = 0, \\ \mathbf{n} \cdot \mathbf{G}_\pm = 0 \qquad \text{(on the surface)}. \end{cases}$$

where v ($\subset \mathrm{R}^3$) is a bounded domain with a smooth boundary s and $\mathbf{n}$ is the unit normal vector onto s. Then

$$\mathbf{B} = c_+\mathbf{G}_+ + c_-\mathbf{G}_- \tag{5.12}$$

with c_+ and c_- as constants, solves (5.5). The corresponding flow using (5.2) is given by

$$\mathbf{V} = (\lambda_+ + \tilde{a})c_+\mathbf{G}_+ + (\lambda_- + \tilde{a})c_-\mathbf{G}_-. \tag{5.13}$$

In order to consider about an equilibrium bifurcation, in the next section, we will derive a set of algebraic relations that express equilibriums in terms of the macroscopic constants of motion.

5.2 Conservation Laws for Double Beltrami Fields

MHD theory give rise to a number of globally conserved physical quantities. Helicity is an important conserved physical quantity in MHD theory and characterizes the topology of a vector field, for example, that of the magnetic field $\mathbf{B} = \nabla \times \mathbf{A}$ in plasmas. Helicity is used to quantify the field properties such as linking, knotting, twisting, writhing, braiding, etc. Helicity properties are widely used to study space plasma physics (solar flares [78, 79], reconnection [80], dynamos [81, 82], turbulence [83]), magnetic confinement devices (tokamaks [84], spheromaks [85, 86], reverse-field pinches [87]), and in basic plasma physics (electron magnetohydrodynamics (EMHD) vortices [88]). In ideal (collision-less) plasmas, magnetic energy and helicities are conserved whereas in nonideal plasmas, due to Taylor's conjecture, magnetic helicity relaxes at a slower rate than energy when the dissipation is highly localized e.g., in current sheets. The conservation of helicity applies for a general vortex dynamics. For the vorticity ω_j that satisfies (5.1) and the boundary condition

$$\mathbf{n} \times (\mathbf{U}_j \times \omega_j) = 0 \quad (\text{on } s),$$

the general helicity is defined as

$$h_j = \frac{1}{2}\int_v (\mathrm{curl}^{-1}\omega_j) \cdot \omega_j dv,$$

where curl^{-1} is the inverse operator of the curl that is represented by the Biot-Savart integral [89]. The relaxation model [37] based on double Beltrami fields supports three invariants of motion: the magnetic helicity h_1, the generalized helicity h_2, and the total magnetofluid energy E, i.e., the sum of kinetic and magnetic energies, defined as

$$h_1 = \frac{1}{2}\int_v \mathbf{A}\cdot\mathbf{B}dv, \tag{5.14}$$

$$h_2 = \frac{1}{2}\int_v (\mathbf{A}+\mathbf{B})\cdot(\mathbf{B}+\nabla\times\mathbf{V})dv, \tag{5.15}$$

$$E = \frac{1}{2}\int_v (\mathbf{B}^2+\mathbf{V}^2)dv, \tag{5.16}$$

where $\mathbf{A}$ is the vector potential. Using these three constants of motion, and choosing λ_+ as a "control parameter" characterizing the length scale of the larger structure (assuming $|\lambda_+| < |\lambda_-|$), we can cast the analysis of double Beltrami fields into algebraic relations. In a cylindrical geometry, the Beltrami fields are expressed by Chandrasekhar-Kendall function. For the axisymmetric solution, we have

$$\mathbf{G}_\pm = \begin{pmatrix} J_1(\lambda_\pm r) \\ J_0(\lambda_\pm r) \end{pmatrix}, \tag{5.17}$$

where J's are ordinary Bessel functions with the subscripts indicating the order.

Using the above equation (5.17) in (5.12) and (5.13), the vector potential $\mathbf{A}$ and vorticity $\nabla\times\mathbf{V}$ can be calculated respectively and are given by

$$\mathbf{A} = \frac{1}{\lambda_+}c_+\mathbf{G}_+ + \frac{1}{\lambda_-}c_-\mathbf{G}_-, \tag{5.18}$$

$$\nabla\times\mathbf{V} = \lambda_+(\lambda_+ + \tilde{a})c_+\mathbf{G}_+ + \lambda_-(\lambda_- + \tilde{a})c_-\mathbf{G}_-. \tag{5.19}$$

We consider a cylindrical volume of radius R and length $L = 2\pi n_\pm/\lambda_\pm$ ($n_\pm$ are integers and only real values of $\lambda_\pm$ are considered). Putting the values of $\mathbf{A}$ and $\mathbf{B}$ in (5.14), we get

$$\begin{aligned} h_1 = {} & \frac{L\pi c_+^2}{\lambda_+}\int_0^R J_1^2(\lambda_+ r)\,rdr + \frac{L\pi c_-^2}{\lambda_-}\int_0^R J_1^2(\lambda_- r)\,rdr \\ & + \frac{L\pi c_+^2}{\lambda_+}\int_0^R J_0^2(\lambda_+ r)\,rdr + \frac{L\pi c_-^2}{\lambda_-}\int_0^R J_0^2(\lambda_- r)\,rdr, \end{aligned}$$

$$= \frac{L\pi c_+^2}{\lambda_+}\left[-\frac{R}{\lambda_+}J_1(\lambda_+R)\,J_0(\lambda_+R)+R^2J_0^2(\lambda_+R)+R^2J_1^2(\lambda_+R)\right]$$
$$+\frac{L\pi c_-^2}{\lambda_-}\left[-\frac{R}{\lambda_-}J_1(\lambda_-R)\,J_0(\lambda_-R)+R^2J_0^2(\lambda_-R)+R^2J_1^2(\lambda_-R)\right] \qquad (5.20)$$

Similarly putting the values of **A**, **B**, **V** and $\nabla \times \mathbf{V}$ in (5.15), we get

$$\begin{aligned}\tilde{h}_2 &= L\pi c_+^2(\lambda_+ + \tilde{a})\,(2+\lambda_+(\lambda_+ + \tilde{a}))\int_0^R \left(J_1^2(\lambda_+r)+J_0^2(\lambda_+r)\right) r\,dr \\ &\quad + L\pi c_-^2(\lambda_- + \tilde{a})\,(2+\lambda_-(\lambda_- + \tilde{a}))\int_0^R \left(J_1^2(\lambda_-r)+J_0^2(\lambda_-r)\right) r\,dr \\ &= L\pi c_+^2(\lambda_+ + \tilde{a})\,(2+\lambda_+(\lambda_+ + \tilde{a}))\left[-\frac{R}{\lambda_+}J_1(\lambda_+R)\,J_0(\lambda_+R)\right. \\ &\quad \left. + R^2J_0^2(\lambda_+R)+R^2J_1^2(\lambda_+R)\right] + L\pi c_-^2(\lambda_- + \tilde{a})\,(2+\lambda_-(\lambda_- + \tilde{a}))\times \\ &\quad \left[-\frac{R}{\lambda_-}J_1(\lambda_-R)\,J_0(\lambda_-R)+R^2J_0^2(\lambda_-R)+R^2J_1^2(\lambda_-R)\right], \qquad (5.21)\end{aligned}$$

and putting the values of **B** and **V** in (5.16), we get

$$\begin{aligned}E &= L\pi c_+^2\left(1+(\tilde{a}+\lambda_+)^2\right)\int_0^R \left(J_1^2(\lambda_+r)+J_0^2(\lambda_+r)\right) r\,dr \\ &\quad + L\pi c_-^2\left(1+(\tilde{a}+\lambda_-)^2\right)\int_0^R \left(J_1^2(\lambda_-r)+J_0^2(\lambda_-r)\right) r\,dr, \\ &= L\pi c_+^2\left(1+(\tilde{a}+\lambda_+)^2\right)\left[-\frac{R}{\lambda_+}J_1(\lambda_+R)\,J_0(\lambda_+R)\right. \\ &\quad \left. + R^2J_0^2(\lambda_+R)+R^2J_1^2(\lambda_+R)\right] + L\pi c_-^2\left(1+(\tilde{a}+\lambda_-)^2\right)\times \\ &\quad \left[-\frac{R}{\lambda_-}J_1(\lambda_-R)\,J_0(\lambda_-R)+R^2J_0^2(\lambda_-R)+R^2J_1^2(\lambda_-R)\right], \qquad (5.22)\end{aligned}$$

In evaluating above integrals we have used the relation

$$\int_0^R rJ_1(\lambda_+R)\,J_0(\lambda_-R)\,dr = 0 \qquad \text{for } \lambda_+ \neq \lambda_-. \qquad (5.23)$$

Considering cylindrical plasma of unit radius and unit length, the macroscopic constants of motion h_1, $\tilde{h}_2(=h_2-h_1)$ and E from equations (5.20), (5.21), and (5.22) respectively read

$$h_1 = \pi\left[\frac{Mc_+^2}{\lambda_+}+\frac{Nc_-^2}{\lambda_-}\right], \qquad (5.24)$$

$$\tilde{h}_2 = \pi c_+^2\left[2+\lambda_+(\tilde{a}+\lambda_+)\right](\tilde{a}+\lambda_+)\,M \qquad (5.25)$$

$$+\pi c_-^2 \left[2+\lambda_- \left(\tilde{a}+\lambda_-\right)\right]\left(\tilde{a}+\lambda_-\right) N, \tag{5.26}$$

$$E = \pi c_+^2 \left[1+\left(\tilde{a}+\lambda_+\right)^2\right] M \tag{5.27}$$

$$+\pi c_-^2 \left[1+\left(\tilde{a}+\lambda_-\right)^2\right] N, \tag{5.28}$$

where

$$M = J_0^2(\lambda_+) + J_1^2(\lambda_+) - \lambda_+^{-1} J_0(\lambda_+) J_1(\lambda_+), \tag{5.29}$$

$$N = J_0^2(\lambda_-) + J_1^2(\lambda_-) - \lambda_-^{-1} J_0(\lambda_-) J_1(\lambda_-). \tag{5.30}$$

In the proceeding calculations to derive the general expression for general equilibrium, we will use the above mentioned relations of Beltrami parameters and eigenvalues. Using these relations, it turns out that $\tilde{h}_2$ of (5.26) can be easily expressed in terms of h_1, E, λ_+, λ_- (h_1, E, a, b). We notice

$$\begin{aligned}
\tilde{h}_2 &= \pi c_+^2 \left[2\left(\tilde{a}+\lambda_-\right)+\lambda_+\right]\left(\tilde{a}+\lambda_+\right)^2 M \\
&\quad +\pi c_-^2 \left[2\left(\tilde{a}+\lambda_+\right)+\lambda_-\right]\left(\tilde{a}+\lambda_-\right)^2 N
\end{aligned}$$

$$\begin{aligned}
&= \pi c_+^2 \left(\lambda_- + b + \tilde{a}\right)\left(\lambda_+ + \tilde{a}\right)^2 M \\
&\quad +\pi c_-^2 \left(\lambda_+ + b + \tilde{a}\right)\left(\lambda_- + \tilde{a}\right)^2 N
\end{aligned}$$

$$\begin{aligned}
&= \pi c_+^2 \left[b\left(\lambda_+ + \tilde{a}\right)^2 + \left(\lambda_+ + \tilde{a}\right)\right] M \\
&\quad +\pi c_-^2 \left[b\left(\lambda_- + \tilde{a}\right)^2 + \left(\lambda_- + \tilde{a}\right)\right] N
\end{aligned}$$

$$\begin{aligned}
&= \pi c_+^2 \left[b\left(\lambda_+ + \tilde{a}\right)^2 + \left(b - \lambda_-\right)\right] M \\
&\quad +\pi c_-^2 \left[b\left(\lambda_- + \tilde{a}\right)^2 + \left(b - \lambda_+\right)\right] N
\end{aligned}$$

$$\begin{aligned}
\tilde{h}_2 &= b\left\{\pi c_+^2 \left[1+\left(\lambda_+ + \tilde{a}\right)^2\right] M \right. \\
&\quad \left. +\pi c_-^2 \left[1+\left(\lambda_- + \tilde{a}\right)^2\right] N\right\}
\end{aligned}$$

$$-\pi\lambda_+\lambda_-\left[\frac{Mc_+^2}{\lambda_+}+\frac{Nc_-^2}{\lambda_-}\right]$$

$$\tilde{h}_2 = bE-\lambda_+\lambda_-h_1, \tag{5.31}$$

which can be cast in several equivalent forms

$$h_2 = h_1+\hat{h}_2 = b\,(E+h_1\tilde{a})\,, \tag{5.32}$$

$$\tilde{h}_2 = \frac{E}{2}\left[(\lambda_++\lambda_-)\pm\sqrt{(\lambda_+-\lambda_-)^2+4}\right] -\lambda_+\lambda_-h_1. \tag{5.33}$$

For a given set of h_1, E, $\tilde{h}_2$ (h_2) and λ_+ (control parameter), we solve (5.33) to find λ_-. Here we assume that L is sufficiently large, so that $\lambda_\pm$ ($=n_\pm/L$) can take continuous real values. It is evident from [35]-[38] that the equilibrium given by (5.32) makes the free energy zero.

$$E-\tilde{a}h_1+\frac{h_2}{b}=0. \tag{5.34}$$

From (5.24) and (5.28), c_+ and c_- are now given by

$$c_+^2 = \frac{1}{\pi MD}\left\{-E+\left[1+(\lambda_-+\tilde{a})^2\right]\lambda_-h_1\right\}\lambda_+, \tag{5.35}$$

$$c_-^2 = \frac{1}{\pi ND}\left\{E+\left[1+(\lambda_++\tilde{a})^2\right]\lambda_+h_1\right\}\lambda_-, \tag{5.36}$$

where

$$\begin{aligned} D &= -\lambda_-\left[1+(\lambda_-+\tilde{a})^2\right]-\lambda_+\left[1+(\lambda_++\tilde{a})^2\right] \\ &= (\lambda_--\lambda_+)\,b(b+\tilde{a}). \end{aligned} \tag{5.37}$$

For given h_1, $\tilde{h}_2$ (h_2), E and λ_+ (control parameter), the preceding system can be solved to determine the physical quantities λ_-, and $c_\pm^2$ which must all remain real for an equilibrium. The expressions for the kinetic energy E_k and the magnetic energy E_B of the magnetofluid read

respectively as

$$E_k = |V|^2 = \pi c_+^2 (\lambda_+ + \tilde{a})^2 M + \pi c_-^2 (\lambda_- + \tilde{a})^2 N, \tag{5.38}$$

$$E_B = |B|^2 = \pi c_+^2 M + \pi c_-^2 N. \tag{5.39}$$

In the next section, we will study the relaxed equilibria admitted by the above mentioned expressions for different values of helicities and energy.

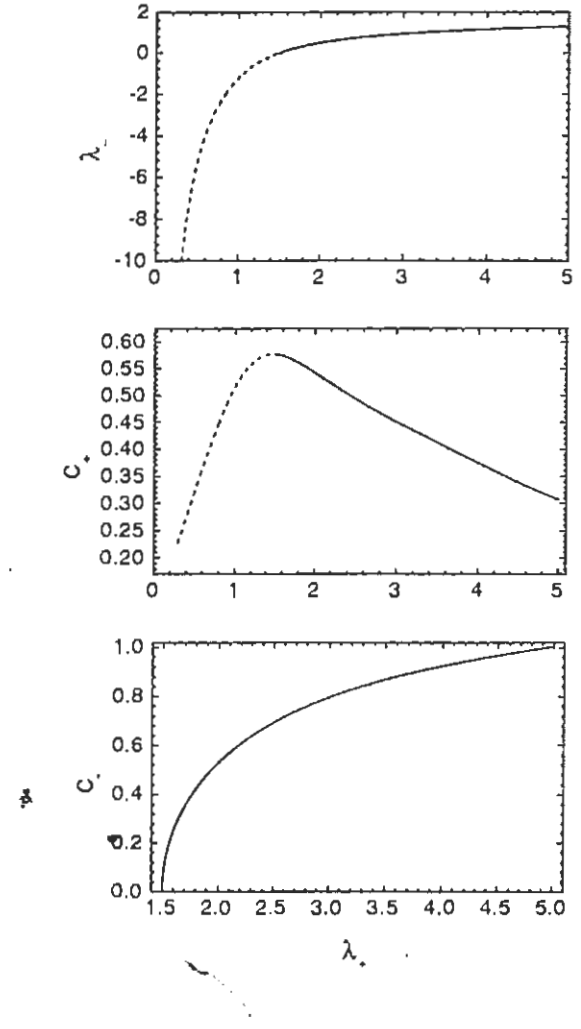

Figure 5-1: Variation of λ_- and $c_\pm$ corresponding to length scale of λ_+ in the case of $h_1 = 1, h_2 = 5$, and $E = 2$.

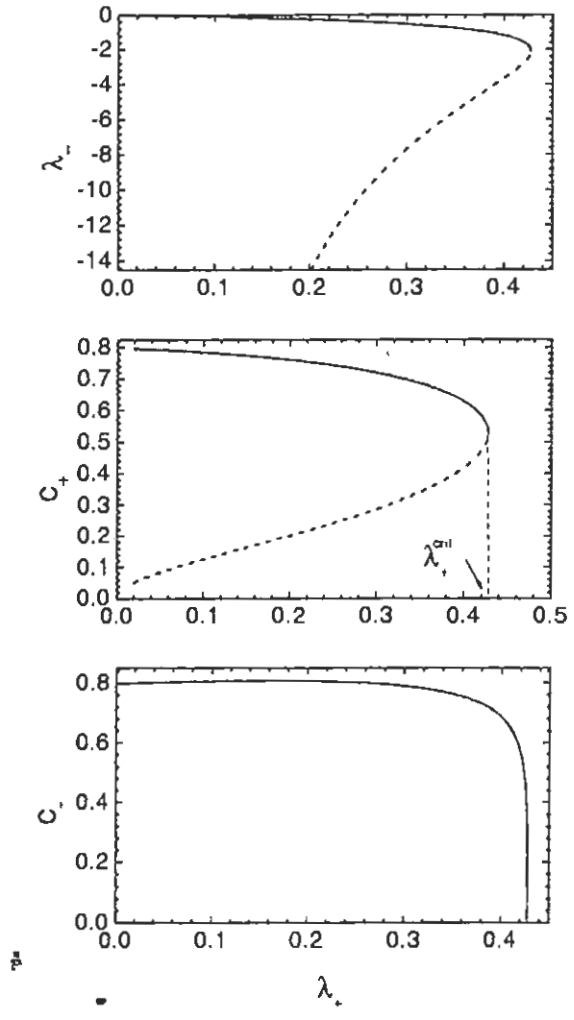

Figure 5-2: Variation of λ_- and $c_\pm$ corresponding to length scale of λ_+ for the case of $h_1 = 1, h_2 = 5$, and $E = 4$.

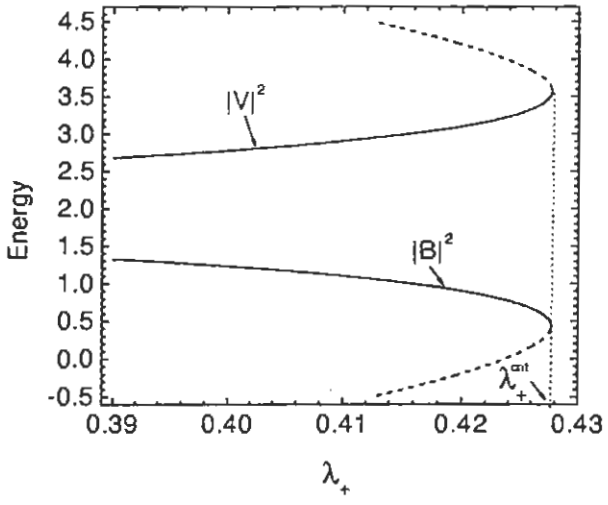

Figure 5-3: Magnetic field and flow energies corresponding to length scale of λ_+ for the case of $h_1 = 1, h_2 = 5$, and $E = 4$.

5.3 Analysis of Relaxed Equilibria

In this section, variations of λ_-, c_+, and c_- by changing the control parameter λ_+ for constant helicities and energy are discussed. The solutions expressed by (5.6), (5.35), and (5.36) are plotted in figures (5-1) - (5-5) where λ_+ is taken as abscissa and corresponding values of λ_- and $c_\pm$ as ordinate. Dashed lines of λ_- and c_+ in these figures express regions of imaginary c_-. In the first two figures h_1 and h_2 are taken as constant whereas energy is varied. In figure (5-1), constant of motions are taken as $h_1 = 1$, $h_2 = 5$, $E = 2$ whereas in figure (5-2), $h_1 = 1$, $h_2 = 5$, $E = 4$. These figures depict that the solutions strongly depends on E i.e., solution behavior changes drastically depending on E. Figure (5-1) shows the continuous variation of λ_- and $c_\pm$ for different values of λ_+. It indicates that a continuous change of the scale of the loop λ_+^{-1} causes only a change in the physical values and equilibrium of the loop is unaffected. It means in this case equilibrium of the loop is preserved subject to different amplitudes and eigenvalues (for small λ_+, however, c_- is imaginary). In contrast, the situation depicted in figure (5-2) is quite different, there is a loss of equilibrium when λ_+ is larger than λ_+^{crit} i.e., when length scale

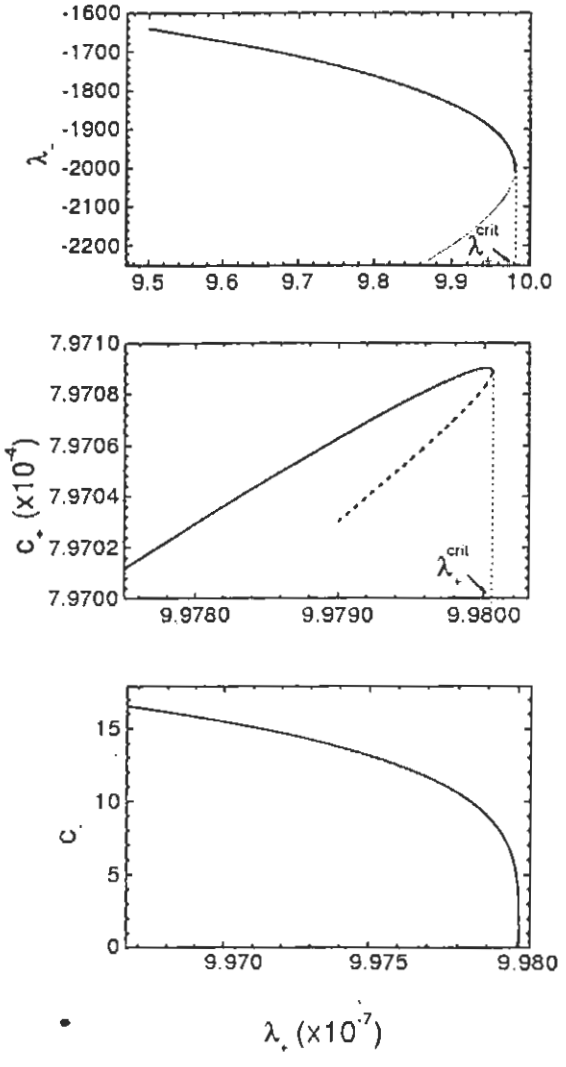

Figure 5-5: Variation of λ_- and $c_\pm$ corresponding to length scale of λ_+ for the case of $h_1 = 1$, $h_2 = 1.004$, and $E = 4$.

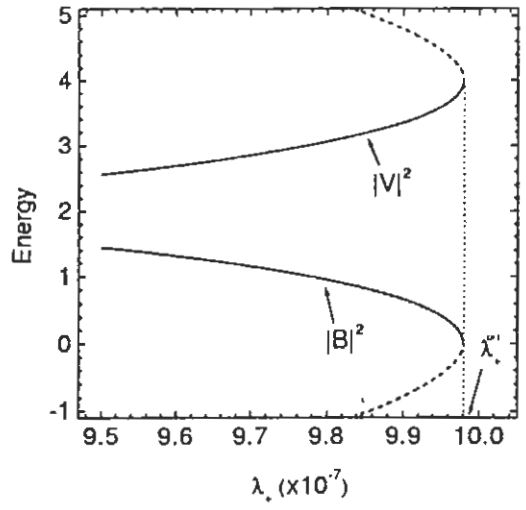

Figure 5-6: Magnetic field and flow energies corresponding to length scale of λ_+ for the case of $h_1 = 1, h_2 = 1.004$, and $E = 4$.

becomes small.

The behaviors of magnetic field energy $|\mathbf{B}|^2$ and flow energy $|\mathbf{V}|^2$ for $h_1 = 1$, $h_2 = 5$, and $E = 4$ are shown in figure (5-3). We observe that at the critical value of control parameter λ_+, magnetic field energy becomes minimum while flow energy attains higher values.

In figures (5-2-5-4), h_1 and E are taken as constant while h_2 is changed. We observe from these two figures that there is no solution (catastrophic loss of equilibrium) for small $\tilde{h}_2$ when the length scale is decreased (flux loops are compressed) beyond a limit.

5.4 Application to Solar Corona

Figure (5-5) shows an example of large scale events (small λ_+) for $h_1 = 1$, $h_2 = 1.004$ and $E = 4$. In this case, the two length scales ($\lambda_\pm$) associated with two different Beltrami fields are quite disparate. The scale of the structure in this case is $l_i/\lambda_+ \sim 10^4$ (km) where l_i represents ion skin depth of the solar corona and is taken to be ~ 10 (m). This scale is appropriate to the coronal loops. To conclude, we find that a decrease in length scale give rise to a loss of

equilibrium where λ_+ reaches to a certain critical value and loops are compressed.

Figure (5-6) shows the energy behaviors with respect to λ_+ for this case. This figure also shows that with the increase in length scale, magnetic field energy decreases and at the critical value of λ_+ where equilibrium is lost, becomes minimum. On the other hand, flow energy increases with scale length and at λ_+^{crit} attains maximum value.

This catastrophic behavior can be used to study the eruptive events in the solar corona. The set of algebraic relations describing the relaxed equilibria in terms of the invariants of the system can also be employed to investigate the equilibrium in different magnetic configurations that are of interest for fusion applications.

Chapter 6

Summary and Conclusions

In this thesis, the relaxed states of MHD plasmas using different models have been studied. There is a strong theoretical, computational and experimental evidence of rapid relaxation in continuous media and turbulent fluids. In the absence of flow energy, the relaxed magnetic field B satisfy the "Beltrami condition"

$$\nabla \times \mathrm{B} = \lambda \mathrm{B}, \tag{6.1}$$

where λ is a scalar field that must satisfy $\mathrm{B} \cdot \nabla\lambda = 0$ to insure $\nabla \cdot \mathrm{B} = 0$. Since the associated Lorentz force ($\mathrm{j} \times \mathrm{B}$) is identically zero, the Beltrami magnetic field represents a flow-less and force-free macroscopic state of the magnetofluid.

Due to force-free feature of Beltrami magnetic field, it has been extensively used to study the relaxation in the solar corona and the evolution of arcade structures of magnetic fields in the corona. Using well-known ABC flow as a solution of Beltrami magnetic field, we have studied the arcade structure of magnetic fields in the corona as shown in figure (2-2) for the two-dimensional case. For three-dimensional case, the magnetic fields represent chaotic behavior as depicted in figure (2-3).

Woltjer derived (6.1) by minimizing the magnetic energy with the constraint that the local magnetic helicity is conserved. Taylor introduced the far-reaching concept of relaxation: He conjectured that a small amount of resistivity present in a realistic plasma would tend to relax all the local helicity constraints leaving only the conservation of global helicity intact. The minimization of the field energy with the global constraint, then, leads to the "relaxed state"

characterized by a spatially homogeneous λ in (6.1) i.e., a "constant-λ Beltrami field".

In 1974, Taylor found an application of his theory to reversed-field pinch (RFP), an experimental configuration of contemporary interest to magnetic fusion physicists. After that Taylor's theory has been paid much attention and extensively used to study plasma relaxation in space and in a variety of plasma devices. Although this theory accounts at least qualitatively (and often quantitatively) for many of the observed properties of laboratory and astrophysical plasmas yet it has some serious inherent shortcomings. It does not take into account the effect of flow and the relaxed state is always force-free. Since the practical plasmas exhibit flow and force-free relaxed state is of no interest for thermonuclear fusion, there is a strong need to modify this theory.

In order to generalize the MHD relaxation theory, different attempts using different kinds of constraints have been made to impart a finite flow and create pressure gradient in the relaxed state. More recently, Mahajan and Yoshida has also presented a relaxation model for an ideal two-species magnetofluid. The novelty of this model lies in its mathematical framework that is different from usual Euler-Lagrange technique but can be proved using variational principle. This model has been described in detail in chapter 3. The relaxed state admitted by this model exhibits strong flow and a finite pressure. The relaxed state of this model can be described by a linear combination of two different Beltrami fields. Let $\mathbf{B}_1$ and $\mathbf{B}_2$ be two different magnetic fields that satisfy the following Beltrami conditions

$$\begin{aligned} \nabla \times \mathbf{B}_1 &= \lambda_1 \mathbf{B}_1, \\ \nabla \times \mathbf{B}_2 &= \lambda_2 \mathbf{B}_2, \end{aligned}$$

where λ_1 and λ_2 are scalar constants. These fields represent force-free magnetic fields. But the linear combination of these force-free magnetic fields that is $C_1\mathbf{B}_1 + C_2\mathbf{B}_2 = \mathbf{B}$, leads to a magnetic field that satisfy the following relaxed state,

$$\nabla \times (\nabla \times \mathbf{B}) - \alpha_1 \nabla \times \mathbf{B} + \alpha_2 \mathbf{B} = 0.$$

It is quite evident and easy to show that

$$(\nabla \times \mathrm{B}) \times \mathrm{B} = C_1 C_2 (\lambda_1 - \lambda_2) \mathrm{B}_1 \times \mathrm{B}_2 \neq 0,$$

revealing that the resulting relaxed state is not a force-free state.

Based on this fact that is the emergence of a force containing relaxed state from the force-free states, the Mahajan-Yoshida relaxation model is very simple but have a very vast potential to illuminate more interesting and far rich features not revealed in a single-fluid description. At one extreme, paramagnetic fields can be recovered and on the other extreme diamagnetic structures can be created subject to different Beltrami parameters and boundary conditions.

This generality of Mahajan-Yoshida model has led us to use it as a paradigm for studying plasma relaxation in different geometries. To probe more deeply into the physics of relaxed states admitted by Mahajan-Yoshida model, we have calculated parallel and perpendicular components of flows and current density for an axisymmetric simple cylindrical geometry. Our results show that when Mahajan-Yoshida model is reduced to a single-Beltrami state, perpendicular components vanish and only large parallel components of said fields that are characteristic of Taylor's relaxed state persist there in the system. But when the double curl Beltrami role of the system is in full play, we get finite value of both the perpendicular as well as parallel components of flows and current densities for the real eigenvalues of the system. When complex or pure imaginary eigenvalues of double curl Beltrami system are taken, then we could get the dominance of perpendicular components throughout the system except at the center of the cylindrical system. In the simple cylinder, $j_\perp = V_\perp = 0$ at $r = 0$ but $j_\parallel(r = 0) \neq 0$ and $V_\parallel(r = 0) \neq 0$. But we are interested to minimize the parallel components of current density and flows throughout the system. Because in dissipative systems, an external agency is required to drive the parallel components and in the presence of strong fast flow, parallel components cause to generate shock waves that in turn, could destabilize the system. Moreover, parallel components cause to dissipate the magnetic helicity in resistive plasmas.

To overcome this problem of simple cylindrical geometry, we have considered internal conductor plasma configuration which is basically a simple cylinder with an additional current carrying conductor at the center. The analytical solution for internal conductor plasma system

are given and the radial profiles of fields and flows are plotted as shown in chapter 4. The system is optimized for certain scale parameters to seek the relaxed states having maximum β accompanied with the minimum value of field-aligned currents and flows for different Beltrami parameters and boundary conditions. A comparison of two configurations is also presented. Our results show that with the help of internal conductor configuration, we can obtain the relaxed state with the dominance of perpendicular components over parallel components throughout the system for certain Beltrami parameters and boundary conditions. Such high-β relaxed states are important regarding thermonuclear fusion. All the results obtained by simple cylindrical plasma configuration can be recovered with this new configuration. Hence, we can use internal conductor plasma configuration to study and understand different features of relaxed states based on double Beltrami fields.

Furthermore, by relating the Beltrami parameters with conserved physical quantities, a set of algebraic relations is obtained that can be investigated to predict the characteristics of the equilibrium state as the control parameter is slowly changed. One such example is worked out in detail, evaluating the Beltrami parameters in terms of the macroscopic constants of motion (helicities and energy). It is found that under certain conditions, the equilibrium can be catastrophically lost. This study could certainly help us in understanding of a variety of eruptive events in the solar atmosphere like the flares, the erupting prominences, and the coronal mass ejections.

This work can be extended further to obtain new results in order to explain the solar flares, heating of solar corona and dynamo process. We know the catastrophe conditions and parameter regimes of different scales while we have not examined the details of the energy flows. It is important to study the preferential conversion of the flow energy into the magnetic energy (small scale or large scale) or vice versa. The control parameter may be λ_+ (scale length) or helicity. The former process may represent the dynamo (in either large or small scale) and the latter may be the flare or heating.

Bibliography

[1] A. Hasegawa, Adv. Phys. **34**, 1 (1986).

[2] S. Ortolani, D. D. Schnack, Magnetohydrodynamics of Plasma Relaxation (World Scientific, 1993).

[3] M. R. Brown, J. Plasma Phys. **52**, 203 (1997).

[4] T. G. Cowling, Mon. Notic. Roy. Astron. Soc. **94**, 39 (1934).

[5] R. Lüst and A. Schlüter, Z. Astrophys. **34**, 263 (1954).

[6] S. Chandrasekhar and L. Woltjer, Proc. Natl. Acad. Sci. U.S.A. **44**, 285 (1958).

[7] L. Woltjer, Proc. Natl. Acad. Sci. U.S.A. **44**, 489 (1958).

[8] L. Woltjer, Proc. Natl. Acad. Sci. U.S.A. **44**, 833 (1958).

[9] H. K. Moffatt, J. Fluid Mech. **35**, 117 (1969).

[10] J. B. Taylor, Phys. Rev. Lett. **33**, 1139 (1974).

[11] M. A. Saunders, C. T. Russel and N. Sckopke, Geophys. Res. Lett. **11**, 131 (1984).

[12] A. Königl and A. R. Choudhuri, Astrophys. J. **289**, 173 (1985).

[13] H. K. Moffatt, J. Fluid Mech. **159**, 359 (1985).

[14] D. Montgomery, L. Turner, and G. Vahala, Phys. Fluids **21**, 757 (1978).

[15] N. Ito and Z. Yoshida, Phys. Rev. E **53**, 5200 (1996).

[16] R. Jordan, Z. Yoshida, and N. Ito, Physica D 114, 251 (1998).

[17] Z. Yoshida, Phys. Fluids 1, 155 (1994).

[18] C. Chu and T. Ohkawa, Phys. Rev. Lett. 48, 837 (1982).

[19] H. E. Moses, J. Math. Phys. **25**,1905 (1984).

[20] H. E. Moses and R. C. Prosser, Proc. R. Soc. London A **422**, 351 (1989).

[21] N. A. Salingaros, Appl. Phys. Lett. **56**, 617 (1990).

[22] J. B. Taylor, Rev. Mod. Phys. **58**, 741 (1986).

[23] Z. Yoshida et al., J. Plasma Phys. **59**, 103 (1998).

[24] R. J. Lahaye, T. H. Jensen, P. S. C. Lee, R. W. Moore, and T. Ohkawa, Nuclear Fusion **26**, 255 (1986).

[25] H. A. B. Bodin and A. A. Newton, Nuclear Fusion **20**, 1255 (1980).

[26] S. O. Knox, C. W. Barnes, G. J. Marklin, T. R. Jarboe, I. Henins, H. W. Hoida, and B. L. Wright, Phys. Rev. Lett. **56**, 842 (1986).

[27] G. R. Tynan, L. Schmitz, R. W. Conn, R. Doerner and R. Lehmer, Phys. Rev. Lett. **68**, 3032 (1992).

[28] T. Peyser and G. C. Goldenbaum, Phys. Rev. Lett. 61, 955 (1988).

[29] B. Barrow and G. C. Goldenbaum, Phys. Rev. Lett. **64**, 1369 (1990).

[30] U. Frisch, A. Pouquet, J. Leorat and A. Mazure, J. Fluid Mech. **68**, 769 (1975).

[31] R. N. Sudan, Phys. Rev. Lett. **42**, 1277 (1979).

[32] L. Turner, IEEE Trans. Plasma Sci. **14**, 849 (1986).

[33] K. Avinash and J. B. Taylor, Comments Plasma Phys. Control. Fusion **14**, 127 (1991).

[34] K. Avinash, Phys. Fluids B **4**, 3856 (1992).

[35] L. C. Steinhauer and A. Ishida, Phys. Rev. Lett. **79**, 3423 (1997).

[36] L. C. Steinhauer and A. Ishida, Phys. Plasmas, **5**, 2609 (1998).

[37] S. M. Mahajan and Z. Yoshida, Phys. Rev. Lett. **81**, 4863 (1998).

[38] Z. Yoshida and S. M. Mahajan, J. Math. Phys. **40**, 5080 (1999).

[39] Z. Yoshida, Y. Ogawa, J. Morikawa, H. Himura, S. Kondo, M. Hashimoto, T. Hirotsu, K. Takemura, H. Kakuno, C. Nakashima, N. Shibayama, S. Tahara, M. Iqbal, S. M. Mahajan, Proceedings of Invited Papers, 17th IAEA Conference on Fusion Energy, Yokohama, 1998, IAEA-CN-69/ICP/10(R).

[40] Z. Yoshida, Y. Ogawa, J. Morikawa, H. Himura, S. Kondo, C. Nakashima, S. Kakuno, M. Iqbal, F. Volponi, N. Shibayama, S. Tahara, Proceedings of Invited Papers, AIP Conference on Non-Neutral Plasma Physics, New Jersey, 1999, edited by J. J. Bollinger, R. L. Spencer and R. C. Davidson (American Institute of Physics, 1999) CP498, p. 397.

[41] F. Wagner et. al., Phys. Rev. Lett. **49**, 1408 (1982).

[42] R. J. Taylor, M. L. Brown, B. D. Fried, H. Grote, J. R. Liberati, G. J. Morales, and P. Pribyl, Phys. Rev. Lett. **63**, 2365 (1989).

[43] R. J. Groebner, K. H. Burrell, and R. R. Seraydarian, Phys. Rev. Lett. **64**, 3015 (1990).

[44] K. Ida et al., Phys. Rev. Lett. **65**, 1364 (1990).

[45] K. Ida et al., Plasma Phys. Controlled Fusion **36**, A279 (1994).

[46] K. C. Shaing and E. C. Crume, Jr., Phys. Rev. Lett. **63**, 2369 (1989).

[47] M. Tendler, Plasma Phys. Controlled Fusion **39**, 371 (1997).

[48] S. M. Mahajan and Z. Yoshida, Phys. Plasmas **7**, 635 (2000).

[49] Z. Yoshida, S. M. Mahajan, S. Ohsaki, M. Iqbal, and N. Shatashvili, Phys. Plasmas **8**, 2125 (2001).

[50] M. Iqbal, A. M. Mirza, G. Murtaza, and Z. Yoshida, Phys. Plasmas **8**, 1559 (2001).

[51] S. Chandrasekhar and P. C. Kendall, Astrophys. J. **126**, 457 (1957).

[52] V. I. Arnold and B. A. Khesin, Topological Methods in Hydrodynamics (Springer-Verlag, New York, 1998).

[53] Z. Mikić, D. C. Barnes, and D. D. Schnack, Astrophys. J. **328**, 830 (1988).

[54] D. Biskamp and H. Welter, Solar Phys. **120**, 49 (1989).

[55] G. E. Vekstein, Astron. Astrophys. **182**, 405 (1990).

[56] R. J. Bray, L. E. Cram, C. J. Durrant and R. E Loughhead, Plasma Loops in the Solar Corona (Cambridge University Press, 1991).

[57] P. Foukal, Astrophys. J. **223**, 1046 (1978).

[58] B. Vrsnak, Solar Phys. **94**, 289 (1984).

[59] M. Kruskal and R. M. Kulsrud, Phys. Fluids **1**, 265 (1957).

[60] D. K. Bhadra and C. Chu, J. Plasma Phys. **33**, 257 (1985).

[61] H. K. Moffatt, Magnetic Field Generation in Electrically Conducting Fluids (Cambridge Univ. Press., Cambridge, 1978).

[62] M. A. Berger, and G. B. Field, J. Fluid Mech. **147**, 133 (1984).

[63] B. N. Kuvshinov and T. J. Schep, Phys. Plasmas **4**, 537 (1997).

[64] T. H. Jensen and M. S. Chu, Phys. Fluids **27**, 2881 (1984).

[65] S. R. Oliveira and T. Tajima, Phys. Rev. E **52**, 4287 (1995).

[66] E. Hameiri and J. H. Hammer, Phys. Fluids **25**, 1855 (1982).

[67] J. M. Finn and T. M Antonsen, Jr., Phys. Fluids **26**, 3540 (1983).

[68] Z. Yoshida and Y. Giga, Math. Z. **204**, 235 (1990).

[69] Z. Yoshida and A. Hasegawa, Phys. Fluids B **3**, 3059 (1991).

[70] M. Abramowitz and I. A. Stegun, Handbook of Mathematical Functions (National Bureau of Standards, Washington DC, 1964).

[71] E. Hameiri and S. T. Chun, Phys. Rev. A **41**, 1186 (1990).

[72] E. Hameiri and H. A. Holties, Phys. Plasmas **1**, 3807 (1994).

[73] T. Sakurai, Solar Phys. **121**, 347 (1989).

[74] D. Biskamp, Non-linear Magnetohydrodynamics (Cambridge University Press, 1993), p.316.

[75] T. G. Frobes and P. A. Isenberg, Astrophys. J. **373**, 294 (1991).

[76] T. G. Frobes and E. R. Priest, Astrophys. J. **446**, 377 (1995).

[77] K. Kusano, Y. Suzuki and K. Nishikawa, Astrophys. J. **441**, 942 (1995).

[78] A. A. Pevtsov, R. C. Canfield, and H. Zirin, Astrophys. J. **473**, 533 (1996).

[79] D. H. Mackay, E. R. Priest, V. Gaizauskas, and A. A. Van Ballegooijen, Sol. Phys. **180**, 299 (1998).

[80] A. Ruzmaikin and P. Akhmetiev, Phys. Plasmas **1**, 331 (1994).

[81] F. Krause and K.-H Rädler, Mean-field Magnetohydrodynamics and Dynamo Theory (Pergamon, New York, 1980)

[82] A. H. Boozer, Phys. Fluids B **5**, 2271 (1993).

[83] M. L. Goldstein, D. A. Roberts, and W. H. Matthaeus, in Annual Review of Astronomy and Astrophysics, edited by G. Burbidge and A. Sandage (Annual Reviews, Palo Alto, CA, 1995), Vol. **33**, p. 283.

[84] J. Aparicio, M. G. Hains, R. J. Hastie, and J. P. Wainwright, Phys. Plasmas **5**, 3180 (1998).

[85] M. Yamada, H. Ji, S. Hsu, T. Carter, R. Kulsrud, N. Bretz, F. Jobes, Y. Ono, and F. Perkins, Phys. Plasmas **4**, 1936 (1997).

[86] Y. Ono, M. Inomoto, T. Okazaki, and Y. Ueda, Phys. Plasmas **4**, 1953 (1997).

[87] C. Litwin and S. C. Prager, Phys. Plasmas 5, 553 (1998).

[88] R. L. Stenzel, J. M. Urrutia, and C. L. Rousculp, Phys. Plasmas 2, 1114 (1995).

[89] Z. Yoshida, Phys. Plasmas B 1, 208 (1994).